CRITICAL STATE FRAMEWORK FOR INTERPRETATION OF GEOTECHNICAL PROPERTIES OF CEMENT TREATED SOILS

By

FARID SARIOSSEIRI

A dissertation submitted in partial fulfillment of
the requirements for the degree of

DOCTOR OF PHILOSOPHY

WASHINGTON STATE UNIVERSITY
Department of Civil and Environmental Engineering

August 2008

To the Faculty of Washington State University:

The members of the Committee appointed to examine the dissertation of FARID SARIOSSEIRI find it satisfactory and recommend that it be accepted.

_____
Chair

_____

_____

_____

ACKNOWLEDGEMENTS

I am grateful for the opportunity to pursue my academic interest at the Washington State University. I would like to express my appreciation to Dr. Balasingam Muhunthan for his unlimited advices and generosity; this research project would not have been possible without his efforts. I wish to acknowledge my committee members Dr. Richard Watts, Dr. Adrian Rodriguez-Marek, and Dr. Shihui Shen. I would like to thank Dr. Mehrdad Razavi at New Mexico Institute of Mining and Technology for his assistance. I also would like to thank many current and former graduate students. I wish to appreciate my family; they have been always supportive. In addition financial support by FHWA is greatly appreciated.

CRITICAL STATE FRAMEWORK FOR INTERPRETATION OF GEOTECHNICAL PROPERTIES OF CEMENT TREATED SOILS

Abstract

by Farid Sariosseiri, Ph.D.
Washington State University
August 2008

Chair: Balasingam Muhunthan

This study examines the effectiveness of cement treatment on geotechnical properties of soils from Aberdeen, Everett, and Palouse regions from the state of Washington. The addition of cement was found to improve the drying rate and compaction characteristics of the soils. Significant improvement in unconfined compressive strength and modulus of elasticity are attained by cement treatment of these soils.

Results of undrained triaxial tests showed that while cement treatment improved shear strength significantly, the type of failure behavior varied greatly. Non-treated, 5%, and 10% cement treated soils displayed ductile, planar, and splitting type of failure, respectively. For 10 % cement treated soils pore pressures raised rapidly to confining pressures resulting in zero effective confining pressure at failure. Consequently, specimens split vertically. Therefore, while increase in strength can be achieved by

cement treatment, high percentages of cement should be used with extreme caution in field applications.

Mohr-Coulomb and Johnston failure criteria were applicable to predict shear strength of non-treated and 5% cement treated soils while Griffith and modified Griffith found to be applicable for non-treated, 5% and 10% cement treated soils.

The results of triaxial tests on Aberdeen soil were interpreted using the critical state framework. As a result of cement treatment interlocking increased, critical state friction remained constant and soils displayed anisotropic behavior. The anisotropic model presented by Muhunthan and Masad (1997) was used to predict the undrained stress path. A combination of this model with extended Griffith theory can be used to predict the complete shear behavior of cement treated soil in q-p′ space. The main contributions of this study to practice are quantifying improvement in mechanical behavior due to cement treatment and highlighting the fact that higher percentages of cement could turn stabilization from beneficial to an extremely dangerous practice.

TABLE OF CONTENTS

Page

LIST OF FIGURES

Page

LIST OF TABLES

Page

This dissertation is dedicated to my family. Thank you for all of the unconditional love, guidance, and support.

CHAPTER ONE

INTRODUCTION

1.1 Introduction

Increased costs associated with the use of high quality materials have led to the need for local soils to be used in geotechnical and highway construction. Often however, high water content and low workability of these soils pose difficulties for construction projects. Frequently, additives such as lime, cement, fly ash, lime-cement-fly ash admixture, cement kiln dust, emulsified asphalt, Geofiber, and polymer stabilizers are used to improve their engineering properties. The choice and effectiveness of an additive depends on the type of soil and its field conditions. Nevertheless knowledge of mechanistic behavior of treated soil is equally important as selecting the stabilizer.

High water content and low workability of local soils in the western side of Washington State have often caused difficulties for highway construction projects. The addition of a few percentages by weight of Portland cement has shown its effectiveness towards better control of workability during compaction in some projects (Lowell 2005). Therefore based on past experience and environmental concerns Washington Department of Transportation decided to use Portland cement as stabilization agent. However, there is a need to systematically examine cement treatment effectiveness for a range of soils encountered and also study the mechanical properties of cement stabilized soils for highway embankment applications. Type and location of the soils that needed improvement prior to use were selected by Department Of Transportation officials.

In this study, the term *modification* is used for improvement in workability and compaction characteristics whereas the term *stabilization* is adopted for improvement in mechanical behavior of cement treated soils.

The beneficial effects of cement on the performance of soils have been widely documented (Balmer 1958; Mitchell 1976; Uddin et al. 1997; Lo and Wardani 2002). Cement treatment leads to improvement in the mechanical properties of soils. However, the findings of different researchers on the role of Portland cement on compacted properties as well as strength and modulus have not been entirely consistent. For example, Balmer (1958) and Clough et al. (1981) reported cement treatment increased cohesion while internal friction angle remained constant. On the other hand, Uddin et al. (1997) stated that internal friction angle increased significantly. Some studies have indicated that at very low cement contents, improvement in strength is due to an increase in friction angle rather than cohesion (Rocha et al. 1961; Abboud 1973). Research has also shown that cohesion increases with curing time while friction angle remains constant (Nash et al. 1965; Wissa et al. 1965; Abboud 1973).

Abboud (1973) reported that cement treated soils exhibit brittle types of failure at low confining pressures and a more plastic failure type at high confining pressures i.e., Mohr-Coulomb failure envelope for cement treated soils is curved. Several failure criteria, including Griffith crack theory and modified Griffith crack theory (Mitchell 1976), have been proposed to account for the strength behavior of soil. The brittle to ductile transition of shear behavior of soils as a function of mean stress is the basis of the modern concept of the Critical State Soil Mechanics (Schofield and Wroth 1968; Schofield 2005). Schofield (1998) has disputed that the Mohr-Coulomb criterion,

popularized by Terzaghi and underpinning the developments of soil mechanics, is valid for a limited range of stress levels. He has argued that the strength of remolded soils (be it sand or clay) is governed by its critical state friction and particle interlocking. The use of friction and particle interlocking may enable us to better interpret the strength of cement stabilized soils.

1.2 Objectives

The overall objective of this research is to study the compaction, strength and deformation characteristics of cement treated soils. The specific objectives of the study are as follows:

1- Investigation of the solidification, workability, and compaction characteristics of Portland cement treated soils.

2- Investigation of the mechanical properties of cement treated soils.

3- Interpretation of mechanical behavior of cement treated soil using critical state frame work.

Tests were performed on three types of soils. They were collected from the Palouse area in Eastern Washington, Aberdeen and Everett area in western Washington. The effect of different percentages of cement was evaluated using Atterberg limits, compaction characteristics, unconfined compressive strength, and modulus of elasticity. In addition, consolidated undrained triaxial tests with pore water pressure measurements, fall cone test, and Oedometer were conducted on Aberdeen soil. The results are interpreted using Mohr-Coulomb, Griffith, modified Griffith, and Johnston (1985) strength criteria as well as using the critical state framework.

1.3 Organization of thesis

Chapter Two presents a background of the study. It includes the effect and performance of different modifiers including lime, Portland cement, fly ash, lime-cement-fly ash admixture, emulsified asphalt, cement kiln dust, polymers, Geofibers, and salt. The chapter also presents an examination of different failure criteria including classical Mohr-Coulomb, Griffith crack theory, modified Griffith crack theory, the criterion suggested by Johnston (1985). This chapter concludes with discussion on the critical state framework.

Experimental methods are given in Chapter Three. This chapter presents a summary of material properties and testing programs. This includes tests on solidification, Atterberg limits, standard proctor, unconfined compressive strength, consolidated-undrained triaxial, fall cone, and Oedometer. Results and discussion are presented in Chapter Four. Interpretation of mechanical behavior of cement treated soil using critical state framework is given in Chapter Five. Chapter Six presents conclusions and recommendations for future work.

CHAPTER TWO

BACKGROUND

2.1 Introduction

A summary of the performance of a number of widely used additives in geotechnical practice is discussed first. It includes, lime, Portland cement, fly ash, lime-cement-fly ash admixture, emulsified asphalt, cement kiln dust (CKD), Geofiber reinforcement, salt, and non-traditional polymer stabilizers. It is followed by discussion of several failure criteria including Griffith and modified Griffith theory, Johnston criterion (1985), and critical state framework and cam clay model.

2.2 Lime stabilization

Lime is one of the oldest and still popular additives used to improve fine-grained soils. Construction of Denver International Airport is an example of using lime stabilization method. Following are the four major lime-based additives used in geotechnical construction; hydrated high calcium lime $Ca(OH)_2$, Calcitic quick lime CaO, monohydrated dolomitic lime $Ca(OH)_2$ MgO, and dolomitic quick lime CaO MgO.

Lime treatment of soil facilitates the construction activity in three ways (Mallela et al. 2004). First, a decrease in the liquid limit and an increase in the plastic limit results in a significant reduction in plasticity index. Reduction in plasticity index facilitates higher workability of the treated soil. Second, as a result of chemical reaction between soil and lime a reduction in water content occurs. This facilitates compaction of very wet soils. Further, lime addition increases the optimum water content but decreases the

maximum dry density and finally immediate increase in strength and modulus results in a stable platform that facilitates the mobility of equipments.

2.2.1 Chemical reaction

When lime is mixed with clayey material in the presence of water several chemical reactions take place. They include cation exchange, flocculation-agglomeration, pozzolanic reaction, and carbonation (Mallela et al. 2004). Cation exchange and flocculation-agglomeration are the primary reactions, which take place immediately after mixing. During these reactions, the monovalent cations that are generally associated with clay minerals are replaced by the divalent calcium ions. These reactions contribute to immediate changes in plasticity index, workability, and strength gain.

Pozzolanic reaction occurs between lime and, the silica and alumina of the clay mineral and produces cementing material including calcium-silicate-hydrates and calcium alumina hydrates. The basic pozzolanic reactions are as follows:

$$Ca(OH)_2 + SiO_2 \rightarrow CaO\text{-}SiO_2\text{-}H_2O \quad (2.1)$$

$$Ca(OH)_2 + Al_2O_3 \rightarrow CaO\text{-}Al_2O_3\text{-}H_2O \quad (2.2)$$

Pozzolanic reactions are time and temperature dependent and may continue for a long period of time. Addition of lime to soil increases its pH; studies have shown that when the pH of the soil increases to 12.4, which is the pH of saturated limewater, the solubility of silica and alumina increase significantly. Therefore, as long as sufficient calcium from the lime remains in the mixture and the pH remains at least 12.4, pozzolanic reaction will continue.

In some instances, lime reacts with carbon dioxide to produce calcium carbonate instead of calcium-silicate-hydrates and calcium alumina hydrates. Such carbonation is an undesirable reaction from the point of soil improvement (Bergado et al. 1996; Mallela et al. 2004).

2.2.2 Lime treatment applications and advantages

Lime treatment has been found to result in an increase in optimum water content, a decrease in maximum dry density, a decrease in swell potential, an increase in strength, an increase in modulus of elasticity, and an increase in fatigue strength. The effect of lime on soil can be categorized into two groups, immediate and long-term stabilization. Increased workability of soil is the result of immediate modification, which is the main contributor in early construction stages. Increased strength and durability is considered long-term stabilization that takes place during and after curing.

2.2.3 Compaction characteristics

Effect of lime treatment in compaction characteristics of a low plasticity clay soil is shown in Figure 2.1. Lime treatment reduces maximum dry density and increase optimum water content (Mallela et al. 2004; Thompson 1966). Increase in optimum water content facilitates compaction of soils which are wet of optimum in their natural condition. Results of studies have also revealed that optimum water content increases with increasing in lime content (Mallela et al. 2004; Tabatabi 1997; Thompson 1966).

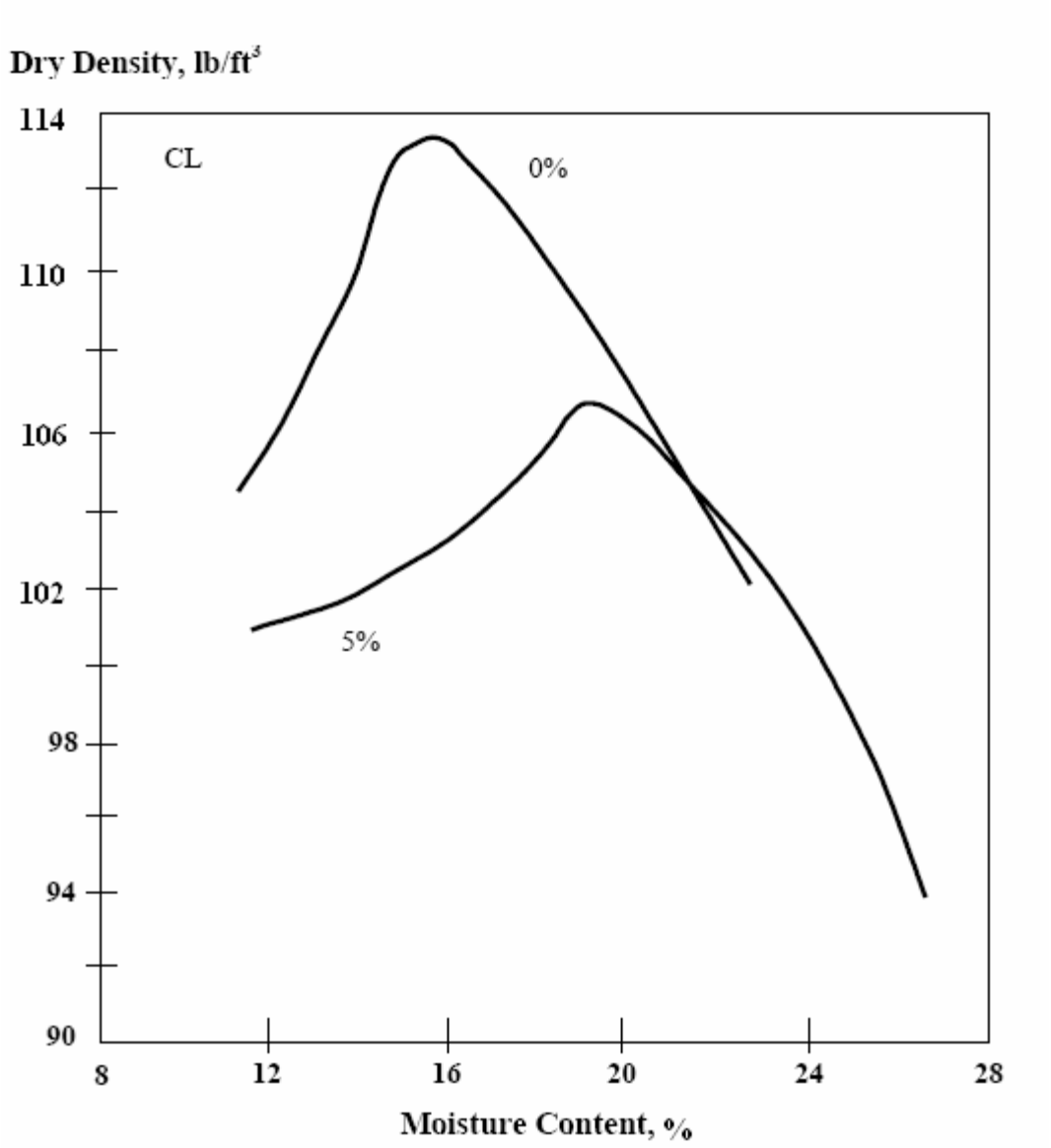

Figure 2.1: Changes in compaction curve by addition of lime to a low plasticity clay soil (Mallela et al. 2004).

2.2.4 Swell potential

Relationship between swell pressure and dry density for Porterville clay is shown in Figure 2.2, for different lime content. It can be observed that as lime content increases, swell pressure decreases significantly. This enables its use in reducing the swelling potential of expansive soils. Figure 2.3, shows the relationship between plasticity index

and percentage of swelling. It is evident that a reduction in plasticity index leads to a significant decrease in swell potential. Lime treatment results in the reduction of plasticity index and removes some of the water that can be absorbed by clay minerals. This coupled with the formation of a cementation skeleton that resist against volume changes contribute to a significant reduction in swell percentage.

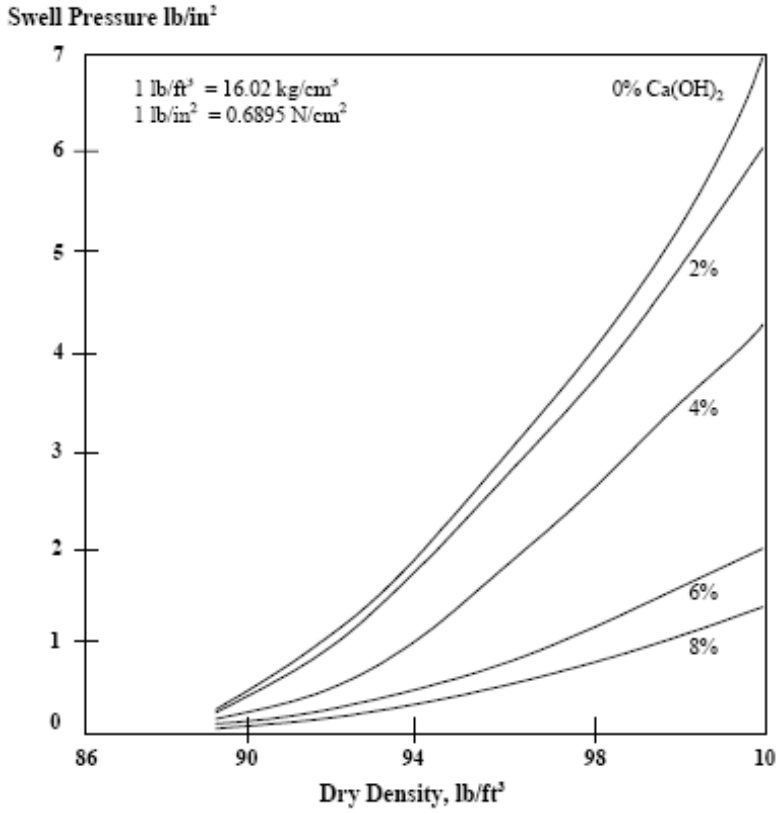

Figure 2.2: Swell pressure-density relationship for lime treated Portterville clay (Mallela et al. 2004).

Addition of lime to clayey material has been shown to reduce swell potential from 8% to 0.1% (Tabatabi 1997). However, it must be noted that the reduction of moisture content and the potential for shrinkage in treated soil may result in development of fissures or small cracks (Tabatabi 1997).

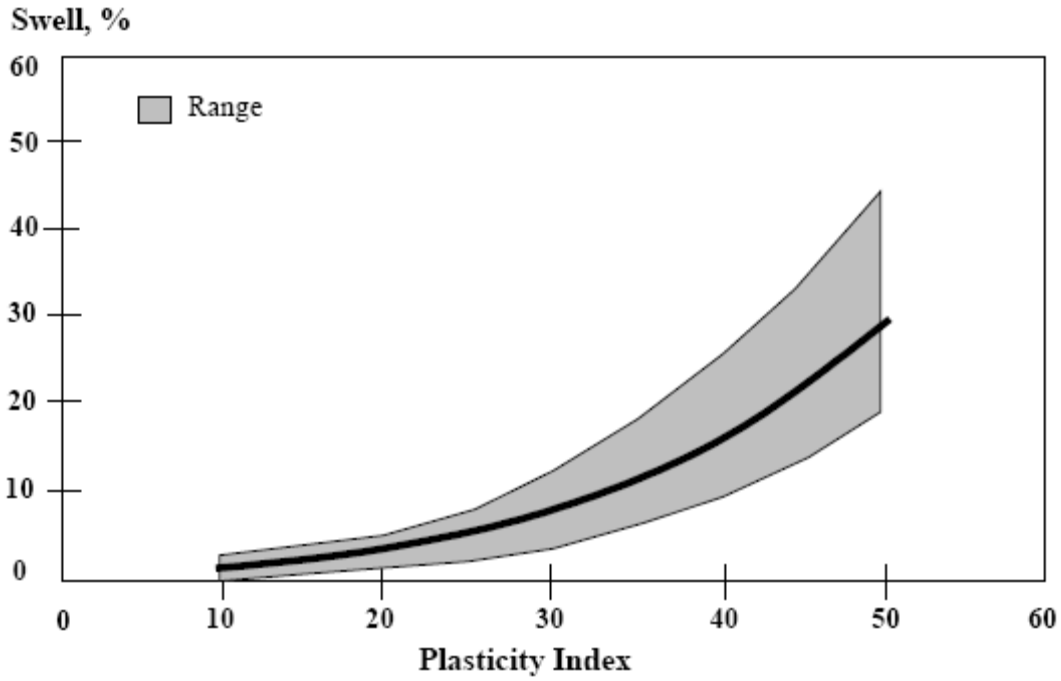

Figure 2.3: Swell potential as a function of plasticity index (Mallela et al. 2004).

2.2.5 Shear strength and stress-strain behavior

Lime treatment leads to significant increase in strength. The immediate increase in strength results from flocculation-agglomeration reaction and leads to better workability, whereas long-term strength gain is due to pozzolanic reactions. Thompson (1966) stated that addition of lime to fine-grained soils yields a substantial increase in cohesion and minor improvement in internal friction angle. The effect of curing time on unconfined compressive strength of the lime treated material is shown in Figure 2.4. It can be observed as that curing time increases, unconfined compressive strength increases while strain corresponding to peak stress decreases. In the other words lime treated soils display brittle behavior.

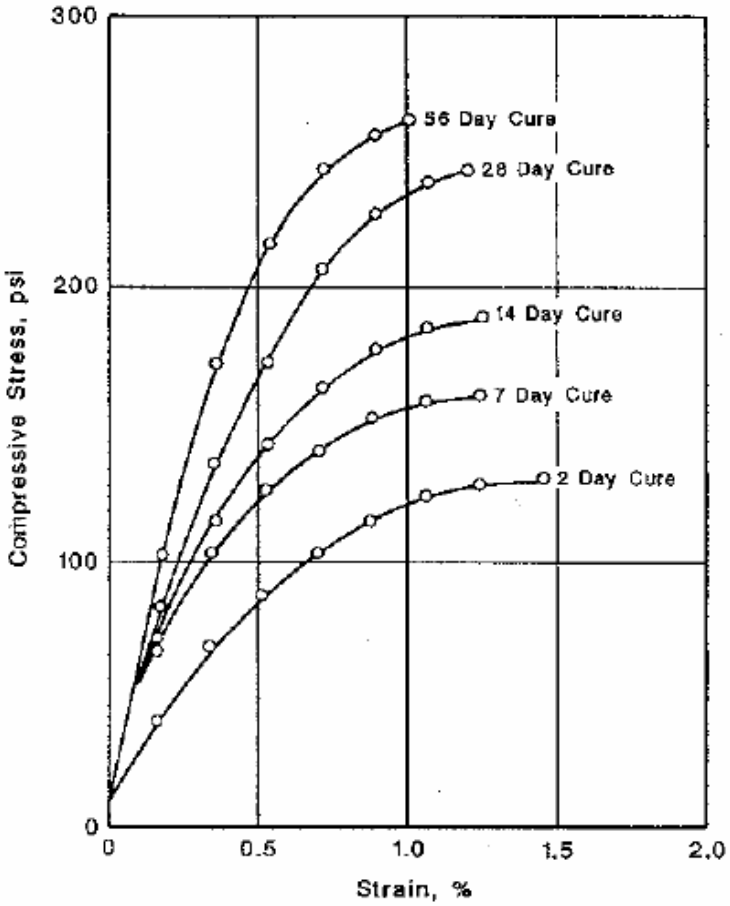

Figure 2.4: Stress-strain characteristics of lime stabilized Goose Lake clay with time (Mallela et al. 2004).

The following relationships suggested by Thompson (1966) can be used to determine the cohesion and modulus of elasticity of lime treated soils based on unconfined compressive strength, respectively.

$$c = 9.3 + 0.292\sigma_c \tag{2.3}$$

$$E = 9.98 + 0.1235\sigma_c \tag{2.4}$$

Where:

c: Cohesion (psi)

E: Modulus of elasticity (ksi)

σ_c: Unconfined compressive strength (psi)

2.2.6 Fatigue and durability

Fatigue strength is related to the number of cycles of loads that the material can carry at a given stress level. Addition of lime to soil increases its fatigue strength significantly. Figure 2.5, shows the fatigue response of lime-stabilized soils. It is evident that as the ratio of applied stress to strength decreases, the number of cycles of loads needed to cause failure of treated material increases (Mallela et al. 2004; Tabatabai 1997). Lime treated soils gain in ultimate strength over time thus contributing to the reduction in applied stress to strength and an increase in fatigue strength.

Studies have shown that moisture and freeze-thaw cycles have less effect on lime treated materials compared with non-treated materials. It has also been recognized that the resistance of lime treated material against freeze-thaw cycles is highly dependent on their immediate strength. The higher immediate strength is associated with resistance to higher number of freeze-thaw cycles (Tabatabai 1997).

2.2.7 Suitability

Lime works best for clayey soils, especially those with moderate to high plasticity index (PI>15). Due to lack of aluminates and silicates in silts and granular material pozzolanic reactions do not take place, therefore lime does not work well for these materials. In order to stabilize silts and granular materials with lime, pozzolanic admixtures such as fly ash need to be used in addition to lime.

Little (1995), suggested that soils classified by Unified Soil Classification System as CH, CL, MH, SC, SM, GC, SW-SC, SP-SC, SM-SC, GP-GC, and GM-GC can be stabilized by lime treatment. Aggregates with plastic fines, caliche and other marginal bases that contain appreciable amount of material passing #40 sieve are also capable of being stabilized with lime (Little 1995). In addition, lime can be used for stabilization of soils with sulfate concentration less than 7000 to 8000 parts per million (ppm) (Harris et al. 2005).

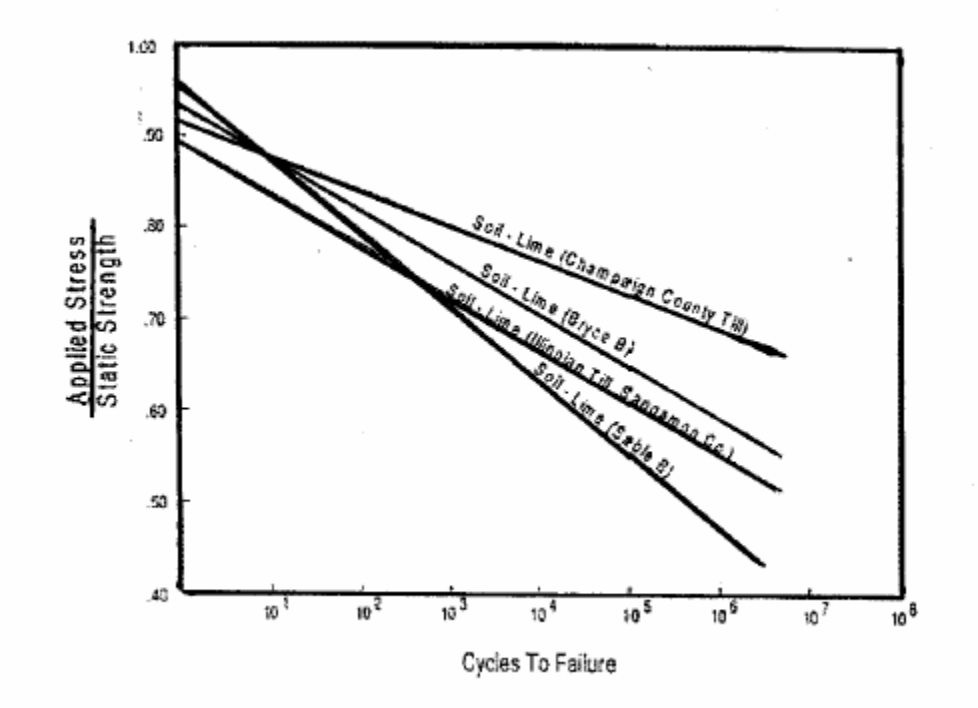

Figure 2.5: Flexural fatigue response curves for different lime-stabilized soils in Illinois (Mallela et al. 2004).

2.2.8 Quantity

The amount of lime required varies based on the characteristics of the material that needs to be treated and the desired degree of stabilization. For modification purposes, normally 2% to 3% by dry weight of the soil is sufficient (Das 1990; Maher et al. 2005). Larger quantities are required for pozzolanic reactions, and thus strength gain to occur. For stabilization purposes, typically 5% to 10% by weight of the dry soil are used (Das 1990).

In order to determine the optimum lime requirement for soil stabilization several methods have been presented. For example Hilt and Davidson (1960) suggested the following for optimum lime content (Bergado et al. 1996):

$$Optimum\ Lime\ Content = \frac{\%\ of\ Clay}{35} + 1.25 \qquad (2.5)$$

U.S. Army Corps of Engineers manuals, EM1110-3-1370 and TM 5-822-14, have presented methods and guidelines to determine the optimum lime content for modification and stabilization purposes. Eades and Grim (1966) suggested that the minimum amount of lime required to stabilize a soil is that can maintain a pH of at least 12.4. Since all available methods are based on empirical observations, additional laboratory testing is needed to identify the optimum lime content for a given soil and environmental conditions.

2.3 Cement stabilization

Soil cement stabilization technique has also been in existence for a long time. A construction project near Johnsonville, South Carolina in 1935 was one of the first controlled construction project in which cement was used as a soil stabilizer in the United

States (Das 1990). Cement treatment causes chemical reaction similar to lime and can be used for both modification and stabilization purposes. Cement can be applied to stabilize any type of soil, except those with organic content greater than 2% or having pH lower than 5.3 (ACI 230.1R-90 1990). Many studies have shown that granular soils and clayey materials with low plasticity index are better suited to be stabilized with cement (Currin et al. 1976; Engineering manual 1110-3-137 1984).

Significant reduction in plasticity index and swell potential, and remarkable increase in strength, modulus of elasticity and resistance against the effects of moisture and freeze-thaw can be achieved by cement stabilization. Note that reduction in plasticity index is due to an increasing of plastic limit, which is highly affected by cement content and curing time (Bergado et al. 1996). The addition of cement was also found to increase optimum water content but decrease the maximum dry density (Tabatabi 1997). However report by ACI committee 230 (1990) states that cement treatment causes changes in maximum dry density and optimum water content, but the direction of changes is not predictable. In addition cement treatment causes immediate decrease in water content (Bergado et al. 1996). Cement treated materials behave in a more brittle manner than non-treated materials. (Bergado et al. 1996) reported that cement treatment changes the behavior of soft clay from normally consolidated to overconsolidated state.

2.3.1 Strength

The effect of cement content and curing time on unconfined compressive strength for 28 days curing is shown in Figure 2.6. It is observed that, as cement content increases unconfined compressive strength of fine-grained as well as coarse-grained soils increases.

Improvement in unconfined compressive strength (in psi) varies from 40 times of cement content for fine-grained soils up to 150 times of cement content for coarse-grained soils. In addition, unconfined compressive strength increases with increasing curing time. Note that improvement due to curing time for coarse-grained soils is significant, as shown in Figure 2.7.

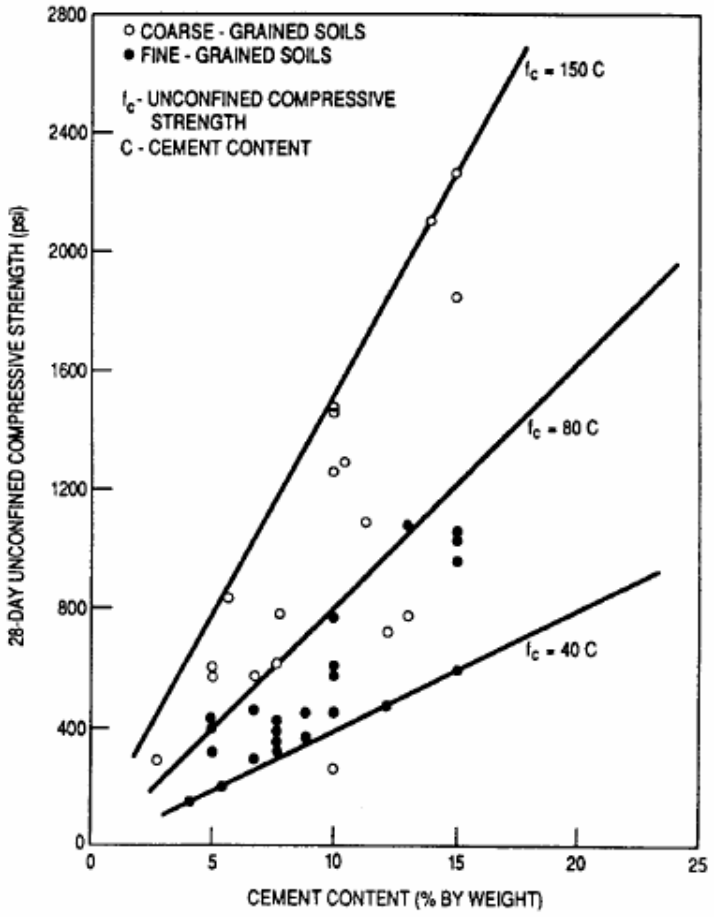

Figure 2.6: Relationship between cement content and unconfined compressive strength for cement treated soils (Mitchell 1976).

The relationship between unconfined compressive strength and curing time for a given soil and cement content was presented by Mitchell (1976):

$$(\sigma_c)_d = (\sigma_c)_{d_0} + K \log\left(\frac{d}{d_0}\right) \tag{2.6}$$

Where:

$(\sigma_c)_d$: Unconfined compressive strength at age of d days (psi)

$(\sigma_c)_{d_0}$: Unconfined compressive strength at age of d_0 days (psi)

K = 70C for coarse-grained soils and K = 10C for fine-grained soils, (C: Cement content, percent by weight)

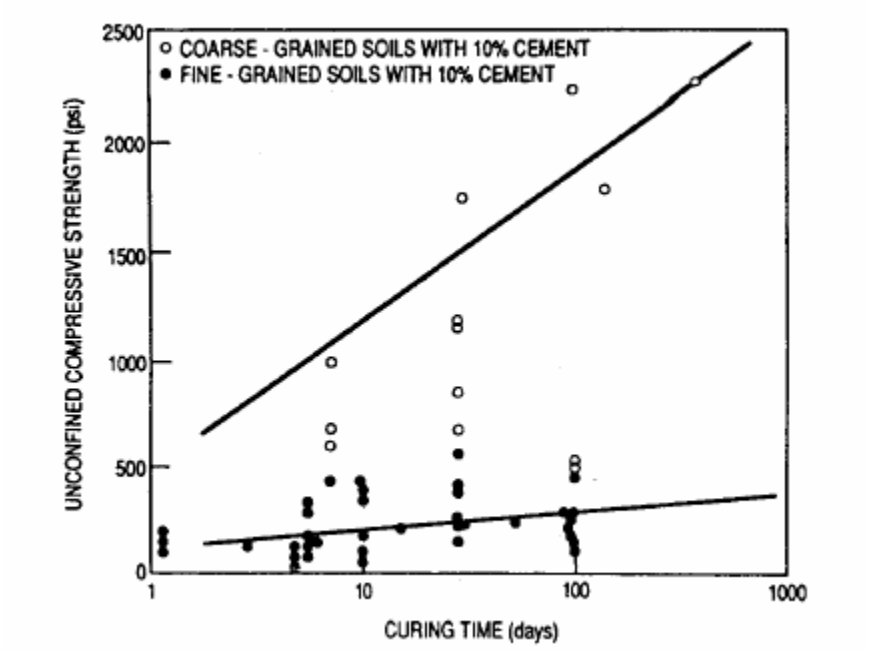

Figure 2.7: Effect of curing time on unconfined compressive strength of cement treated soils (Mitchell 1976).

Recent studies have also reported that addition of cement increases the effective cohesion significantly (Lo and Wardani 2002). Figure 2.8, shows the effect of cement content on effective cohesion of several coarse-grained and fine-grained soils. It is noted that, this plot was obtained for 90 days curing time and 413.64 kPa (60 psi) confining pressure. It can be seen that cement treatment leads to an increase in effective cohesion.

The increase in cohesion can be expressed as a function of unconfined compressive strength directly (Mitchell 1976):

$$c = 7.0 + 0.225(\sigma_c) \tag{2.7}$$

Where, σ_c is unconfined compressive strength (psi) and c is effective cohesion.

Studies have shown that internal friction angle remains relatively constant for cement treated soils regardless of cement content and curing time (Clough et al. 1981; Balmer 1958). The average values of internal friction angle are 43.8˚ and 36.1˚ for granular and fine-grained cement treated soils, respectively (Balmer 1958). On the other hand, recent studies have reported that cement stabilization leads to significant increase in internal friction angle (e.g. Uddin et al. 1997). In addition, the results of undrained triaxial test have shown that cohesion and friction angle increase with increasing curing time and cement content. The cohesion of cement treated clay disappears at large strain, and it behaves as purely frictional material (Bergado et al. 1996).

Delays between mixing and compaction leads to significant reduction in unconfined compressive strength of cement treated material. Results of a particular research showed that, losses in unconfined compressive strength were 10% to 20% and up to 40% for four and 24 hours delay, respectively (White and Gnanendran 2005).

Results of investigations showed that unconfined compressive strength increases with increasing relative compaction (Figure 2.9). It can be observed that, each 1% increase in relative compaction leads to about 200 kPa increase in unconfined compressive strength (White and Gnanendran 2005).

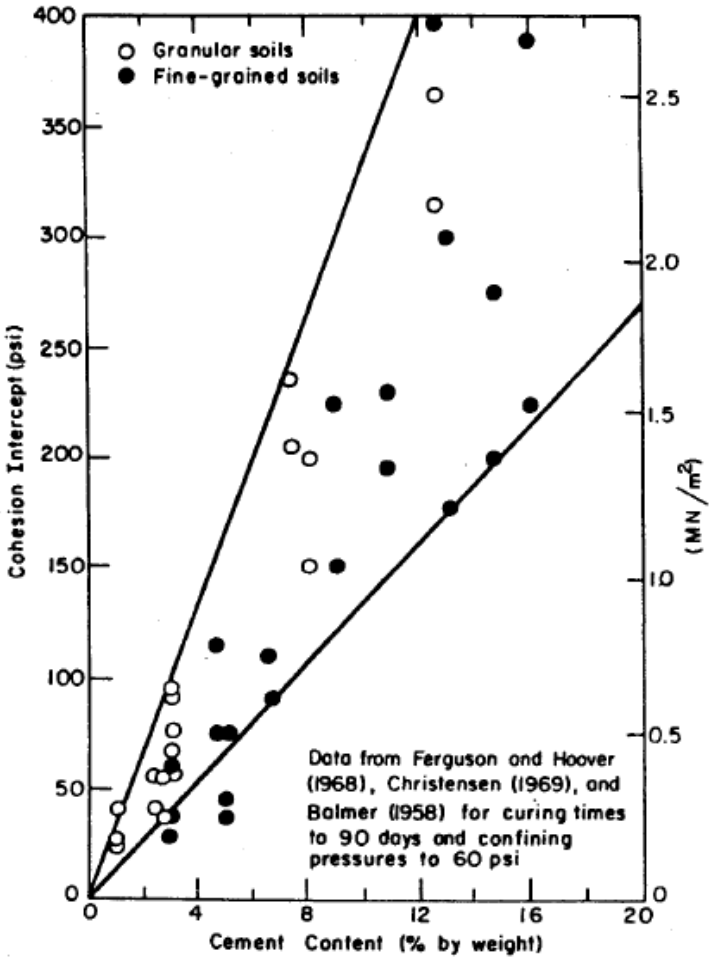

Figure 2.8: Effect of cement content on effective cohesion for several coarse-grained and fine-grained soils (Mitchell 1976).

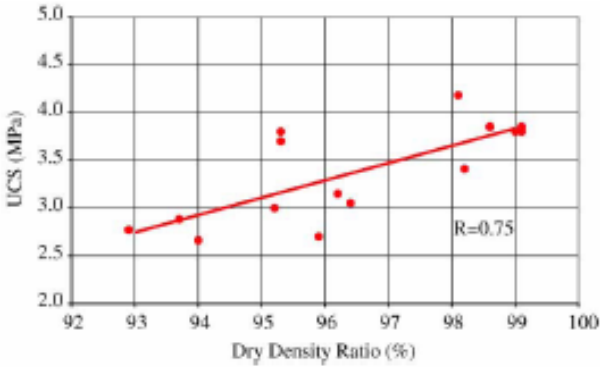

Figure 2.9: Unconfined compressive strength versus relative compaction for cement treated material (White and Gnanendran 2005).

2.3.2 Durability

In most stabilization projects, achieving a maximum level of durability is desirable. Cement treatment has been documented to provide resistance against freeze-thaw cycles. Relationship between unconfined compressive strength and freeze-thaw and wet-dry cycle tests is shown in Figure 2.10. It is observed that, resistance against freeze-thaw and wet-dry cycling increase with increasing unconfined compressive strength. As a result the greater the percentage of cement content the better the durability.

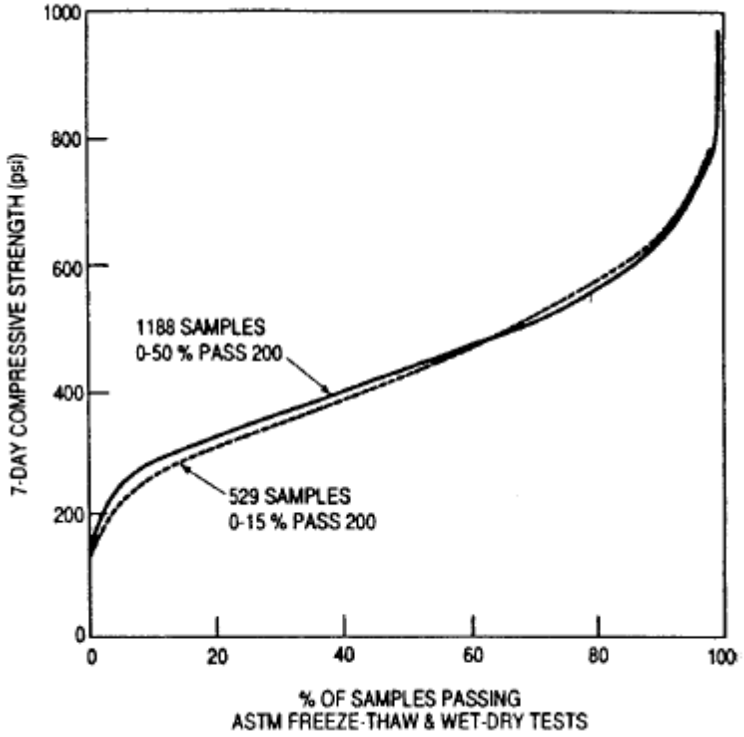

Figure 2.10: Relationship between unconfined compressive strength and durability of cement treated soils based on Portland Cement Association durability criteria (ACI 230.1R-90 1990).

2.3.3 Compressibility

The results of Oedometer test on Bangkok clay is shown in Figure 2.11. Significant improvement on the compressibility of cement treated soils is evident. It is observed that preconsolidation pressure increases significantly due to addition of cement. Coefficient of consolidation of cement treated soils gradually decreases, approximately linearly, with increasing consolidation pressure. Results have shown that higher cement content is associated with the greater value of coefficient of consolidation.

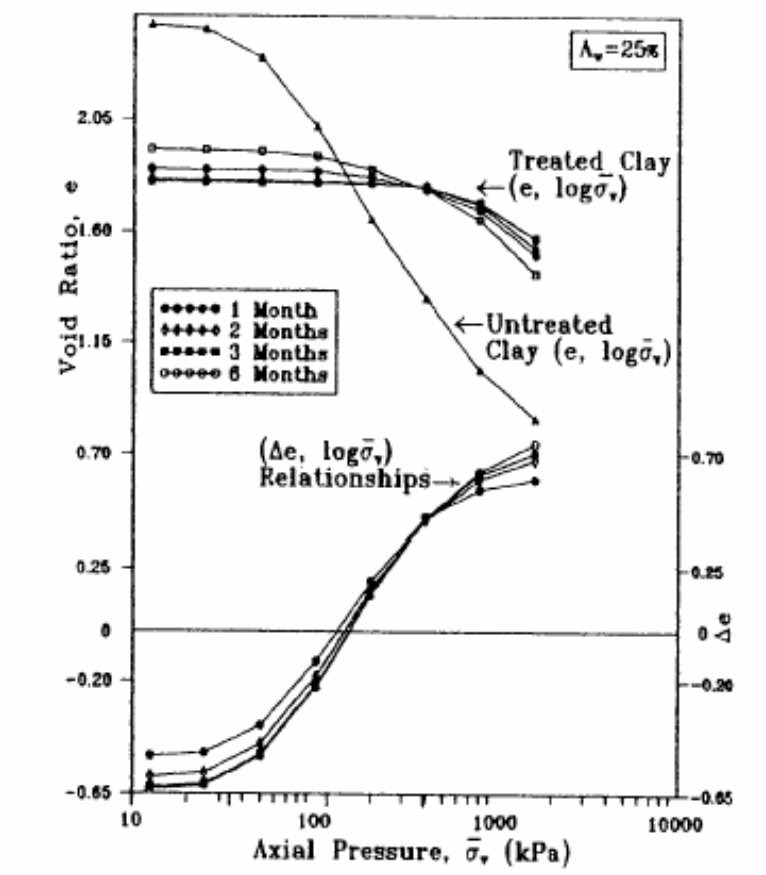

Figure 2.11: Consolidation curve for Bangkok clay with 25% cement content (after Bergado et al. 1996).

Typical amounts of cement for stabilization purposes vary from 5% to 10% of weight of dry soil. U.S. Army Corps of Engineers, EM1110-03-137, TM 5-822-14, and Portland Cement Association laboratory handbook (1992) provide guidelines to determine the optimum cement content for stabilization purposes. Note, that most of the manuals and guidelines in U.S do not recommend cement stabilization for soils with plasticity index greater than 15. In order to overcome this, small amount of lime can be added to soil prior to cement stabilization.

Cement treatment is more expensive than lime. For example, a cost analysis of a project at Joshua Tree National Park, CA showed that the cost of cement stabilization for 6 inches (15 cm) of mixing depth ranged from $2.80 to $3.40 per square yard (0.836 m^2) (Maher et al. 2005). In comparison, the cost of lime stabilization for 8 inches (20 cm) of mixing depth based on a project at Natches Trace Parkway, Madison, MS, and Bald Knob National Wildlife Refuge, White County, AR was only $1.30 to $2.00 per square yard (0.836 m^2).

2.4 Fly ash

Fly ash is a by-product of coal combustion in power plants. Fly ash contains silica, alumina, and different oxides and alkalis in its composition, and is considered as a pozzolanic material (Das 1990). The most common elemental compositions of fly ash include SiO_2, TiO_2, Al_2O_3, Fe_2O_3, MnO, MgO, CaO, Na_2O, K_2O, P_2O_5, SO_3 and organic carbons. A guideline for selecting fly ash as soil stabilizing agent is provided in ASTM C593.

There are two types of fly ash, type “C” and type “F”. This classification is based on the chemical composition. Fly ash type “C” contains significant amount of free lime. This type of fly ash produces pozzolanic and cementitious reactions. Cockrell et al. (1970), have shown that the lighter color fly ash indicates the presence of high calcium oxide and the darker color reflects high organic content. Fly ash can improve the engineering properties of soil. However it must be noted that fly ash properties are highly variable and depend on chemical composition of coal and combustion technology.

2.5 Lime-Cement-Fly ash

Construction of runway 9-27 at Houston International Airport is an example of using Lime-Cement-Fly ash stabilization (Little et al. 2000). Coarse-grained soils with little or no fines can be stabilized by a combination of lime and fly ash. The presence of various chemical components in fly ash enables it to produce a hardened cementitious material with improved compressive strength when mixed with lime and water. In order to accelerate the reaction and obtain the higher compressive strength a small amount of cement can be added. It is noted that for this admixture to be useful, fly ash must contain components that can react with the lime.

US Army Corps of Engineers manual EM1110-03-137 and TM 5-822-14, recommend that soils with less than 12% of material passing sieve #200 and plasticity index of material passing sieve #40 less than 25 are suitable to be stabilized with lime-cement-fly ash. The amount of required lime and fly ash can be obtained per guidance from ASTM C593. In addition, 1% cement is added for additional strength gain. If the achieved strength does not meet requirements, cement should be added in increments of

0.5% until the desired strength is obtained. The total added material should not exceed 15% of the dry weight of the soil.

The stabilization reactions in fly ash applications are a function of the hydration modulus defined as the ratio of the percentages of amount of CaO to that of the sum of amounts of SiO_2, Al_2O_3, and Fe_2O_3 in a given fly ash composition. Kamon and Nontananadh (1991) have suggested that in order to reactions take place, the hydration modulus must be greater than 1.7:

$$\frac{\%CaO}{\%SiO_2 + \%Al_2O_3 + \%Fe_2O_3} \geq 1.7 \qquad (2.8)$$

The above equation can be used to determine the portion of fly ash and lime in an admixture design. For example, if a certain type of fly ash has a hydration modulus of 1.0, the remainder has to be provided by addition of lime in order to satisfy Equation 2.8. Nicholson and Ding (1997) have observed that use of the above equation often resulted in the need for a large amount of lime addition which was higher than that was necessary to achieve desired improvement. However, the equation can be useful to obtain a preliminary estimate of amount of required lime. It is also noted that in order to obtain an effective mixture of lime and fly ash their amounts can be varied from 10% to 15% and 2% to 8% for fly ash and lime, respectively (Little et al. 2000). But typical mixture ratios range 3% to 4%, 10% to 15%, and 0.5% to 1.5% for lime, fly ash, and cement, respectively (Little et al. 2000). Results of investigation revealed that one hour delay between mixing and compaction lead to significant increase in unconfined compressive strength and resilient modulus of lime-fly ash treated material (White and Gnanendran 2005).

2.6 Emulsified asphalt

Stabilization with emulsified asphalt is more applicable for coarse-grained soils; however this method can also be applied to stabilize fine-grained soils as well. The tendency of the soil to adsorb water decreases with increase in the amount of emulsified asphalt. A study by Santoni et al. (2004) showed that a sample stabilized with emulsified asphalt had the minimal loss in unconfined compressive strength when tested under the wet condition, compared with the other samples that had been stabilized with the other stabilization agents.

Sandy soils can be stabilized by emulsified asphalt easily, if they contain less than 25% fine material with plasticity index of less than 12. The emulsified asphalt binds sand particles together and leads to significant increase in soil bearing capacity especially if the soil contains some fine material (Tabatabi 1997). Typical amount of emulsified asphalt that is used to stabilize the sandy soils is 2% to 6% of the dry weight of soil.

In order to obtain better performance of emulsified asphalt in gravelly soils the amount of fines with the plasticity index of less than 12 must be less than 15%. Typical amount of emulsified asphalt required to stabilize gravely soils is 2% to 6% of the dry weight of soil.

In order to stabilize the fine soils with emulsified asphalt, the soil should have the liquid limit less than 40 and plasticity index no grater than 18 (12 to 18). Rapid curing asphalt emulsions work better for fine soils stabilization rather than medium and slow curing asphalt emulsions. Typical amount of emulsified asphalt required to stabilize fine soils is 4% to 8% of the dry weight of soil.

The type and amount of emulsified asphalt highly depends on type of soil and other parameters such as atmospheric condition of the area. In order to obtain better stabilization results soil should be mixed with water slightly less than optimum water content, before adding emulsified asphalt. Unlike stabilization with lime, cement, and fly ash use of emulsified asphalt does not cause pozzolanic reactions. Therefore, the strength gain is attained based on the binding of particles alone. Consequently, the soil should be compacted carefully. In the other words, the better results can be achieved by the better compaction.

2.7 Cement kiln dust (CKD)

Cement Kiln Dust is a fine powdery by-product of the Portland cement manufacturing process. Approximately, 12.9 million metric tons of CKD is generated in the Unites States, annually. About 8.3 million tons of generated CKD is reused in Cement manufacturing, 3.7 million tons is landfilled or stockpiled, whereas the balance is consumed off site. The beneficial properties of CKD and its cost effectiveness compared with other type of stabilizers have led to its use as a popular stabilization agent in recent times. For example cement kiln dust has been used in road base stabilization purposes by some cities and counties in the state of Oklahoma (Miller and Azad 2000).

Table 2.1, shows the percentages of the main chemical compositions of CKD. Values in the first row are provided by Lafarge North America for a specific product and those in the second row are mean values of 63 different CKD's calculated from published data by Sreekrishnavilasam et al. (2006).

Table 2.1: Cement kiln dust (CKD) composition.

	SiO_2(%)	Al_2O_3(%)	Fe_2O_3(%)	CaO(%)	MgO(%)	SO_3(%)	Na_2O(%)	K_2O(%)	Total Alkali(%)
Lafarge	12.47	2.89	1.58	41.84	0.59	7.25	0.9	1.21	1.69
Mean	15.05	4.43	2.23	43.99	1.64	6.02	0.69	4	3.32

Based on the values of each component in Table 2.1, the hydration modulus (Equation 2.8) of CKD is found to vary between 2.47 and 2.03, respectively. It indicates that CKD can be considered a soil stabilizer. In addition, CKD has high surface area. Past studies have shown that the specific surface area of CKD varies within 0.46 -1.4 m^2/g (Sariosseiri and Muhunthan 2008). This feature enables CKD to absorb water off the surface of soil particles. This would be advantageous during early stages of compaction (modification) especially when the natural water content is higher than the optimum water content.

Results of study on comparison of effect of CKD and cement on geotechnical properties of Palouse loess showed that addition of CKD and cement led to an increase in optimum water content and a decrease in maximum dry density (Sariosseiri and Muhunthan 2008). Plasticity index increased initially but decreased at higher percentage of additives. In addition, CKD treatment resulted in a significant improvement in unconfined compressive strength and modulus of elasticity, it must be noted these increases for CKD treated soil are noticeably lower than that attained by addition of cement (Sariosseiri and Muhunthan 2008). However, it is noted that due to lack of standards and guidelines, use of CKD has not been fully accepted by government agencies. Further research is necessary in this regard.

2.8 Selection of additive

Guidelines to determine the appropriate stabilizer agent for different type of soils are abundant in the literature. Two methods that are widely used in practice are presented below. The first one is based on Currin et al. (1976) and the second one is based on U.S. Army Corps of Engineers publications (EM1110-03-137 and TM 5-822-14).

2.8.1 Currin et al. Method

This method uses the percentage of material passing #200 sieve and the plasticity index of the soil in its selection as shown in Figure 2.12. This method is specifically developed for pavement sub-grade stabilization purposes. It is supported with a number of tables and plots to determine the amount of stabilizers.

2.8.2 U.S. Army Corps of Engineers Method

The US Army Corps Engineering manuals EM1110-3-137 and TM 5-822-14 provide valuable guidelines for soil stabilization purposes. These guidelines are summarized in Figure 13 and in Table 2.2. Soils are first classified into selected areas based on their gradation characteristics as in Figure 2.13. The type of stabilization techniques and any restrictions imposed on specific areas are provided in Table 2.2. In addition, the Army Corps of Engineers manuals also provide the required amount for the different stabilizers based on soil type and other considerations. As noted earlier, the above guidelines must be supplemented with extensive laboratory testing to determine the most efficient admixture design in practice.

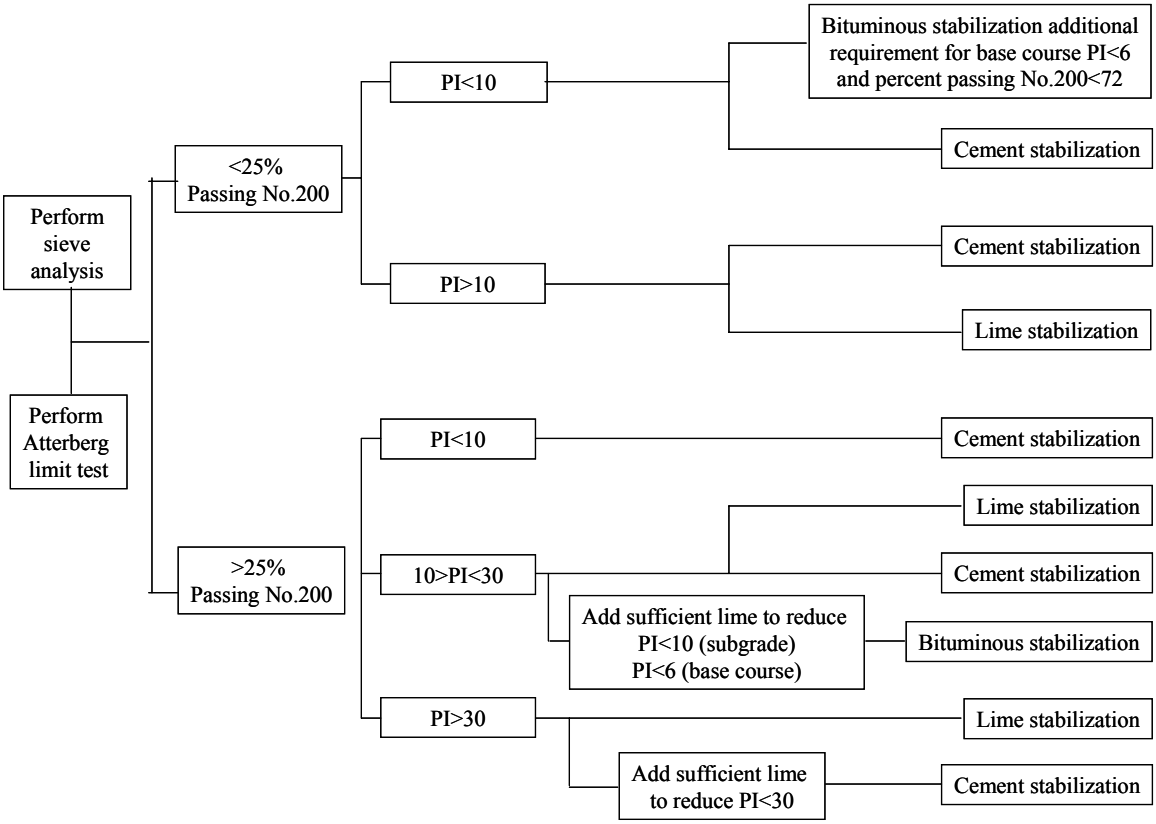

Figure 2.12: Determination of appropriate stabilizer (Currin et al. 1976).

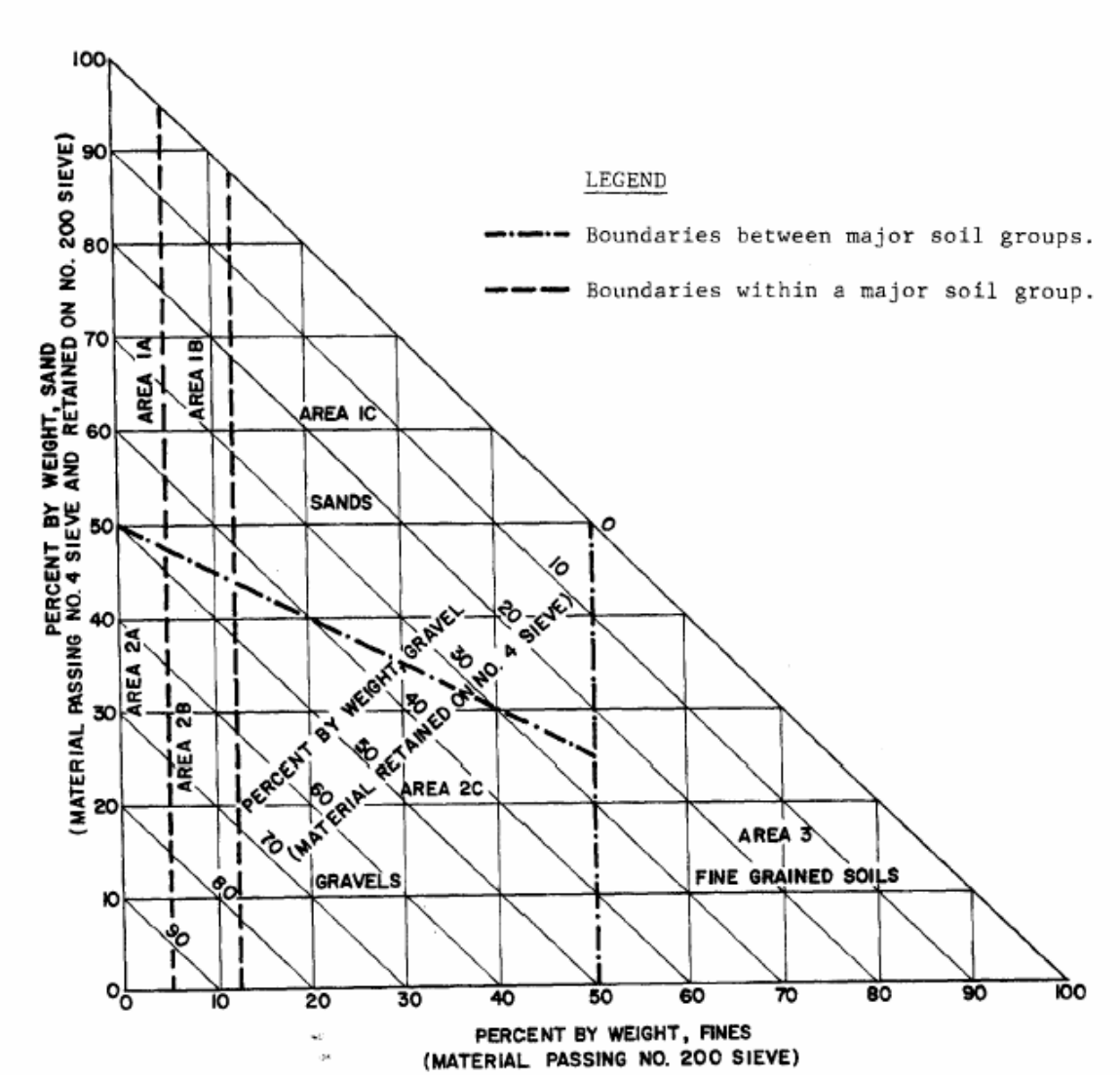

Figure 2.13: Gradation triangle for selecting a commercial stabilizing agent, (EM 1110-3-137).

Table 2.2: Guide for selecting stabilizing additives, (EM 1110-3-137).

Area	Soil classification*	Type of stabilizing additive recommended	Restriction on liquid limit and plasticity index	Restriction on percent passing sieve # 200	Remark
1A	SW or SP	Bituminous			
		Portland cement			
		Lime-Cement-Fly ash	PI not to exceed 25		
1B	SW-SM or SP-SM or SW-SC or SP-SC	Bituminous	PI not to exceed 10		
		Portland cement	PI not to exceed 30		
		Lime	PI not to exceed 12		
		Lime-Cement-Fly ash	PI not to exceed 25		
1C	SM or SC or SM-SC	Bituminous	PI not to exceed 10	Not to exceed 30% by weight	
		Portland cement	b**		
		Lime	PI not less than 12		
		Lime-Cement-Fly ash	PI not to exceed 25		
2A	GW or GP	Bituminous			Well graded material only
		Portland cement			Material should contain at least 45% by weight of material passing sieve #4
		Lime-Cement-Fly ash	PI not to exceed 25		
2B	GW-GM or GP-GM or GW-GC or GP-GC	Bituminous	PI not to exceed 10		Well graded material only
		Portland cement	PI not to exceed 30		Material should contain at least 45% by weight of material passing sieve #4
		Lime	PI not less than 12		
		Lime-Cement-Fly ash	PI not to exceed 25		
2C	GM or GC or GM-GC	Bituminous	PI not to exceed 10	Not to exceed 30% by weight	Well graded material only
		Portland cement	b**		Material should contain at least 45% by weight of material passing sieve #4
		Lime	PI not less than 12		
		Lime-Cement-Fly ash	PI not to exceed 25		
3	CH or CL or MH or ML or OH or OL or ML-CL	Portland cement	LL less than 40 and PI less than 20		Organic and strongly acid soils falling within this area not susceptible to stabilization by ordinary means
		Lime	PI not less than 12		

* Soil classification corresponds to MIL-STD-619. Restriction on liquid limit (LL) and plasticity index (PI) in accordance with method 103 in MIL-STD-621.

** $b \leq 20 + (\%\,pass\#200 / 4)$

2.9 Non-traditional stabilizers

In recent years an increasing number of non-traditional additives have been developed for soil stabilization purposes. Non-traditional stabilizers can be generally classified into major categories, including, salts, acids, enzymes, lignosulfonates, emulsions, polymers, tree resin, and geofibers. Each group has its own suite of sub categories of products. Shorter curing time and lack of need for special equipment and particular construction skills have made the use of these materials favorable for construction projects lately. Unfortunately, only few independent studies have been conducted to verify the claim of manufacturers. Since the chemical formulas of the products are modified often based on market tendency, it is rather difficult to evaluate the performance of a single product. As a result, documentation on soil stabilization performance with non-traditional additives continues to be subjective. A summary of the results of some independent studies conducted to examine the performance of a few non-traditional additives as a guide for future evaluations are presented below.

2.9.1 Polymers

Results of the research by Little et al. (2005) show the benefit of the polymer Soil-Sement® on stabilizing Eolian and Fluvial soils. Both types of soils are classified as poorly graded sand based on Unified Soil Classification System. Addition of this polymer to dry Eolian soils increased its CBR value by 992%. In addition, CBR value after freeze-thaw cycles increased by 872%. Similarly, Soil-Sement® treated Fluvial soils showed CBR increase of 497% and 3751% for dry and after freeze-thaw cycles, respectively. It is noted, however, studies conducted by the same authors show that some other brands of

polymers actually decreased the CBR values of treated material compared with non-treated material. The unconfined compressive strength of silty sand treated with Soil-Sement Engineering Formula®[1] by Santoni et al. (2004) also showed significant increase.

2.9.2 Fiber reinforcement

Use of hair sized polypropylene fibers in geotechnical applications has been accepted because of its cost competitiveness compared with other stabilization agents. These materials are not affected by chemical and biological degradation and do not cause leaching in soil (Puppala and Musenda 2000).

Puppala and Musenda (2000) have conducted a series of tests to study the engineering properties of clayey materials reinforced with randomly oriented fibers. The study used polypropylene fibers of nominal size of one inch and two inches in length. The physical and chemical properties of the fibers are as shown in Table 2.3. These fibers have high chemical resistance and can be applied in high temperature conditions. The results showed that mixing soils with fibers increased the unconfined compressive strength by 44% for Irving clay and 19% for San Antonio clay. In addition, mixing of fibers also resulted in the reduction of swell pressures and shrinkage volume. The study also showed that the length and amount of the fibers very much affect the level of improvement. In some cases, addition of fibers resulted in the reduction of unconfined compressive strength. Therefore, extensive laboratory testing must be conducted to determine optimum length and amount of the fiber for a given soil.

[1] Soil-Sement Engineering Formula and Soil-Sement are different products from the same manufacturer.

Table 2.3: Properties of polypropylene fibers (after Puppala and Musenda 2000).

Property	Value
Specific gravity	0.91
Tensile stregth, (MPa)	551.6 to 758.45
Modulus, (MPa)	3502.66
Melting point, (˚F)	324
Ignition point, (˚F)	1100
Absorption	None
Acid and salt resistance	High
Alkali resistance	High
Electrical conductivity	Low

Santoni and Tingle (2002) reported the results of sand fiber stabilization technology developed by the U.S. Army Corps of Engineers Research Center in Vicksburg, MS. In this study, two inch long polypropylene fibers were mixed with moist sand and the sand-fiber mixture was compacted with a smooth-drum vibratory roller. In order to bond the sand particles with fibers, a surface-wearing coat of material such as resin modified emulsion or emulsified asphalt were sprayed. While this method is more applicable to immediate military constructions, the results indicated that roads built using sand fiber stabilization method served for a reasonable length of time with little or no maintenance. The fiber technology can be applied to a very wide variety of soils without the need for special equipments or skills.

2.9.3 Salt (Sodium chloride)

Singh and Das (1999) reported significant improvement in CBR, unconfined compressive strength, and indirect tensile strength of salt treated material. Soil samples were prepared from commercial clay (BB1), River Aire soil, sand, and gravel. The study

further showed that addition of salt resulted in increase in resilient modulus. This is potentially useful for long-term highway pavement subgrade applications.

2.10 Environmental issues

Since most of the soil stabilization techniques using additives involve chemicals of some kind, care must be taken toward environmental considerations. If the application area is not appropriately protected from surface runoff the stabilized material can be washed onto surrounding areas and damage adjacent vegetation. In the case of lime treatment there is a potential for the rise of pH on contaminated areas. Fly ash composition is dependent on the source of coal and the type of combustion technology used. Most of the fly ash products have heavy metals in their composition. Therefore, fly ash treated materials have the potential to leach and contaminate water bodies. Many federal and state laws, regulations and specifications limit the amount of fly ash that can be used in highway construction projects (EPA-530-K-05-002 2005). Cement appears to have the least environmental impact compared with lime and fly ash. No environmental impact studies on the use of polymers have been reported to date.

Based on applicability and feasibility of available stabilization method, type of soils in sites, previous experiences, and environmental concerns Washington State Department of Transportation decided to use cement as stabilization agent. Therefore, the study here focuses on cement modification and stabilization, from this point onwards.

2.11 Failure criteria for cement treated soils

2.11.1 Introduction

The Mohr-Coulomb criterion popularized by Terzaghi, has been used extensively to characterize the failure of soils. It can be written as: $\tau_f = c + \sigma \tan\phi$ where, τ_f is the shear strength of the soil, and σ is the applied normal stress. ϕ and c are called internal friction angle and intrinsic cohesion, respectively. However, as pointed out before, the use of strength parameters, c and ϕ to soils and cement treated soils have led to number of anomalies. Results of many studies have shown that failure envelope of cement treated soils are curved. Consequently, it is impossible to report a particular internal friction angle (ϕ) to characterize the strength over the wide range of confining pressures. Several failure criteria such as, Griffith crack theory, modified Griffith crack theory, Hoek and Brown, and Johnston (1985) have been presented to improve the strength description of geo materials. It must be noted that application of each failure criteria is limited to type of material and stress conditions.

2.11.2 Griffith, modified, and extended Griffith crack theory

Griffith crack theory states that fracture initiation for a two dimensional loaded brittle body with microscopic flaws can be expressed as:

$$(\sigma_1 - \sigma_3)^2 = -8\sigma_t(\sigma_1 - \sigma_3) \qquad (2.9)$$

For $\sigma_1 + 3\sigma_3 > 0$ and if $\sigma_1 + 3\sigma_3 < 0$, then $\sigma_3 = \sigma_t$, where σ_t is tensile strength of material. Microscopic flaw includes small cracks, fissures, or grain boundaries (Parry 1995). The Griffith crack theory in terms of shear and normal stresses can be expresses in form of Equation 2.10.

$$\tau^2 + 4\sigma_t.\sigma_n - 4\sigma_t{}^2 = 0 \qquad (2.10)$$

Schematic failure envelope based on the Griffith crack theory for plane compression in terms of principal stresses, and shear and normal stresses are shown in Figures 2.14 and 2.15, respectively. It is clear that the ratio of unconfined compressive strength to uniaxial tensile strength is -8.

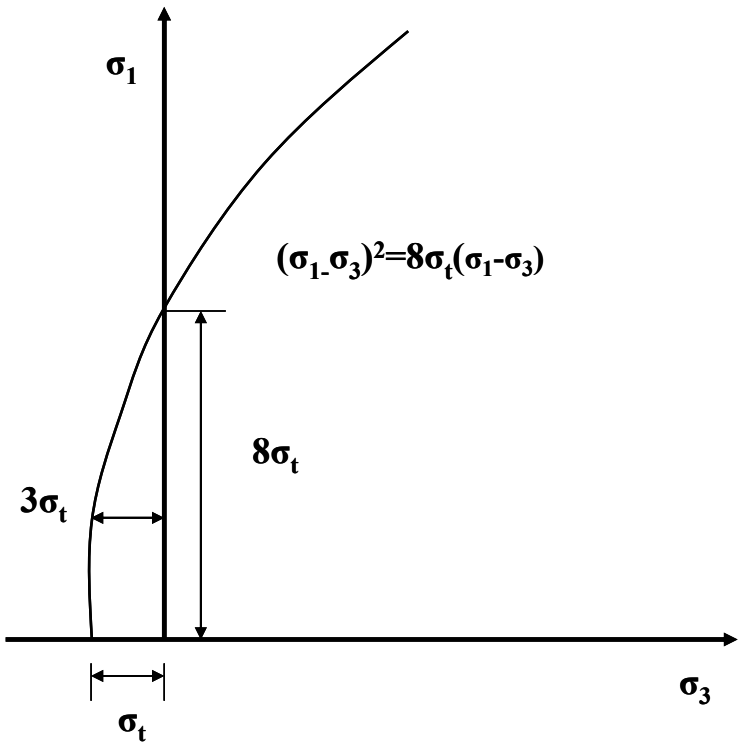

Figure 2.14: Failure envelope based on Griffith theory in terms of principal stresses.

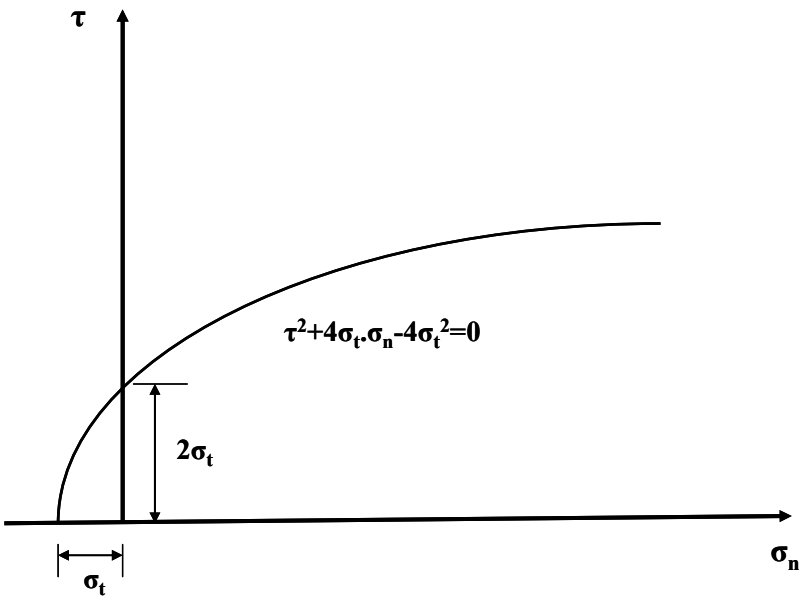

Figure 2.15: Failure envelope based on Griffith theory in terms shear and normal stresses.

The original Griffith failure envelope does not account for friction in closed cracks. Based on data from concrete and rock, McClintock and Walsh (1962) modified the Griffith crack theory to account for friction in closed cracks. Equation 2.11 expresses this modification in terms of principal stresses, where μ is the coefficient of internal friction (Jaeger and Cook 1976). The modified Griffith theory in terms of shear and normal stresses expressed in Equations 2.12 and 2.13, and illustrated in Figure 2.16.

$$\sigma_1\left[\left(\mu^2+1\right)^{\frac{1}{2}}-\mu\right]-\sigma_3\left[\left(\mu^2+1\right)^{\frac{1}{2}}+\mu\right]=4\sigma_t \tag{2.11}$$

$$\tau^2+4\sigma_t.\sigma_n-4\sigma_t{}^2=0 \qquad \text{For } \sigma_n<0 \tag{2.12}$$

$$\tau=2\sigma_t+\mu\sigma_n \qquad \text{For } \sigma_n>0 \tag{2.13}$$

McClintock and Walsh (1962) also recommended it can be assumed that $\mu = 1$ and the ratio of $\frac{\sigma_c}{\sigma_t}$ is -10. Details of the development and derivation of Griffith and modified Griffith crack theory are presented in Appendix A.

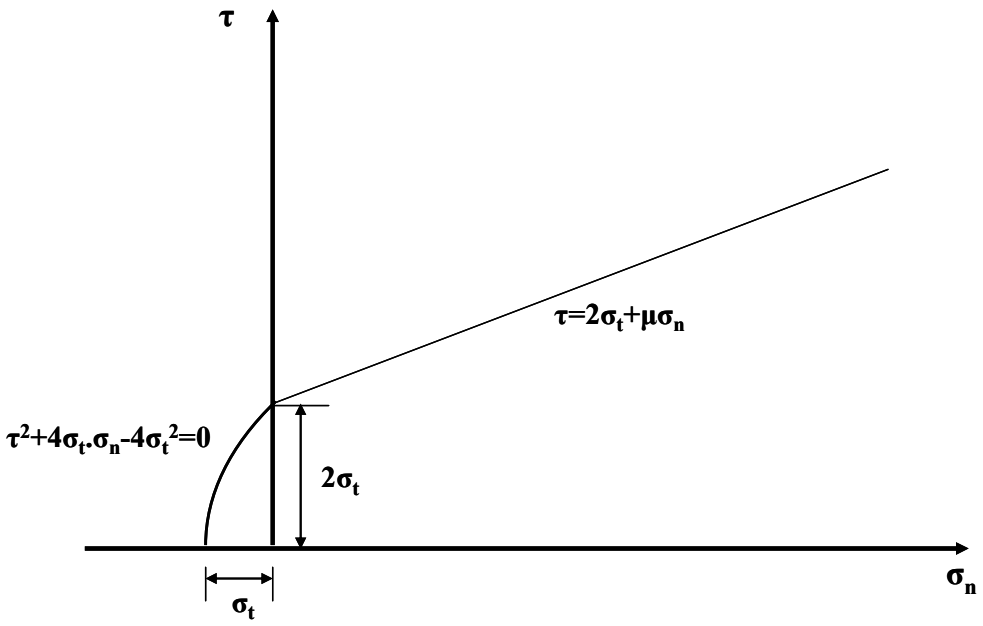

Figure 2.16: Failure envelope based on modified Griffith theory in terms of shear and normal stresses.

Griffith and modified Griffith failure envelopes assumed that the ratio of $\frac{\sigma_c}{\sigma_t}$ is -8 and -10 respectively, while results of studies on 13 different rocks showed that this ratio varies between -5 and -22. However, results of study by Abboud (1973) revealed close agreement between measured and predicted values for cement treated materials by using Griffith and modified Griffith theory, as shown in Figures 2.17 and 2.18 for gravel and silty clay soils, respectively.

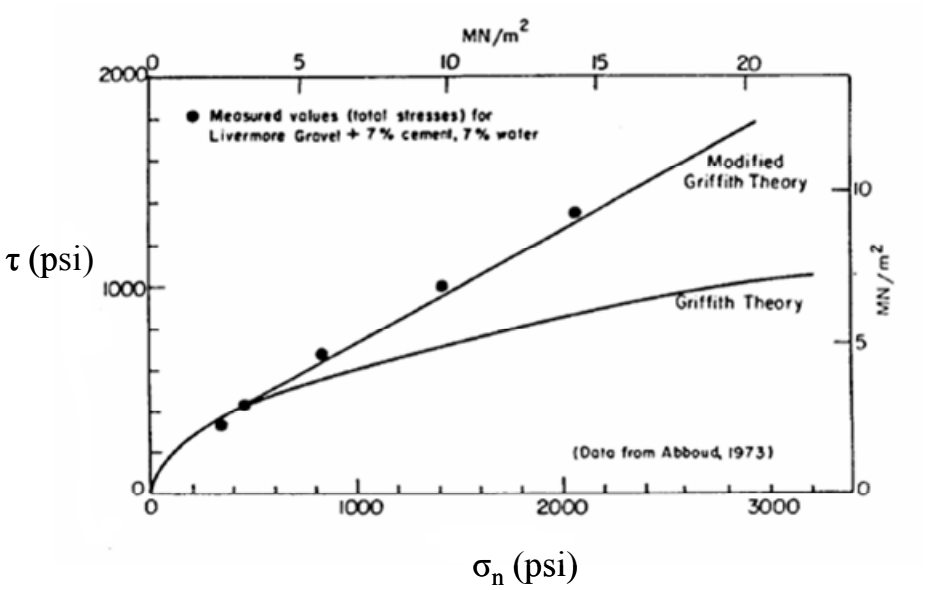

Figure 2.17: Comparison between measured strength and predicted values by Griffith theory for cement treated gravel (Mitchell 1976).

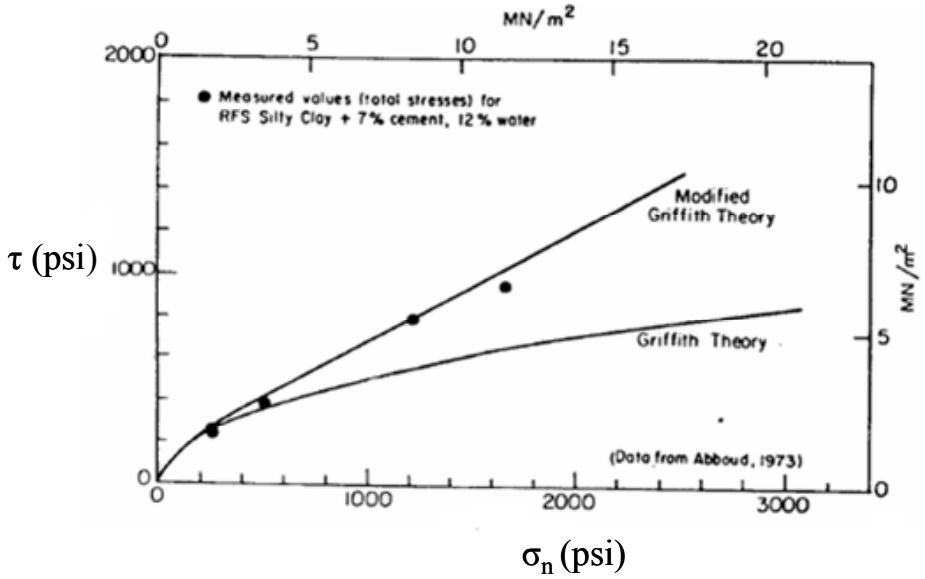

Figure 2.18: Comparison between measured strength and predicted values by Griffith theory for cement treated silty clay soil (Mitchell 1976).

It can be observed that modified Griffith theory can be applied for cement treated soils. Figure 2.19 presented by Mitchell (1976) shows the variation of σ_{1N} and σ_{3N} (principal stresses at failure normalized by unconfined compressive strength, $\frac{\sigma}{\sigma_c}$) for published data. It can be observed that Griffith theory can be applied in tensile range and low stress levels ($\frac{\sigma_3}{\sigma_c} < 0.1$), whereas modified Griffith theory can be applied for a wide range of stress levels. Mitchell (1976) found that μ can be assumed 0.89 instead of 1.0.

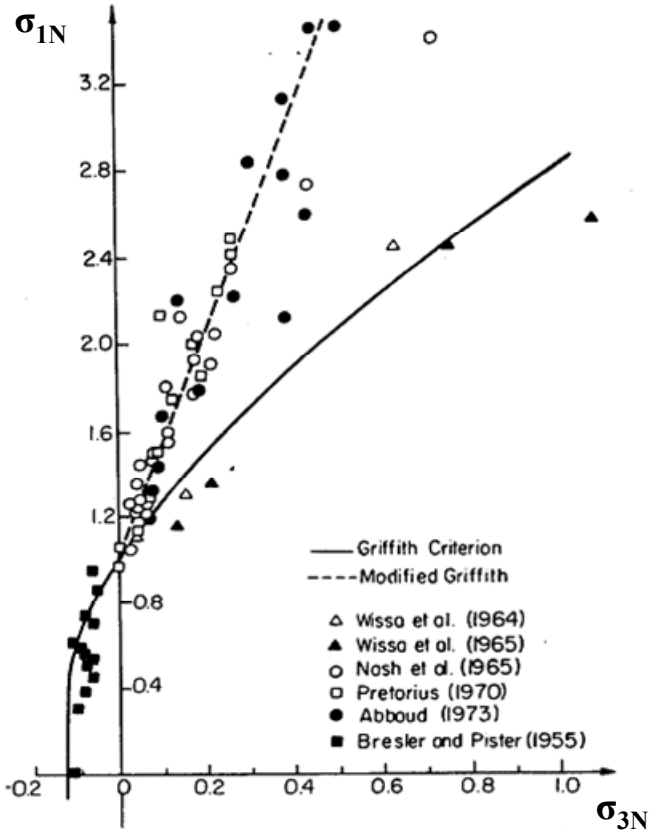

Figure 2.19: Failure envelope for cement treated soils (Mitchell 1976).

The original Griffith and modified Griffith theory assume that intermediate principal stress σ'_2 does not have an effect on initiation of cracks. Griffith theory has been extended by Murrell (1963) to account for effect of intermediate principal stress and known as extended Griffith theory. It is assumed that the ratio of unconfined compressive strength to tensile strength is -12. The extended Griffith theory for triaxial compression test at which $\sigma'_2=\sigma'_3$ in terms of major and minor principal stresses are as:

$$(\sigma'_1 - \sigma'_3)^2 = -12\sigma'_t(\sigma'_1 + 2\sigma'_3) \tag{2.14}$$

2.11.3 Johnston failure criterion

Extensive study by Johnston and Chiu (1984) on Melbourne mudstone resulted in a new failure criterion for soft rocks. This failure criterion is given by:

$$\sigma'_{1N} = \left(\frac{M}{B}\sigma'_{3N} + S\right)^B \tag{2.15}$$

Where:

M and B: Intact material constant

S: Parameter that accounts for strength of discontinuities of rock or soil, for intact material S=1.

If $\sigma'_{3N}=0$, then σ'_1= Unconfined compressive strength and if $\sigma'_1=0$, and assume $\sigma'_3 = \sigma'_t$ (σ'_t : tensile strength) then the ratio of unconfined compressive strength to uniaxial tensile strength can be expressed as:

$$\frac{\sigma_c}{\sigma'_t} = -\frac{M}{B} \tag{2.16}$$

Based on a broad range of data for clays and rocks Johnston (1985) suggested that Equations 2.17 and 2.18 can be used to determine the B and M, respectively.

$$B = 1 - 0.0172(Log\sigma_c)^2 \quad (2.17)$$

$$M = 2.065 + 0.276(Log\sigma_c)^2 \quad (2.18)$$

Where, unconfined compressive strength is measured in kPa. In order to specify M for different rock types he presented Equations 2.19 to 2.22 for Limestone, Mudstone, Sandstone, and Granite, respectively.

$$M = 2.065 + 0.170(Log\sigma_c)^2 \quad (2.19)$$

$$M = 2.065 + 0.231(Log\sigma_c)^2 \quad (2.20)$$

$$M = 2.065 + 0.270(Log\sigma_c)^2 \quad (2.21)$$

$$M = 2.065 + 0.659(Log\sigma_c)^2 \quad (2.22)$$

It can be seen that M depends on unconfined compressive strength as well as material type.

2.11.4 Critical state frame work and Cam-clay failure criterion

2.11.4.1 Introduction

None of the failure criteria extant in the field of soil mechanics account for the changes in shear behavior of soils with confining stress. This important feature is captured by Critical State Soil Mechanics (CSSM). While its original developments were based on remolded clay, the frame work has been shown to be applicable for a wide range of soils. Chiu and Johnston (1984) showed its applicability for soft Melbourne mudstone.

The state of soil specimen in a triaxial test is defined by the following variables (Wood 1990):

$$p' = \frac{\sigma_1' + 2\sigma_3'}{3} = \frac{\sigma_1 + 2\sigma_3}{3} - u \tag{2.23}$$

is the mean normal effective stress.

$$q = \sigma_1' - \sigma_3' = \sigma_1 - \sigma_3 \tag{2.24}$$

is the mean shear stress, and

$$V = 1 + e \tag{2.25}$$

is the specific volume. Note e is the void ratio.

The critical state line projected onto the q- p' space is defined by:

$$q = Mp' \tag{2.26}$$

M is the critical state frictional constant and the slope of the line. The critical state line projected onto the $V - ln\ p'$ plane is given by:

$$V = \Gamma + \lambda \ln p' \tag{2.27}$$

Where Γ is the specific volume corresponding to $p' = 1$ and λ is the slope of the critical state line. In addition, the normal consolidation line during isotropic consolidation is given by:

$$V = N + \lambda \ln p' \tag{2.28}$$

Where N is the specific volume corresponding to p' = 1. Note that this line falls on the V– ln p′ plane since q = 0.

Finally, the isotropic elastic line is given by:

$$V = V_\kappa + \kappa \ln p' \tag{2.29}$$

Where κ is the slope of swelling and recompression lines and V_κ is the specific volume corresponding to p' = 1. The four basic parameters of the critical state framework, M, Γ, λ and κ are shown in Figures 2.20 and 2.21.

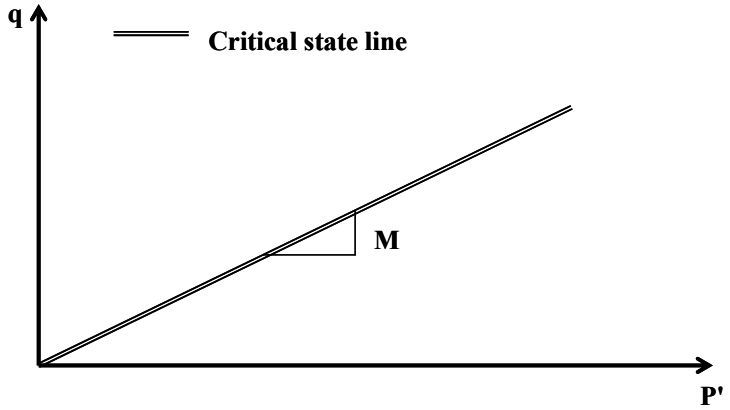

Figure 2.20: Critical state parameter M in q-p' spaces.

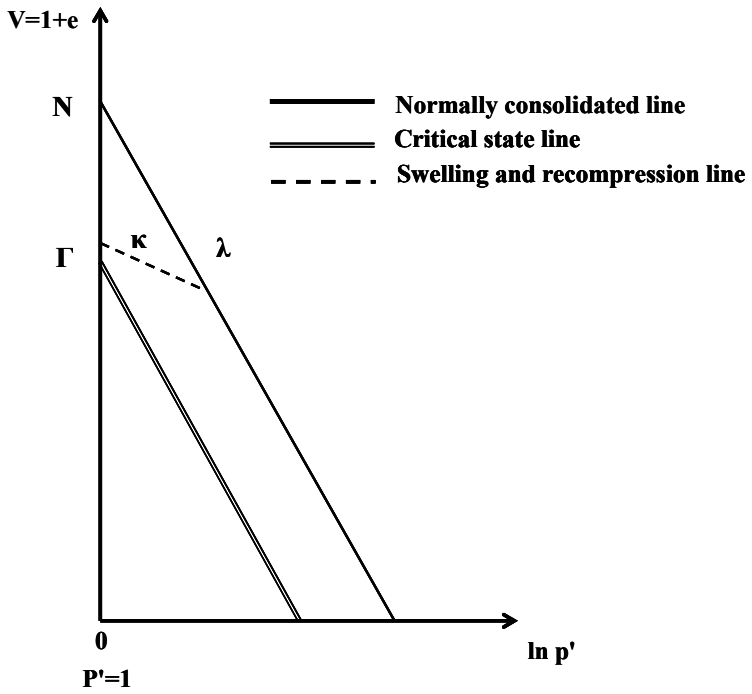

Figure 2.21: Critical state parameters in V-ln p' space.

At the core of CSSM was the creation of the constitutive model called Cam-clay based on the theory of plasticity and the prediction of the successive ductile yielding states of specimens on the wet side of critical state (Schofield and Wroth 1968). For the Cam-clay model, the parameters N, Γ, λ, and κ are related by the simple expression:

$$N - \Gamma = \lambda - \kappa \tag{2.30}$$

and therefore if three are known the fourth may be established. By performing isotropic consolidation and swelling tests in triaxial system on normally consolidated specimens and plotting V as a function of ln p' the parameters *N, Γ, λ*, and κ may be obtained. For the Cam-clay model:

$$\eta = \frac{q}{p'} = \frac{M}{\lambda - \kappa}(\Gamma + \lambda - \kappa) - \frac{M}{\lambda - \kappa} V_\lambda \tag{2.31}$$

$$V_\lambda = V + \lambda \ln p' \tag{2.32}$$

Therefore, by plotting η against V_λ, a straight line with slope of –M/(λ-κ) should be obtained. Since (λ-κ) is evaluated from the isotropic consolidation and swelling tests, M can then be determined.

2.11.4.2 State of soils

In the critical state framework, the state of soils is defined in a 3-D, mean effective normal stress (p'), shear stress (q) and void ratio or specific volume (V) space. Limits to stable states of yielding are defined by the state boundary surface in the 3-D, q-p'-V space. The 2-D representations of the normalized state boundary surface in the q/p'_{crit} - p/p'_{crit} (p'_{crit} : mean effective confining pressure at critical state) and V-ln p' spaces are as shown in Figure 2.22. Critical state soil mechanics divides the soil behavior

at limiting states into three distinct classes of failure; the limiting lines OA and OG (Figure 22a) indicate states of soils undergoing fractures or cracks; AB and GE indicate that Hvorslev's Coulomb faults on rupture planes; BD and ED indicate Cam-clay yield and fold of a sediment layer. Soil states on the crack surface result in the development of unstable fissures and cracks openings. Heavily overconsolidated clays and overcompacted sands at low confining stresses could reach this limiting state. Collapse similar to fracture on the dilative side can also exist on the contractive domain but outside the normal consolidation line (Figure 2.22b).

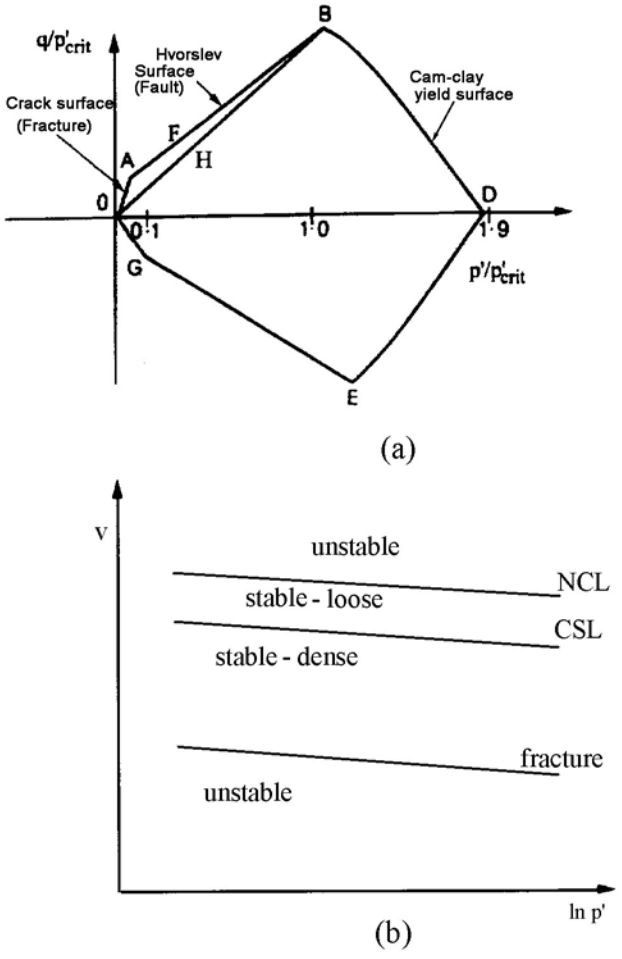

Figure 2.22: Limits of stable states of soils in (a) normalized q/p_{crit} - p/p_{cri}stress space stress (b) V– ln p' space (Pillai and Muhunthan 2002) (schematic).

Such states outside the stable yielding exist in wind deposited loose sands, air pluviated or moist-tamped sands and result abrupt collapse upon shearing of these materials (Pillai and Muhunthan 2001; Pillai and Muhunthan 2002). For sands and clayey silts of low plasticity, stable yield behavior occurs only within a narrow band on both the looser and denser side of the critical state line (Figure 2.22b).

The "no tension" or "limiting tensile strain" criteria are the most widely used among the alternative theories to quantify tensile fracture (Schofield 1980). For the triaxial specimen the no tension criterion with $\sigma'_3 = 0$ results in $p' = \sigma'_1/3$ or $q/p' = 3$ and leads to vertical split cracks which is the case of line OA. For horizontally spalling cracks, $\sigma'_1 = 0$ results in $p' = 2/3\ \sigma'_3$, $q = -\sigma'_3$, or $q/p' = 1.5$ which is the case of line OG. For clays or silty clays, Schofield (1980) had suggested that the change from rupture to tensile crack occurs at a pressure $p' = 0.1\ p'_c$, where p'_c is the effective confining stress at critical state.

When the effective stress path crosses the crack surface OA, the soil element begins to disintegrate into a clastic body and unstressed grains become free to slide apart. In that case the average specific volume of the clastic mass can increase (large voids/cracks) and consequently its permeability can increase significantly and instantly. A significant internal/external shear stress at low confining stresses can cause the crossover of the crack-surface OA and a large increase in specific volume. When such condition occurs, the opening within the soil body may be an extensive crack or a local pipe or channel.

2.11.4.3 Liquidity index, confining stress, and soil behavior

Critical state soil mechanics (Schofield and Wroth 1968) has shown that it is possible to generalize the density or specific volume axis by converting to a liquidity basis. It was further shown that the critical pressure is about 5 kPa at the liquid limit and 500 kPa at the plastic limit. In his Rankine lecture, Schofield (1980) mapped the remolded soil behavior on a liquidity against pressure diagram as shown in Figure 21 utilizing the hundred fold increase in pressure from the liquid limit critical state to the plastic limit critical state which is two log cycles, so the rupture band has half the width of PI and will intersect the line p' = 5 kPa at LI = 0.5. This intersection is a consequence of putting the lower limit of Coulomb rupture at $p/p_{crit} = 0.1$ (Schofield 1980). In the LI-p' space, clear boundaries exists that separate the regions of fracture, rupture, and ductile behavior. This is an independent and convenient approach to separate the states of fracture/rupture/ductile yield behavior of the soil using its index properties.

Considering a body of soil initially at LI = 0.5 and subjected to an elastic compression the map suggests at shallow depths where p' < 5kPa there may be cracks, but for depths where 5 kPa < p' < 50 kPa the soil will remain water-tight while deforming. In contrast a body of soil initially at LI = 0 will undergo fracture at depths for which p < 50 kPa or about 3 m of the overburden depth. In other words, the overburden depth should be larger than 3 m to ensure that deformation caused rupture planes (water tight) rather than open cracks. If LI = -0.25, the depth could be about 100 kPa or 6 m of depth.

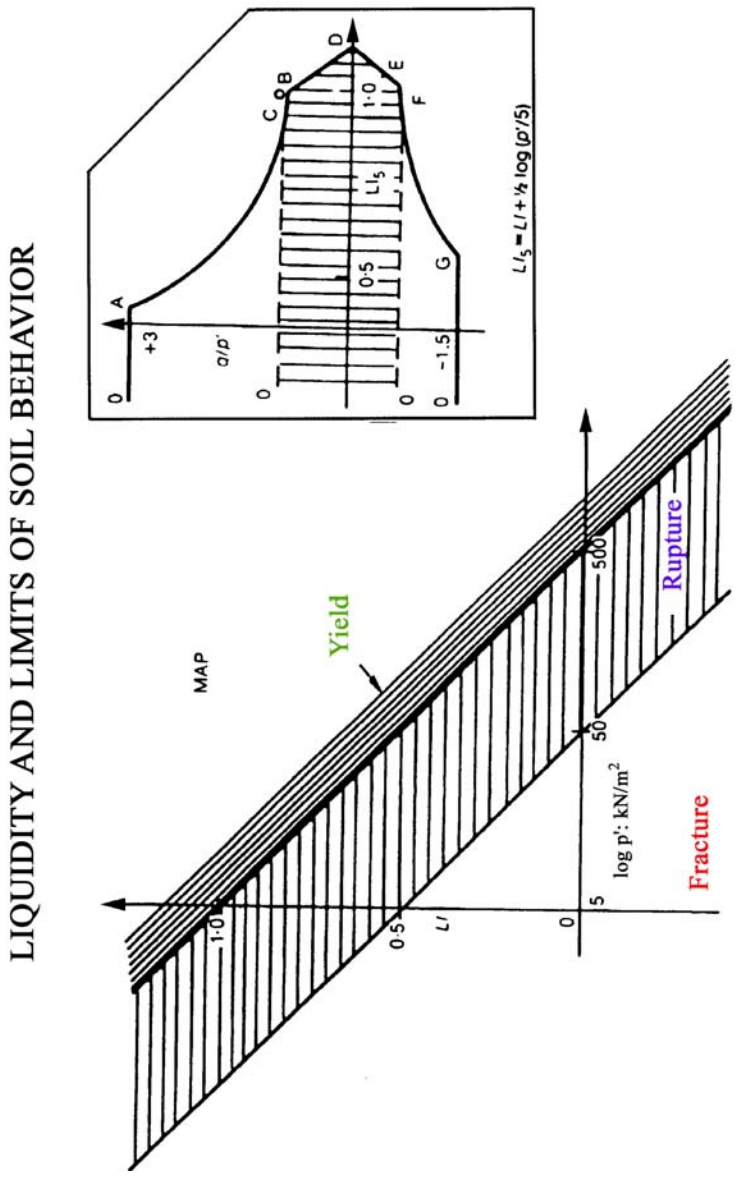

Figure 2.23: Liquidity and limits of soil behavior in LI-Log p' space (after Schofield 1980).

In order to identify the band of behavior in which various states of soil lie in the LI-p' space, Schofield (1980) defined their equivalent liquidities by projecting these states in the direction parallel to the critical state line towards the ordinate through p' = 5 kN/m^2. The equivalent liquidity LI_5 can be shown to be $LI_5 = LI+1/2 \log (p'/5)$ (Schofield

1980). Therefore, the equivalent liquidity equals liquidity as found in the ground plus a correction for stress. A value of LI_5 of less than 0.5 generally would indicate the fracture zone. Values of 0.5 to 1.0 represent the rupture zone. Values larger than 1.0 represent Cam-clay ductile zone.

The inset of Figure 2.23 shows the section of the behavior map at constant p'. Stress ratios q/p' will increase as equivalent liquidity falls. In the high equivalent liquidity range, stress ratio increases linearly as liquidity of Cam-clay falls. The Hvorslev's surface gives the rupture limits which allow higher stress ratios as lower values of p/p_{crit} are approached, but at the no tension limits, q/p' = 3 in compression, and –1.5 in extension. There is a general increase of limiting stress ratio as equivalent liquidity falls, but this is not a continuous change because there is a change of limiting behavior from continuous yield, to discrete rupture , to fracture of stiff fissured soil at equivalent liquidity below 0.5 (Schofield 1980).

The above concepts provide two independent approaches to analyze the cracking of soils. The first approach makes use of mechanical properties determined from triaxial tests and Oedometer tests to separate the three regions of soil behavior, the fractures, the faults, and the ductile yield. The second approach relies on index properties (plasticity index and liquidity index) to identify such regions. The analysis herein employed both approaches to complement each other.

CHAPTER THREE

EXPERIMENTAL METHODS

3.1 Materials

Soils from Palouse, Everett, and Aberdeen areas were collected for the study. Table 3.1, presents a summary of the geotechnical properties of these soils. The soil collected from Palouse area, known as Palouse loess, was a relatively homogeneous, unconsolidated, Eolian deposit, generally considered to have a glacio-fluvial origin (Jennings 1994). Loess is abundant in many places of the world. Figure 3.1, shows the loess distribution in North America.

Table 3.1: Geotechnical properties of Aberdeen, Everett, and Palouse soils.

Property	Aberdeen	Everett	Palouse	Standard method
USCS	ML	SP-SM	ML-CL	ASTM D 2487
Particle size analysis				ASTM D 422
Passing # 200 sieve, (%)	100	8.6	100	
Specific gravity	2.75	2.70	2.73	ASTM D 854
Liquid limit, (%)	54.2	32.5*	33.1	ASTM D 4318
Plastic limit, (%)	42.8	29.3*	19.6	ASTM D 4318
Plasticity index, (%)	11.4	3.2	13.6	ASTM D 4318
Maximum dry unit weight, (kN/m^3)	14.3	18.7	17.3	ASTM D 698
Optimum water content, (%)	27.0	9.7	17.0	ASTM D 698

* These values were obtained from material passing #200 sieve.

Glacial till collected from Everett, had glaciated at least seven times during the Quaternary Period by glaciers from British Columbia (Troost et al. 2003). Distribution of glacial till in the United States is shown in Figure 3.2. Soil collected from Aberdeen area was mainly an offshore marine deposit and consists of tuffaceous siltstone and tuffaceous fine-grained sand stone (Beikman et al. 1967). It is part of the Grays Harbor basin, known

as Lincoln Creek formation. Grays Harbor basin and Lincoln Creek formation are shown in Figures 3.3 and 3.4, respectively.

Figure 3.1: Loess distribution map in North America (United States Geological Survey).

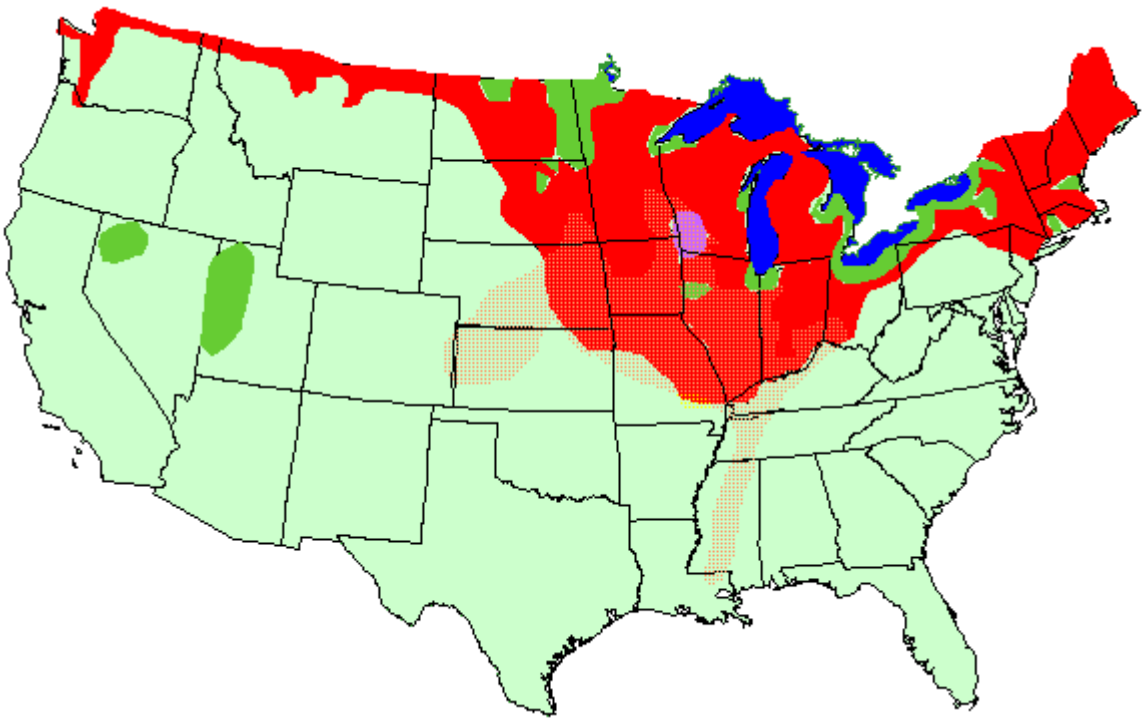

Figure 3.2: Glacial till distribution map (University of Florida).

Figure 3.3: Grays Harbor basin area (Beikman et al. 1967).

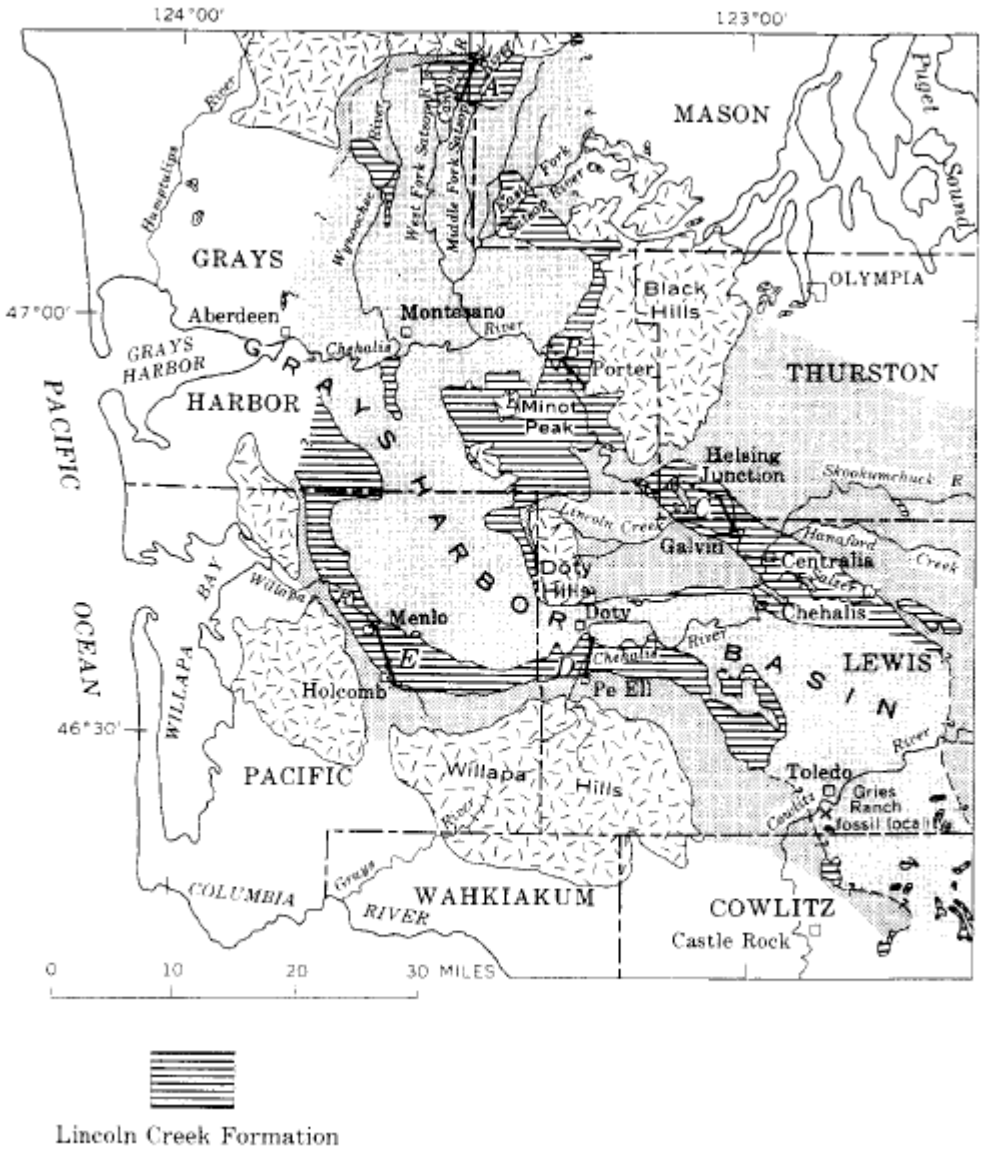

Figure 3.4: Distribution of Lincoln Creek formation in Grays Harbor basin (Beikman et al. 1967).

3.2 Testing program

In order to accomplish and clarify the objectives of this research, a series of soil mechanics laboratory tests including drying rate of soils, Atterberg limits using Casagrande and fall cone method, standard proctor (compaction), unconfined compressive strength, consolidated-undrained triaxial, and Oedometer (consolidation) tests were conducted on non-treated, as well as, cement treated soils.

3.2.1 Drying rate of the soils (solidification)

Solidification is the process that removes excess water from soil mass by hydration reaction induced by addition of stabilization agent (Bennert et al. 2000). This process was investigated by recording the reduction of moisture content of the material with time for addition of different cement content. The soils were first oven dried, water was added to bring them back to a certain water content. Different amounts of cement was added to the mixture, changes in water content were measured with time. Results are presented in a plot of water content versus time.

3.2.2 Atterberg limits, Casagrande method

Enhanced workability of materials has been shown to be associated with reduction in plasticity index (Baran et al. 2001; Mallela et al. 2004). A series of tests with different cement content were conducted to determine the effect of cement content on the Atterberg limits of Palouse and Aberdeen soils. Note that, since the Everett soil is sandy, plasticity limits were not considered. Tests were conducted 30 minutes after addition of cement according to ASTM D4318.

3.2.3 Atterberg limits, fall cone test (cone penetration)

The fall cone test is a method to determine the liquid limit of soils based on penetration of a standard cone (shape and mass) into the soils. It was originally developed as a technique to determine the undrained shear strength of remolded cohesive soils in Scandinavia (Koumoto and Houlsby 2001). Reliability of this technique to determine the liquid limit of soils is widely documented (Koumoto and Houlsby 2001; Sivapullaial and Sridharan 1985; Feng 2000). In the fall cone test (Figure 3.5), a cone with an apex angle of 30˚ and total mass of 80 grams is suspended above, but just in contact with the sample. The cone is permitted to fall freely for a period of 5 seconds. The water content corresponding to a cone penetration of 20 mm is defined by British Standard 1377 as the liquid limit (Head 1992).

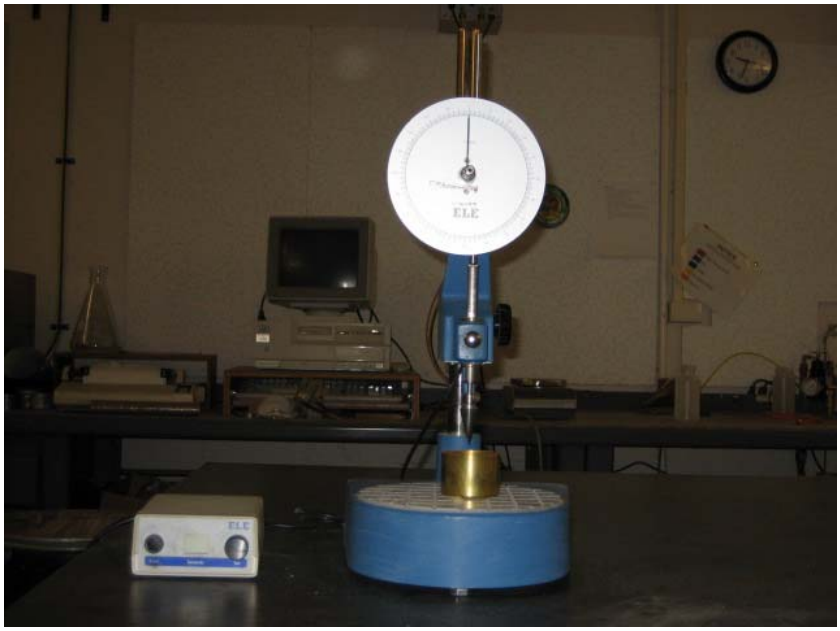

Figure 3.5: Fall cone (cone penetration) test apparatus.

Independently, Lawrence (1980) and Wasti (1987) used two cones with different masses to measure penetration, which can be associated to plasticity index. A typical result of fall cone test is shown in Figure 3.6. The plasticity index is determined by:

$$PI = \frac{(W_1 - W_2)Log100}{Log\left(\frac{M_2}{M_1}\right)} \tag{3.1}$$

Where,

W_1: Water content corresponding to 20mm penetration of M_1

W_2: Water content corresponding to 20mm penetration of M_2

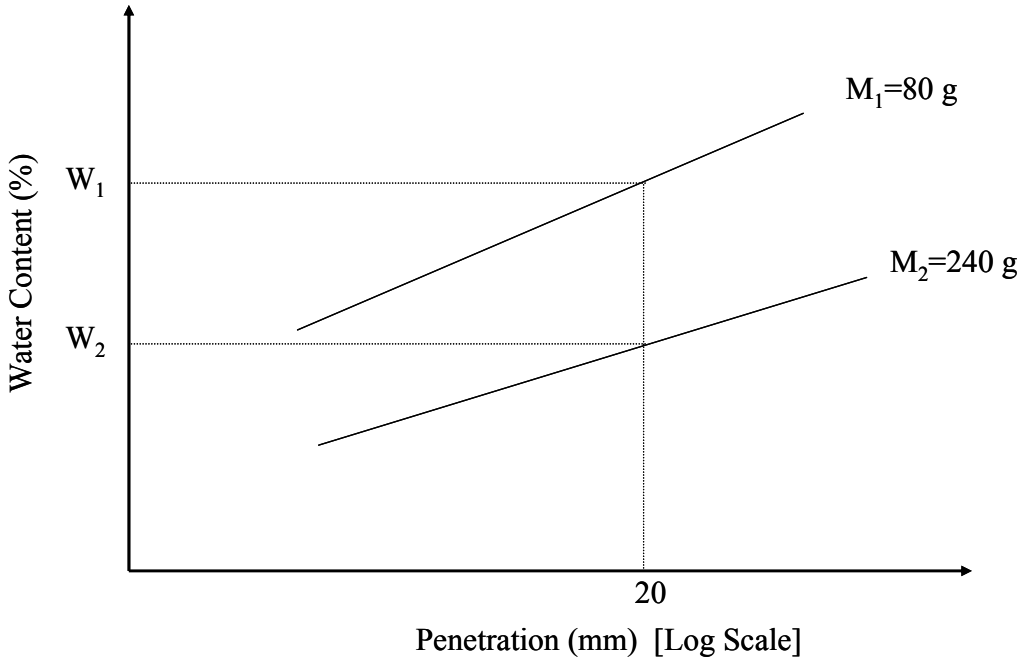

Figure 3.6: Schematic results of fall cone test.

In order to determine the effect of addition of cement on plasticity of Aberdeen soil, a series of fall cone tests on native soil and cement treated soil were conducted. For cement treated soils two sets of sample were prepared. One was tested half an hour after addition of cement and the other was tested after 7 days curing in an air tight container.

3.2.4 Standard proctor (compaction)

In order to investigate the effect of addition of cement on optimum water content and maximum dry unit weight of the selected soils, a series of standard proctor tests on non-treated and cement treated soils (2.5, 5, 7.5, and 10% cement content) were conducted according to ASTM D 698. Cement was added to oven dried soils and mixed until uniform color was observed before compaction. It must be noted that tests were completed in less than an hour.

3.2.5 Unconfined compressive strength

Despite its limitations on replicating conditions in the field, the unconfined compression test is one of the widely used laboratory tests in pavement application and soil stabilization application. The unconfined compression strength is often used as an index to quantify the improvement of soils due to treatment. For example, ASTM D 4609 (Standard guide for evaluating effectiveness of admixture for soil stabilization) states that an increase in unconfined compressive strength of 345 kPa (50 psi) or more must be achieved for a treatment to be considered effective. In addition, if specimens do not slake during immersion, the treatment may be effective; and if no significant strength is lost due to immersion, the treatment may be effective for waterproofing soils. Based on

ASTM D2166 suggestion (the largest particle diameter should be smaller than 1/6 mold diameter), particle sizes retained on sieve #6 were removed from the soils prior to performing the unconfined compression test. A series of unconfined compressive strength tests were conducted on the host soils as well as cement treated soils according to ASTM D2166 and ASTM D4609. Axial load increment was applied at a rate of 1% strain per minute.

3.2.5.1 Specimen preparation

Specimens were prepared at optimum water content and maximum dry density for each mixture (0, 2.5, 5, 7.5, and 10% cement content) by using the Harvard miniature apparatus. For each cement content, two sets of specimens were prepared. One set was tested after 7 days curing time in an air tight container with a wet sponge placed upon it. The other set was wrapped in a plastic sheet and placed in an air tight container with a wet sponge for seven days, then immersed in water for two days prior to testing (Figure 3.7a and 3.7b). Weights of the samples were measured before and after immersion in water.

(a) (b)

Figure 3.7: (a) Specimens during curing period, (b) Specimens being immersed in water.

3.2.6 Consolidated-Undrained triaxial

While unconfined compressive strength is widely used as an index in quantifying improvement, it is evident from the discussion in Chapter Two that soil behavior is controlled by confining pressure. In order to examine the strength behavior in detail, a series of consolidated-undrained (CU) triaxial tests with pore pressure measurements were conducted. This information is required for evaluating the suitability of treated material for construction of embankments. Confining pressures were varied from 0 to 600 kPa. The latter simulates the effect of a 30 m height embankment confining pressures.

3.2.6.1 Specimen Preparation

Everett and Aberdeen soils were used in this part of the study. Consolidated-undrained triaxial test were conducted on host soils as well as cement treated soils. The dry material was mixed with cement thoroughly until a uniform color was observed. Formation of clumps was avoided when water was added to soil cement mixture. Samples were prepared at optimum water content and maximum dry density. In order to prepare compacted specimens compatible with the triaxial machine at our laboratory and minimize sample disturbance prior to loading, a split mold was custom-built (Figure 3.8). The diameter and height of the mold were 7 cm and 16.4 cm, respectively. However for Aberdeen soil splitting the mold without disturbing the sample was not possible, therefore a sample extruder was used to extrude the compacted specimens. After the material was placed in the mold standard proctor hammer was used to compact the soil in five equal layers to achieve target density. The mixing and compaction was completed within an hour. Specimens were cured for seven days. Cement treated samples were kept

for a day in an air tight container with a wet sponge in it, after that with the intention of help saturation samples were immersed in water for six days prior to testing. It must be noted that unconfined compressive strength samples in this part of the study were prepared similar to triaxial specimens.

Figure 3.8: Custom built mold for triaxial test.

3.2.6.2 Saturation

Cured specimens were set on the base of the triaxial chamber, a filter paper and pre-boiled porous stone were placed between the base and bottom of the sample and between the cap and top of it. A rubber membrane was used to seal the specimen from the chamber around it and secured with O rings at the cap and the base. Chamber was assembled, filled with water and small confining pressure (40 kPa) was applied, then CO_2 was percolated from bottom to top for 2-3 minutes to expedite displacement of the air.

Air bubbles were forced out of the system by injecting de-aired water in to the tubes. De-aired water was allowed to percolate from bottom to top of the sample under a small gradient (5 kPa). Percolation was continued until amount of the water flowing into

the sample was equal to amount water flowing out of the sample. The sample was then saturated by applying back pressure.

Skempton's pore pressure parameter $B = \frac{\Delta u}{\Delta \sigma_3}$ was determined by measuring the corresponding pore pressure increase due to increase in cell pressure. Saturation process was continued until achieved B value for non-treated and cement treated Everett soil were 0.95 and 0.7, respectively and for non-treated and cement treated Aberdeen soil were 0.9.

Skempton's B parameter can be shown to be equal to (Holtz and Kovacs 2004):

$$B = \frac{1}{1 + \frac{nC_s}{C_{sk}}} \tag{3.2}$$

Where,

n: Porosity

C_s: Compressibility of the voids

C_{sk}: Compressibility of soil skeleton

Therefore, the B values are dependent on the compressibility of soils. Since cement treatment decreases the compressibility of soils significantly, the corresponding B values are much smaller to begin with. Thus, achieving B value of unity is almost impossible.

Results of an extensive study by Black and Lee (1973) are shown in Figure 3.9 (see also Table 3.2). It is seen that while B value of unity ensures complete saturation, a value of B around 0.7 or higher tends to achieve saturation percentages well above 95% for most of soils. Thus, it is deemed the saturation achieved in all specimens is sufficient to ensure that the results are not affected much by the presence of air voids.

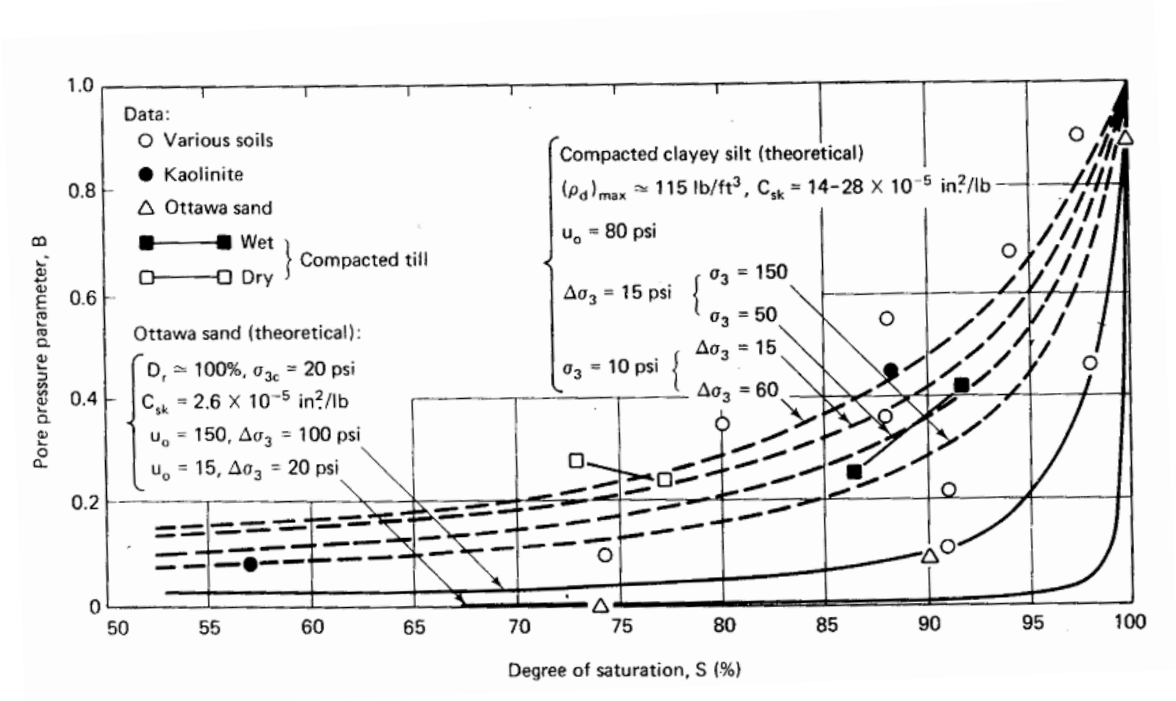

Figure 3.9: Relationship between pore pressure parameter B and degree of saturation, (Black and Lee 1973).

Table 3.2: B values for different soils at complete or nearly complete saturation (Black and Lee 1973).

Soil type	Saturation		
	100%	99.5%	99%
Soft normally consolidated clays	0.9998	0.9920	0.9860
Medium (compacted clays)	0.9988	0.9630	0.9390
Stiff (Stiff clays-sands)	0.9877	0.6900	0.5100
Very stiff (very high consolidated pressure)	0.9130	0.2000	0.1000

3.2.6.3 Consolidation and shearing

Specimens were consolidated at different cell pressures. Consolidation was continued until the height of water in burettes (on triaxial panels) did not rise. Once consolidation was completed, samples were sheared at a deformation rate of 0.5 mm per minute (strain controlled). Pore pressure changes during shearing were recorded.

3.2.7 Oedometer test (consolidation)

In order to determine the effect of addition of cement on consolidation parameters of Aberdeen soil, series of Oedometer tests on host soil as well as cement treated soils were conducted. Specimens were prepared similar to triaxial test, then trimmed to fit into the Oedometer ring. Non-treated and cement treated specimens were immersed in water three days and six days prior to testing.

CHAPTER FOUR

RESULTS AND DISCUSSION

4.1 Introduction

This chapter presents the results of laboratory tests on host as well as cement treated soils and a discussion on their relevance to practice. The tests include, grain size analysis, drying rate (solidification), Atterberg limits, compaction characteristics, unconfined compressive strength, consolidated-undrained triaxial, and Oedometer. The applicability and limitations of the different failure criteria including Mohr-Coulomb, Griffith, modified Griffith, and Johnston's are also discussed.

4.2 Grain size analysis

The grain size distribution of the soils is shown in Figure 4.1. It is seen that Everett soil is coarse-grained whereas Aberdeen and Palouse soils are fine-grained.

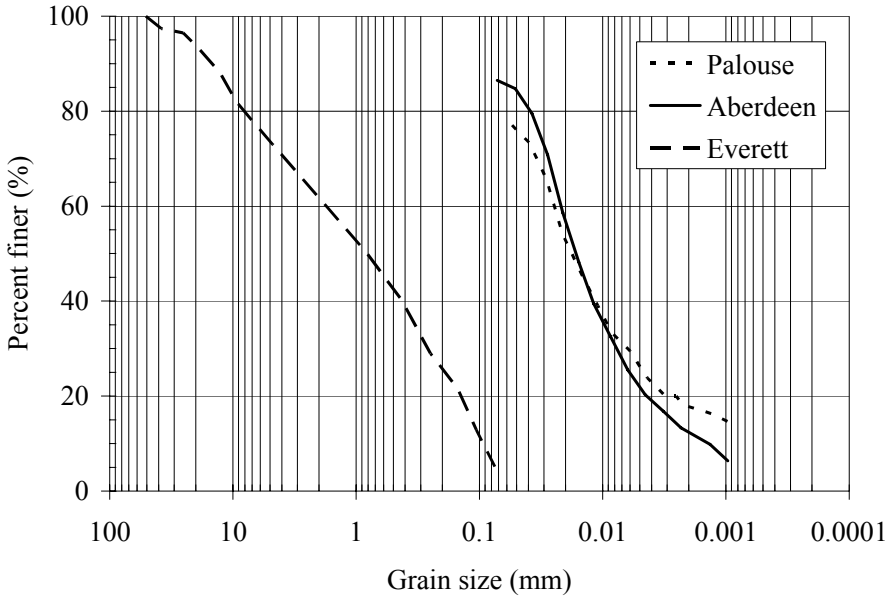

Figure 4.1: Grain size distribution of the soils

4.3 Solidification

The effect of cement treatment on the solidification characteristics of Aberdeen, Everett, and Palouse soils in the laboratory is as shown in Figures 4.2, 4.3, and 4.4, respectively. These observations were made at room temperature (24˚C) for conditions of different cement contents. It can be observed that addition of cement leads to significant reduction in water content of the soils. Initial drying rate increased with cement content, soils displayed nearly equal drying rate after 30 minutes of addition of cement. The results also show that mixed soils could lose significant amount of water depending on the type of soils. This will facilitate the compaction of soils wet of optimum that are often encountered in west of Washington state. However, it is necessary to perform compaction within the first few minutes to avoid loss of large amount of water.

Use of a drying rate curve as has been done here in the laboratory would facilitate contractors with the choice of appropriate mixing time to achieve a given reduction of water content in practice. In addition, it is suggested that allowance be made for prevailing atmospheric and site conditions on the drying rate for field applications.

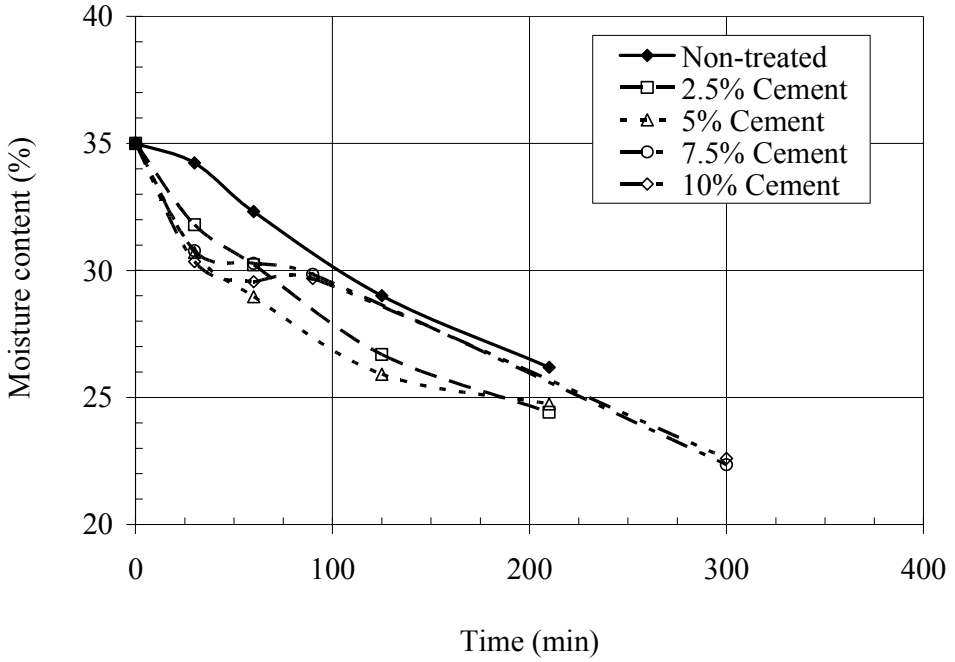

Figure 4.2: Solidification characteristics of Aberdeen soil.

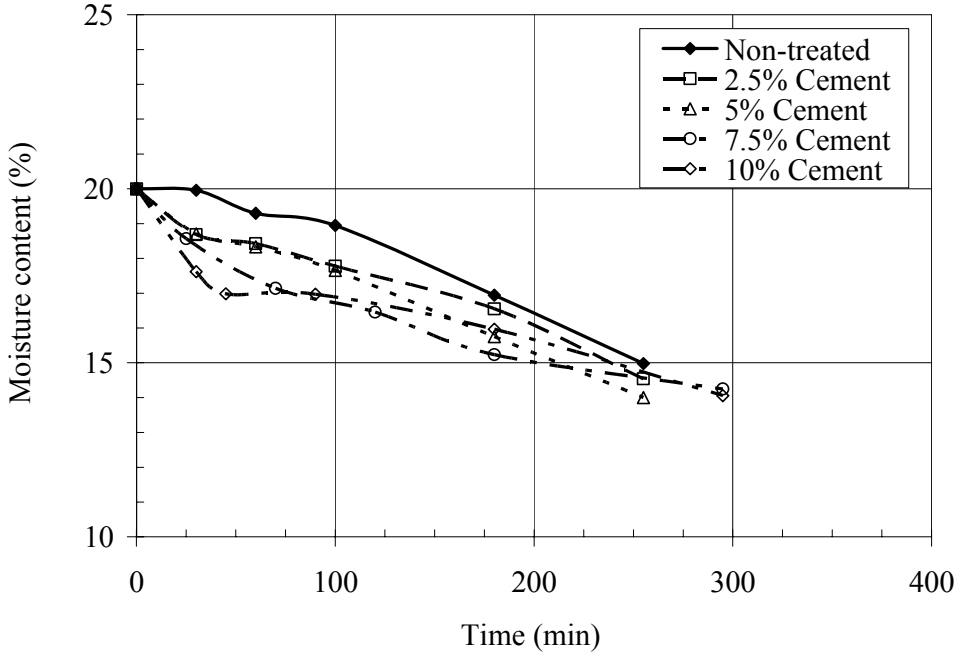

Figure 4.3: Solidification characteristics of Everett soil.

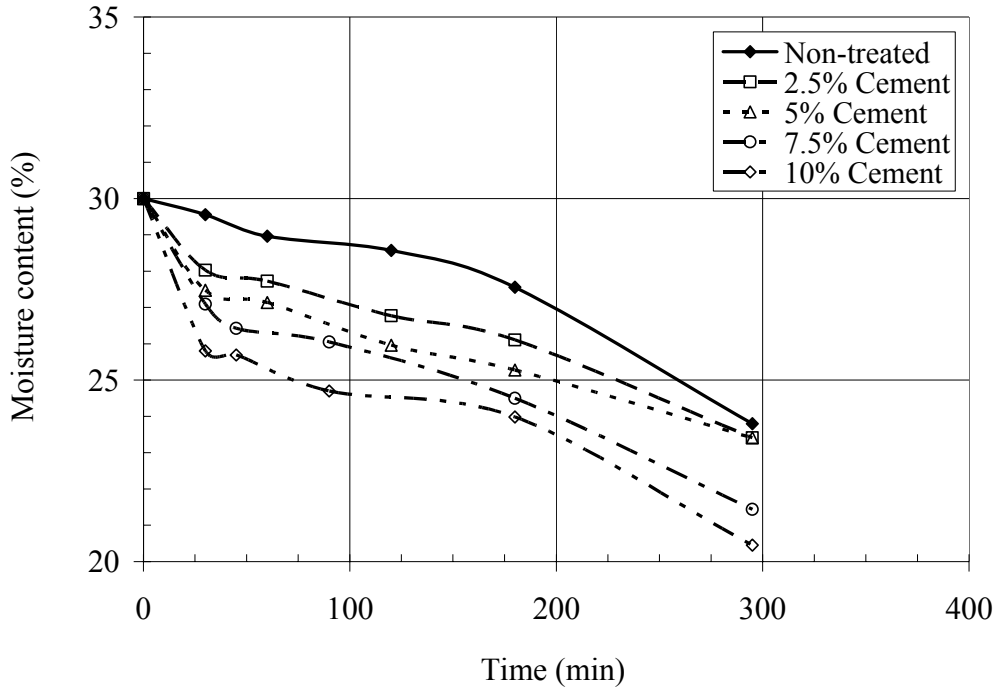

Figure 4.4: Solidification characteristics of Palouse loess.

4.4 Atterberg limits

The results of Atterberg limits test using Casagrande and fall cone method for Aberdeen soil is as shown in Table 4.1. Note that fall cone tests were performed 30 minutes and seven days after addition of cement. As observed in the past by some investigators (Wasti 1987), it is seen that the results of Casagrande and fall cone do not match well.

Table 4.1: Atterberg limits for Aberdeen soil using Casagrande and fall cone method for different cement content.

	Casagrande method			Fall cone test					
	LL (%)	PL(%)	PI(%)	LL (%)		PL (%)		PI (%)	
	30 min	30 min	30 min	30 min	7 days	30min	7 days	30 min	7 days
Non-treated	54	42.8	11.4	60.6		53		7.6	
2.5% Cement content	56.4	41.8	14.6	NP	NP	NP	NP	NP	NP
5.0% Cement content	54.9	44.8	10.1	67.2	57.2	58.1	50.9	9.1	6.3
7.5% Cement content	54.1	45.7	8.4	NP	NP	NP	NP	NP	NP
10% Cement content	53.1	46.9	6.2	66.6	61.5	57.1	56.4	9.5	5.1

NP: Not performd.

Since the Casagrande method is widely used in North America, the effect of cement addition on Atterberg limits discussed here based on it from this point onwards. Variation of liquid and plastic limits for different cement content for Aberdeen soil is shown in Figure 4.5. It can be seen that liquid limit increased slightly (initially) and decreased with increasing in cement content, while plastic limit remained relatively constant. Consequently the plasticity index increased initially followed by a decrease with increase in cement content.

Variation of liquid limit and plastic limit for Palouse loess for different cement content is shown in Figure 4.6. It can be seen that liquid limit increased initially and decreased gradually as cement content increased. Plastic limit increased initially and remained relatively constant with increasing in cement content. Therefore plasticity index increased initially and decreased as cement content increased.

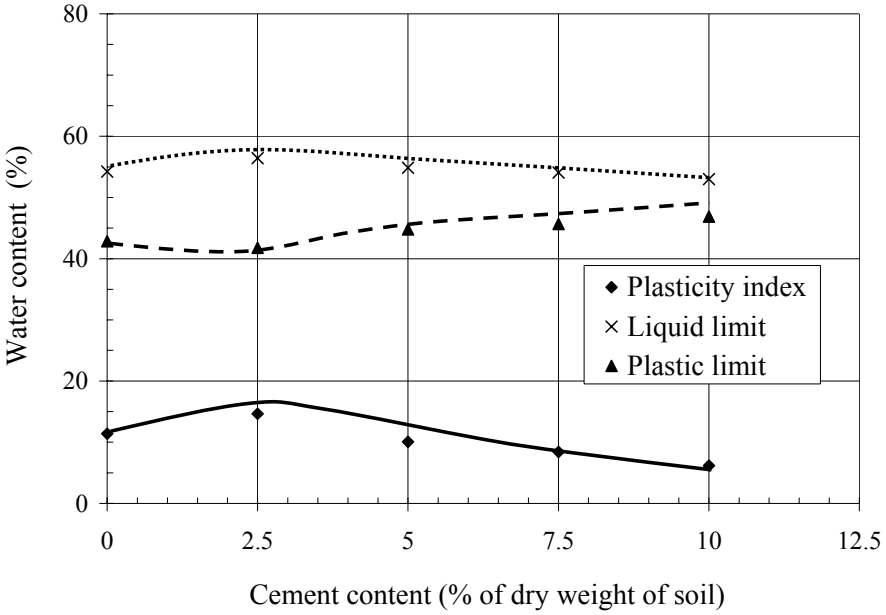

Figure 4.5: Variation of plastic behavior of Aberdeen soil for different cement content

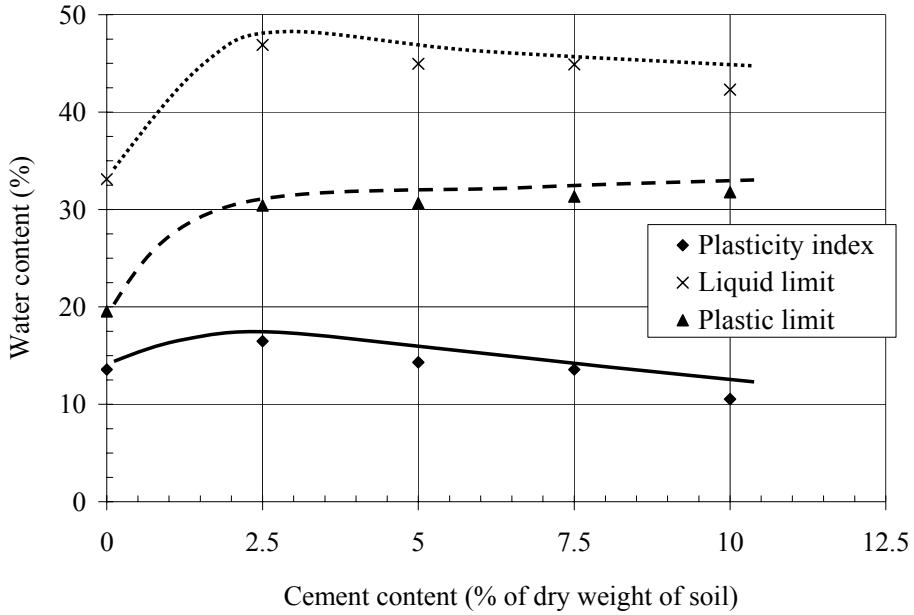

Figure 4.6: Variation of plastic behavior of Palouse loess for different cement content

4.5 Compaction characteristics

The effect of cement treatment on optimum water content and maximum dry unit weight of soils were determined from standard compaction tests and are as shown in Figures 4.7 and 4.8, respectively. It can be observed, generally, as cement content increased, optimum water content increased whereas maximum dry unit weight decreased. It can also be seen that, changes in compaction characteristics are significant at lower percentages of cement content. However at higher percentages of cement, the changes in compaction characteristics of treated soils are minimal.

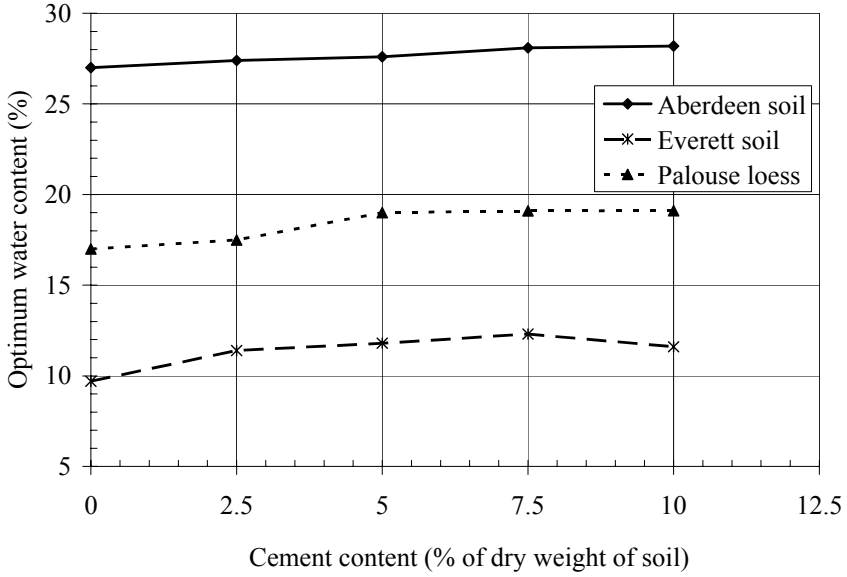

Figure 4.7: Effect of cement treatment on optimum water content of the soils.

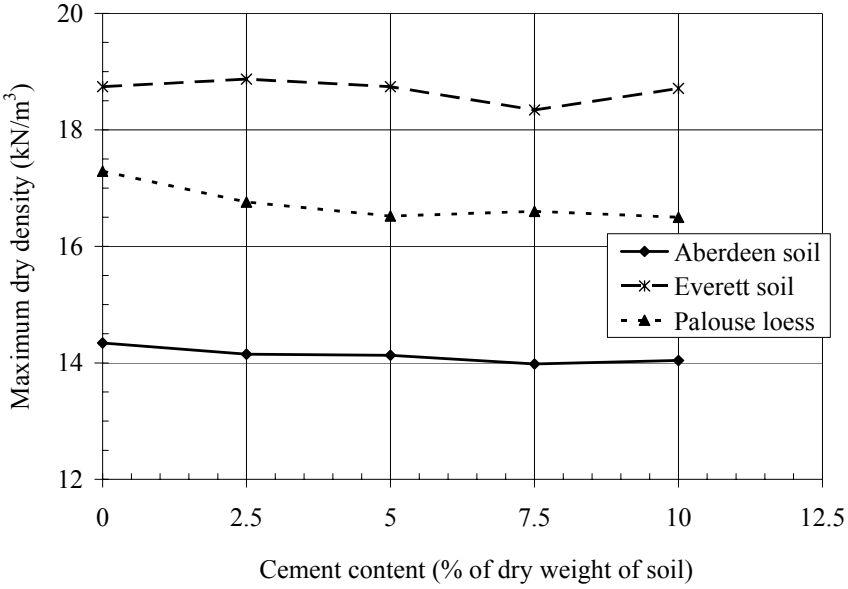

Figure 4.8: Effect of cement treatment on maximum dry density of the soils.

4.6 Unconfined compressive strength

4.6.1 Aberdeen soil

The effect of cement treatment on unconfined stress-strain behavior of Aberdeen soil for unsoaked and soaked samples is shown in Figures 4.9 and 4.10, respectively. It is observed that the peak axial stress increased significantly due to cement treatment, but the corresponding strain to peak axial stress decreased from approximately 4% to slightly greater than 1%. Thus, cement treated soils exhibited much more brittle behavior than non-treated soils. It is noted that non-treated specimens and those with 2.5% cement content disintegrated after being immersed in water (Figure 4.11).

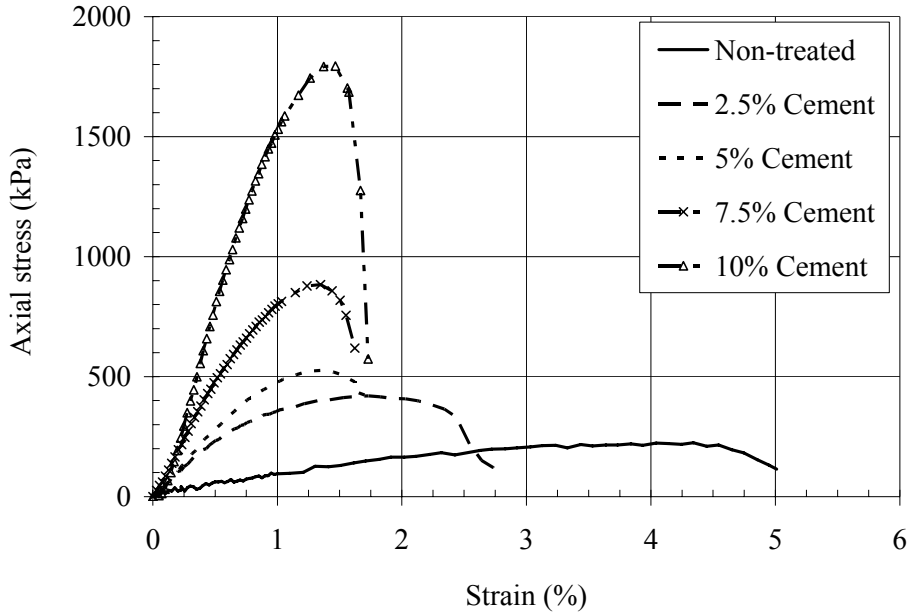

Figure 4.9: Effect of cement treatment on unconfined stress-strain behavior of Aberdeen soil, unsoaked samples.

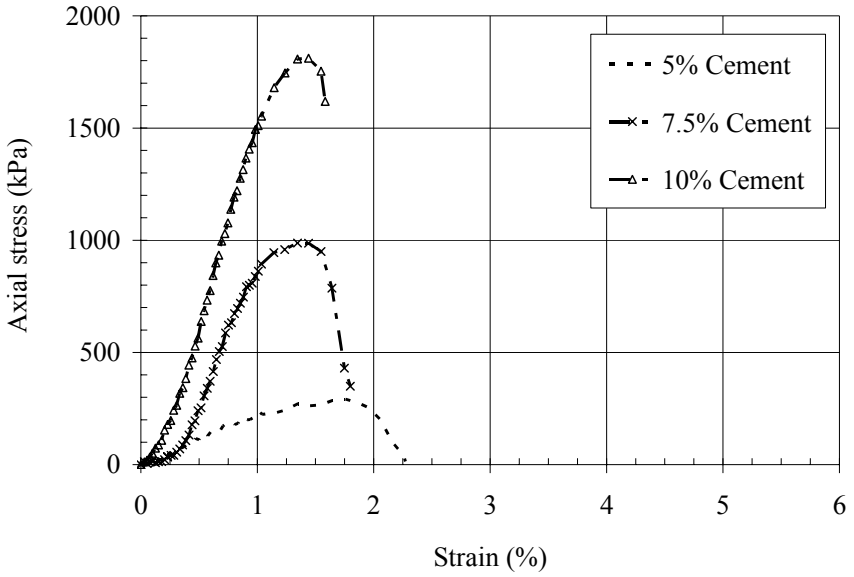

Figure 4.10: Effect of cement treatment on unconfined stress-strain behavior of Aberdeen soil, soaked samples.

Figure 4.11: Disintegration of specimens after being immersed in water.

The effect of addition of cement on unconfined compressive strength of Aberdeen soil is shown in Figure 4.12, for unsoaked and soaked samples. It can be observed that cement treatment leads to significant increase in unconfined compressive strength especially for cement contents greater than 5%. Surprisingly, soaked samples with 7.5% and 10% cement content exhibited greater unconfined compressive strength compared with unsoaked samples. Figure 4.13, shows the effect of cement treatment on modulus of elasticity at 30% of peak axial stress for soaked and unsoaked samples. It can be observed that modulus of elasticity increased significantly with cement content.

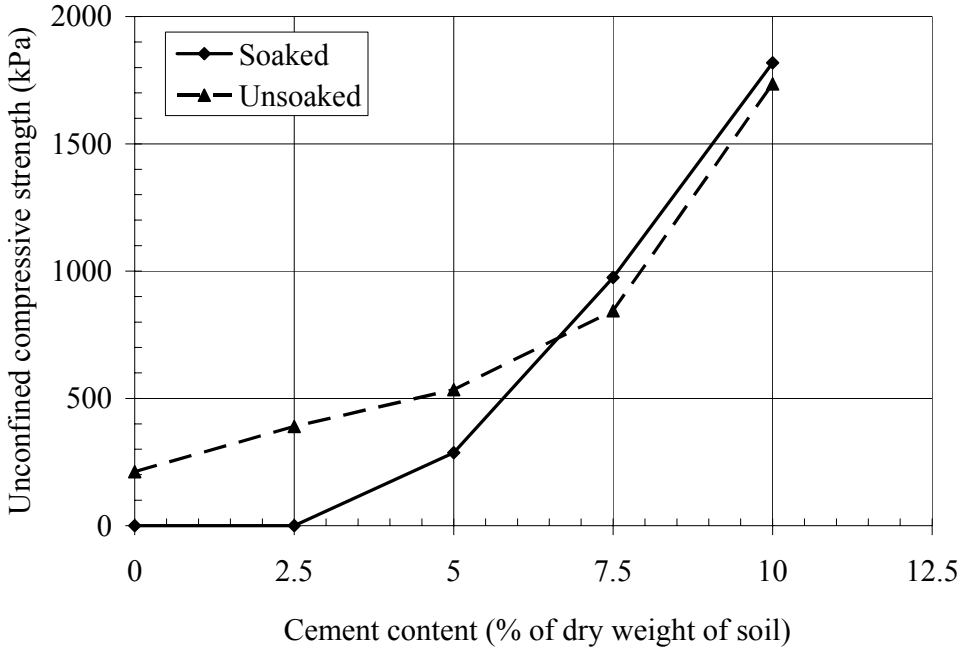

Figure 4.12: Effect of cement treatment on unconfined compressive strength of Aberdeen soil.

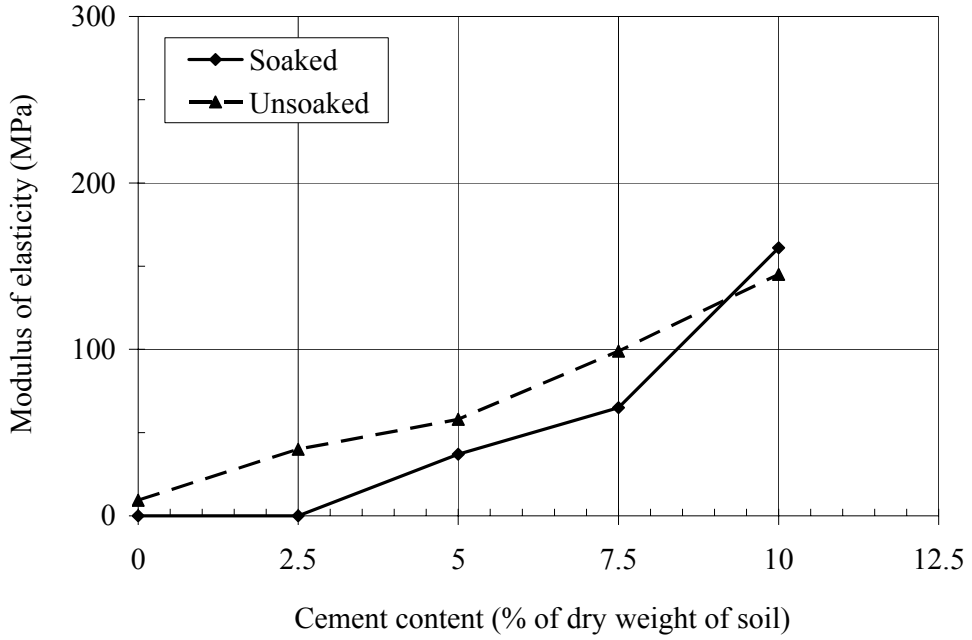

Figure 4.13: Effect of cement treatment on modulus of elasticity of Aberdeen soil.

4.6.2 Everett soil

The effect of cement treatment on unconfined stress-strain behavior of Everett soil for unsoaked and soaked samples are shown in Figures 4.14 and 4.15, respectively. It is observed that, cement treatment led to significant increase in peak axial stress, but corresponding strain to peak axial stress decreased slightly. Therefore treated soils exhibited more brittle behavior compared with non-treated soils. Non-treated specimens disintegrated after being immersed in water. The effect of cement treatment on unconfined compressive strength and modulus of elasticity at strain corresponding to 30% of peak axial stress are shown in Figures 4.16 and 4.17, respectively.

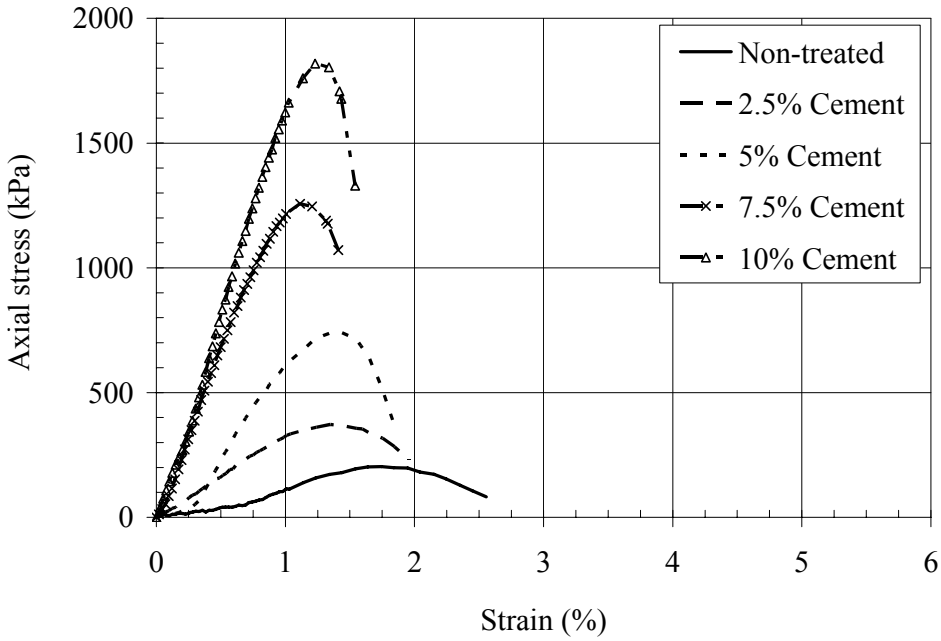

Figure 4.14: Effect of cement treatment on unconfined stress-strain behavior of Everett soil for unsoaked samples.

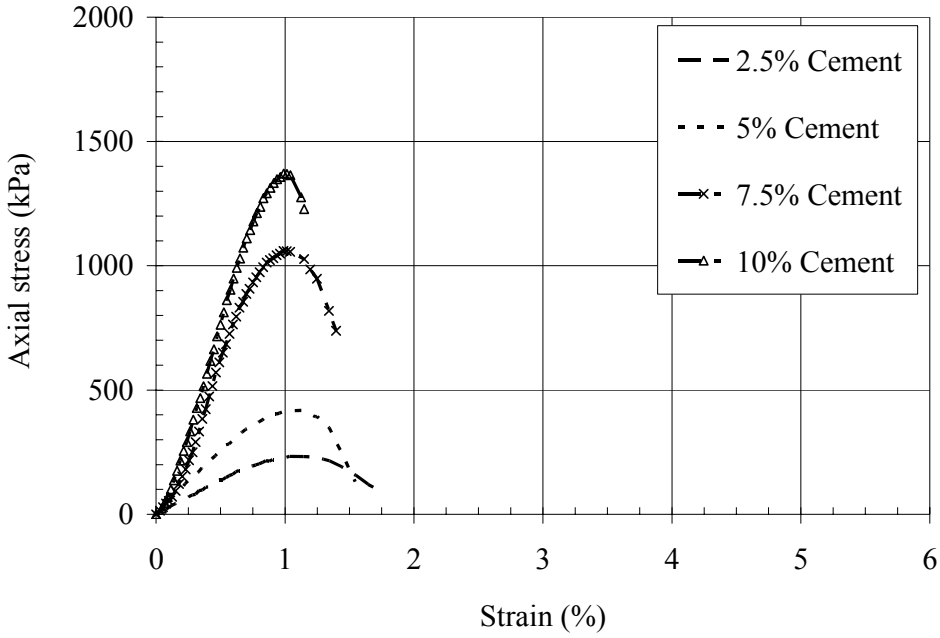

Figure 4.15: Effect of cement treatment on unconfined stress-strain behavior of Everett soil for soaked samples.

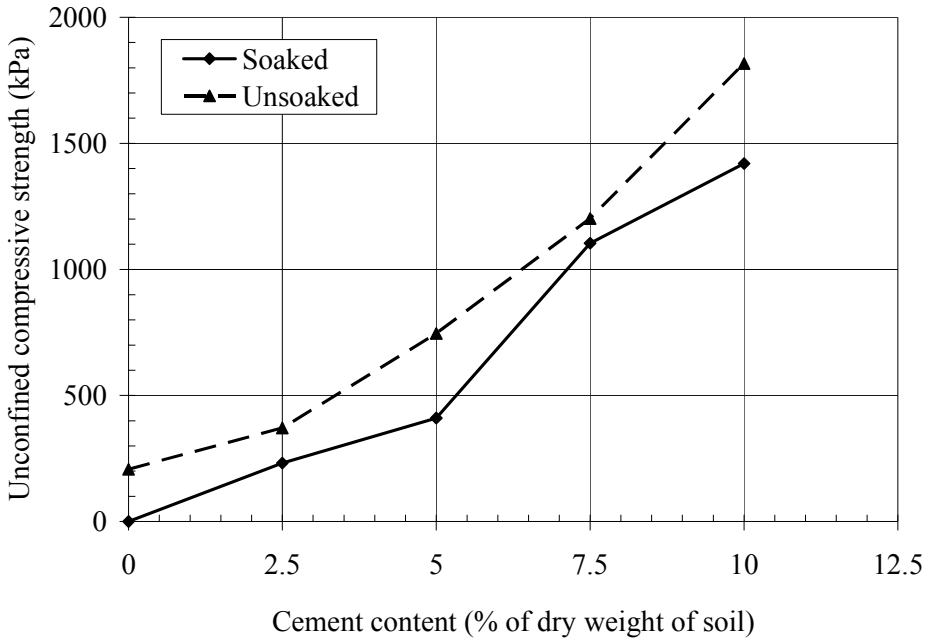

Figure 4.16: Effect of cement treatment on unconfined compressive strength of Everett soil.

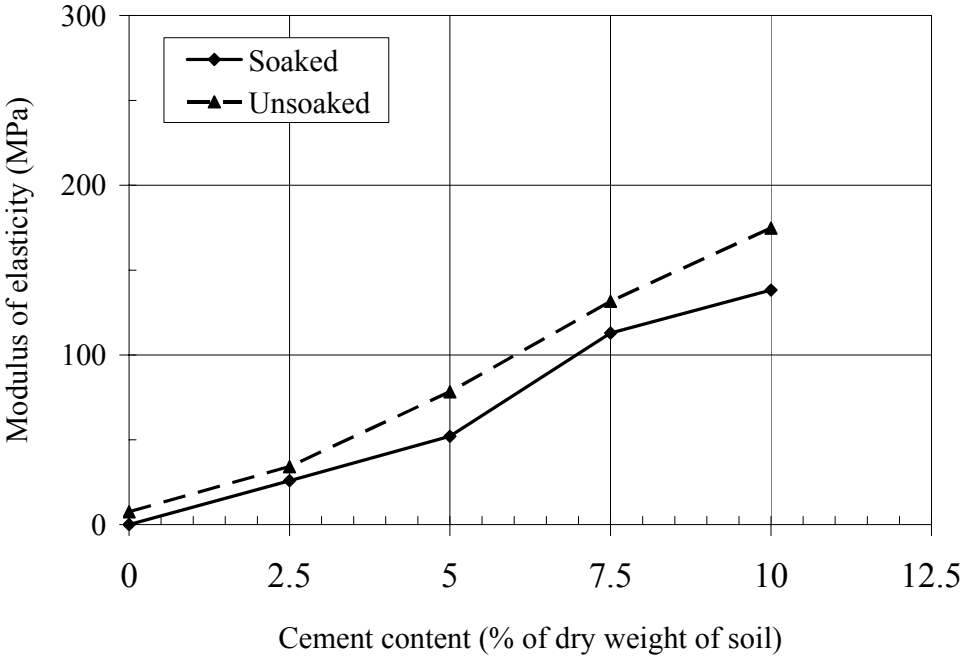

Figure 4.17: Effect of cement treatment on modulus of elasticity of Everett soil.

It can be observed that cement treatment resulted in significant increase in unconfined compressive strength and modulus of elasticity. It is noted that, unsoaked samples exhibited significant greater unconfined compressive strength compared with soaked samples.

4.6.3 Palouse loess

The effect of cement treatment on unconfined stress-strain behavior of Palouse loess for unsoaked and soaked samples are shown in Figures 4.18 and 4.19, respectively. It is observed that, peak axial stress increased significantly due to cement treatment, but corresponding strain to peak axial stress decreased from approximately 5% to slightly greater than 1%. Thus, cement treated soils exhibited much more brittle behavior compared with non-treated soils. As with the other soils, non-treated specimens of Palouse loess disintegrated after being immersed in water.

The effect of cement treatment on unconfined compressive strength and modulus of elasticity at strain corresponding to 30% of peak axial stress is shown in Figures 4.20 and 4.21, respectively. It can be observed that cement treatment resulted in significant increase in unconfined compressive strength and modulus of elasticity of Palouse loess.

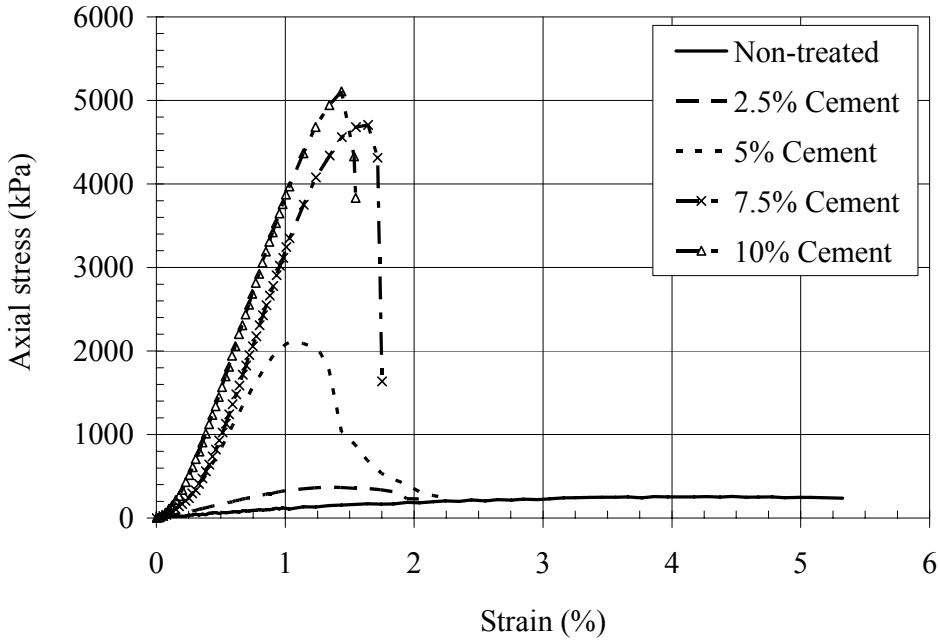

Figure 4.18: Effect of cement treatment on unconfined stress-strain behavior of Palouse loess for unsoaked samples.

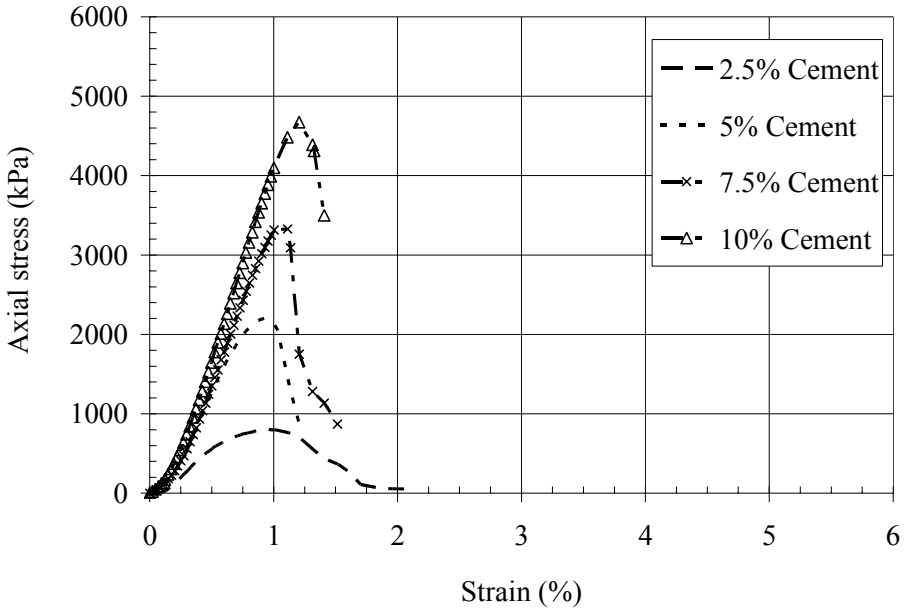

Figure 4.19: Effect of cement treatment on unconfined stress-strain behavior of Palouse loess for soaked samples.

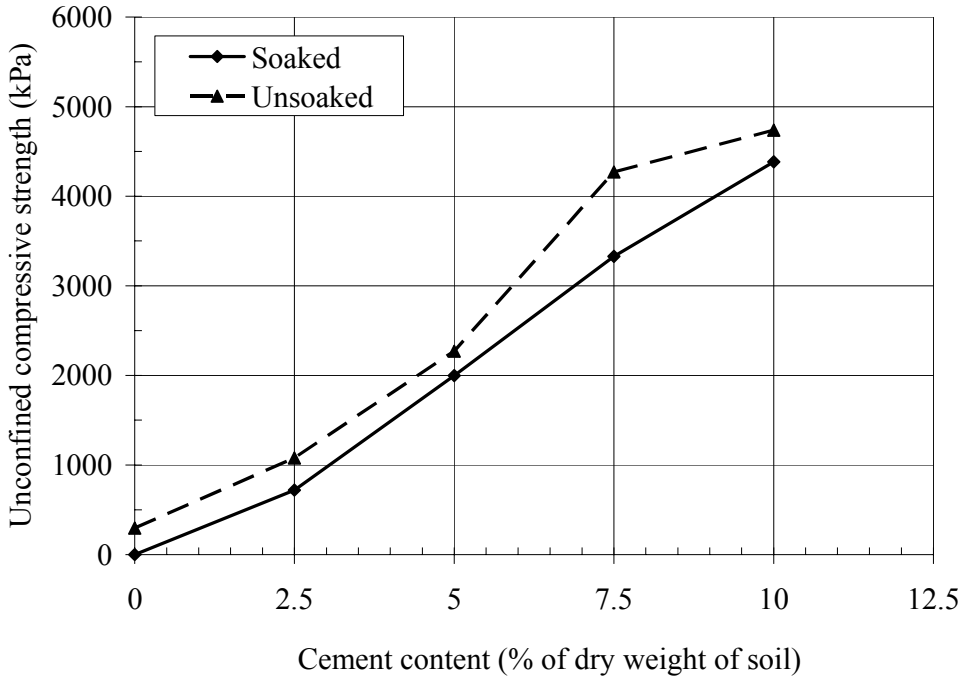

Figure 4.20: Effect of cement treatment on unconfined compressive strength of Palouse loess.

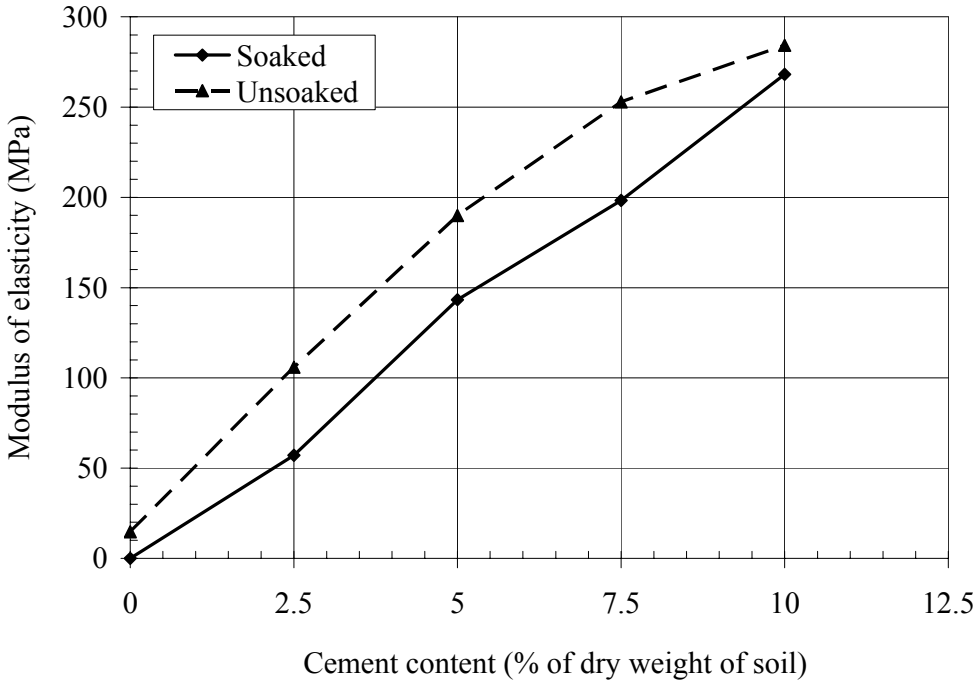

Figure 4.21: Effect of cement treatment on modulus of elasticity of Palouse loess.

A summary of unconfined compressive strength and modulus of elasticity of the soils, for unsoaked and soaked conditions, is given in Table 4.2. It can be seen that addition of small percentages of cement led to significant improvement in unconfined compressive strength of Palouse loess, whereas higher percentages of cement were needed to improve Aberdeen and Everett soils. Note that Palouse loess and Aberdeen soil had nearly the same grain size distribution yet their unconfined compressive strength varied with cement addition. For comparison purposes, a summary of the variation of mean unconfined compressive strength of different types of cement treated soils as reported by Kasama et al. (2007) is presented in Table 4.3. It can be seen that in general sandy and clay soils attained the maximum unconfined compressive strength (see also Mitchell 1976). Since Everett soil is coarse-grained it was expected to exhibit higher strength compared with Palouse and Aberdeen soils. However, this was not the case here.

Table 4.2: Summary of unconfined compressive strength and modulus of elasticity of non-treated and cement treated soils.

Soils	Cement content (%)	Unconfined compressive strength (kPa)		Modulus of elasticity (Mpa)	
		Unsoaked	Soaked	Unsoaked	Soaked
Aberdeen	0	211.7	0	9.33	0
	2.5	389.3	0	40	0
	5	534.3	286.4	58	37
	7.5	843.8	975	99	65
	10	1735.4	1818	145.1	161
Everett	0	206.9	0	7.55	0
	2.5	371.1	231.8	34.2	25.9
	5	746.3	410.4	78.35	52
	7.5	1202.3	1104	131.7	112.9
	10	1816.6	1420.1	174.8	134.2
Palouse	12.5	294.3	0	14.76	0
	15	1077	719.1	105.9	57.1
	17.5	2270.2	1997	190	143.3
	20	4270.1	3328.3	253	198.3
	22.5	4736.7	4383.1	284.2	268.2

Table 4.3: Mean value of unconfined compressive strength of different soils modified from Kasama et al. (2007).

Soil type		Mean (Mpa)
Gravel		1.58
Sandy soil		4.77
Cohesive soil	Silt	1.92
	Clay	4.72
	Unknown	2.92
Organic soil		1.15
Volcanic soil	Kanto laom	1.86
	Kuroboku	0.26
	Other	0.63
Waste		3.49
Unusual soil	Masado	10.74
	Peat	0.43
	Diatom soil	3.24

4.7 Consolidated-undrained triaxial

4.7.1 Aberdeen soil

Figures 4.22 to 4.27 show the deviator stress (q) and pore pressure versus axial strain increment for non-treated and cement treated Aberdeen soil for different confining pressures. It is observed that deviator stress increased with increasing in confining pressure. The increase was significant with the addition of cement. The stress strain and pore pressure response of non-treated soil is typical of ductile material behavior. This was also reflected in the bulging of the specimens nearing failure (Figure 4.28). Addition of 5% cement resulted in the soils attaining a peak deviator stress at about 2% strain increment and progressive softening afterwards. These cement treated specimens failed

with either single or double shear band as shown in Figure 4.29. Slight negative pore pressure was developed during shearing of non-treated and 5% cement treated at low confining pressures. It is noted in the case of 10% cement treated soil pore pressures raised up to almost confining pressure at very low strain (1%). As a result, the effective confining pressure dropped to near zero. This suggests split failure of the specimen with cracks transferring pressures immediately to the pore water resulting in such dramatic increase. Figure 4.30 shows the failed specimen with split crack.

Sangrey (1972) and Pillai and Muhunthan (1999) have reported split cracks in naturally cemented soils. They described that as a result of breakage of cemented bonds resulting in a significant amount of free water. This causes a large immediate build-up of pore pressure equal to confining pressure. Therefore it appears while higher percentages of cement results in higher peak strength, there is a danger of such specimens failing dramatically at very low strains during undrained loading negating the beneficial effect of cement treatment.

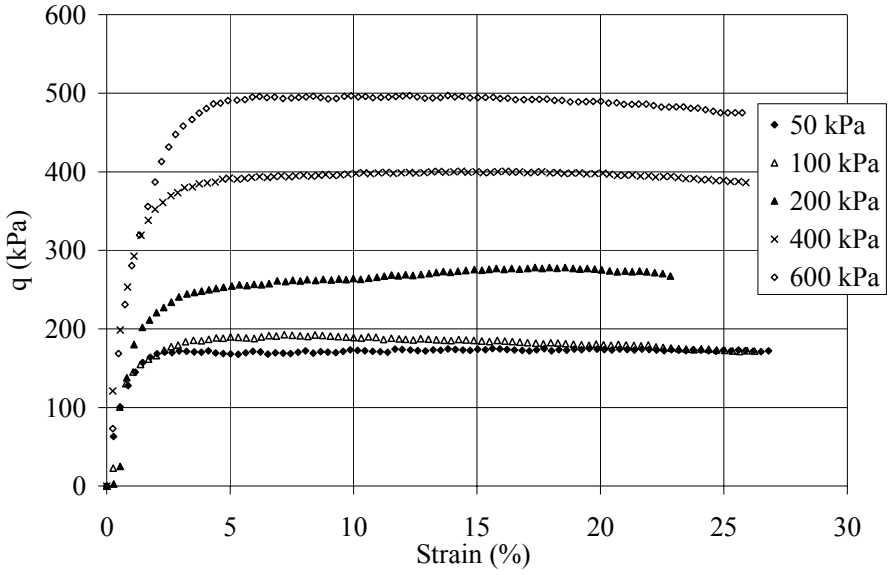

Figure 4.22: Deviator stress versus axial strain increment for non-treated Aberdeen soil.

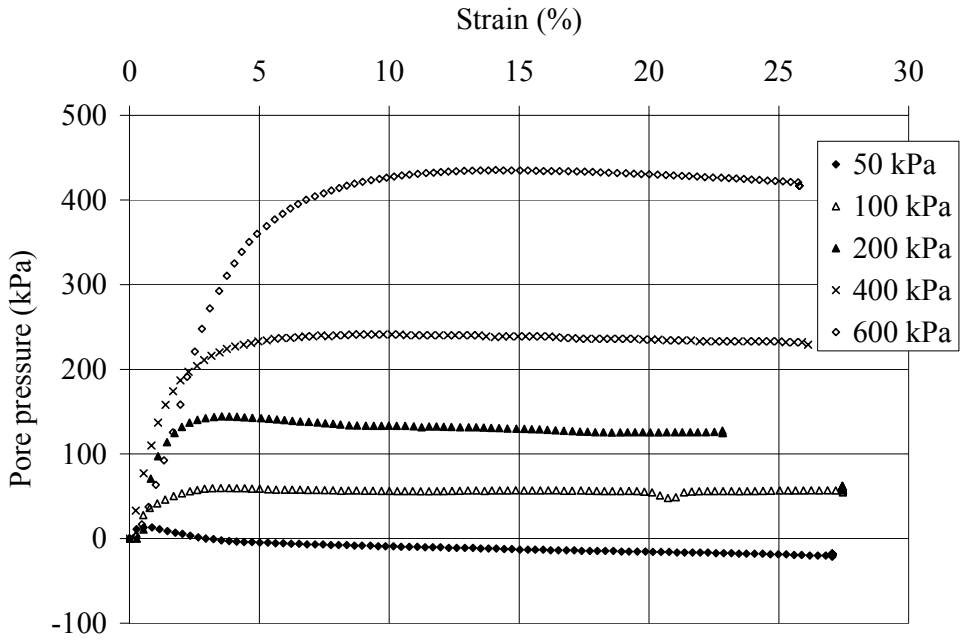

Figure 4.23: Pore pressure versus axial strain increment for non-treated Aberdeen soil.

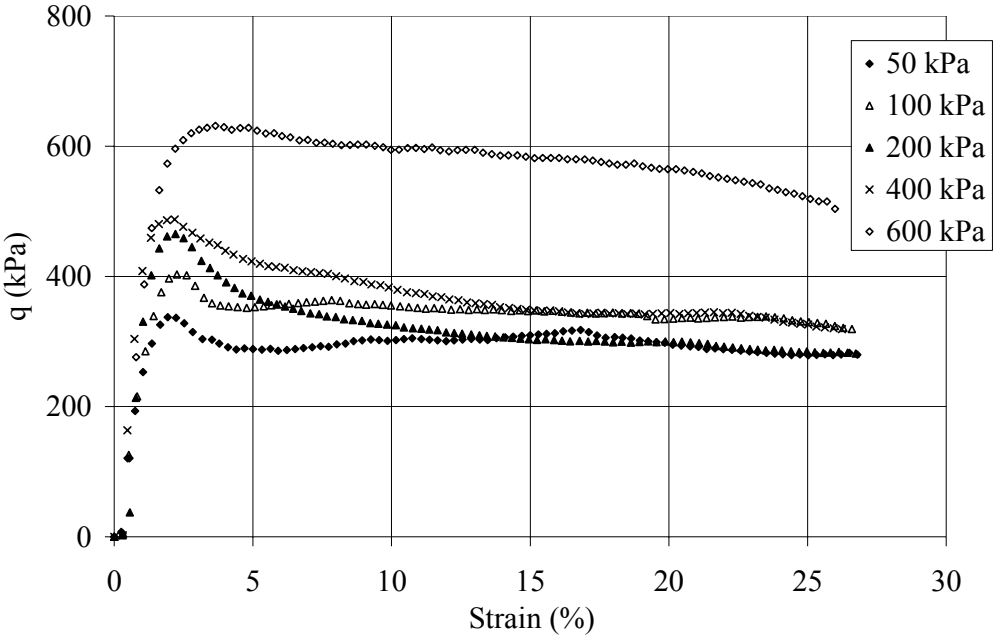

Figure 4.24: Deviator stress versus axial strain increment for 5% cement treated Aberdeen soil.

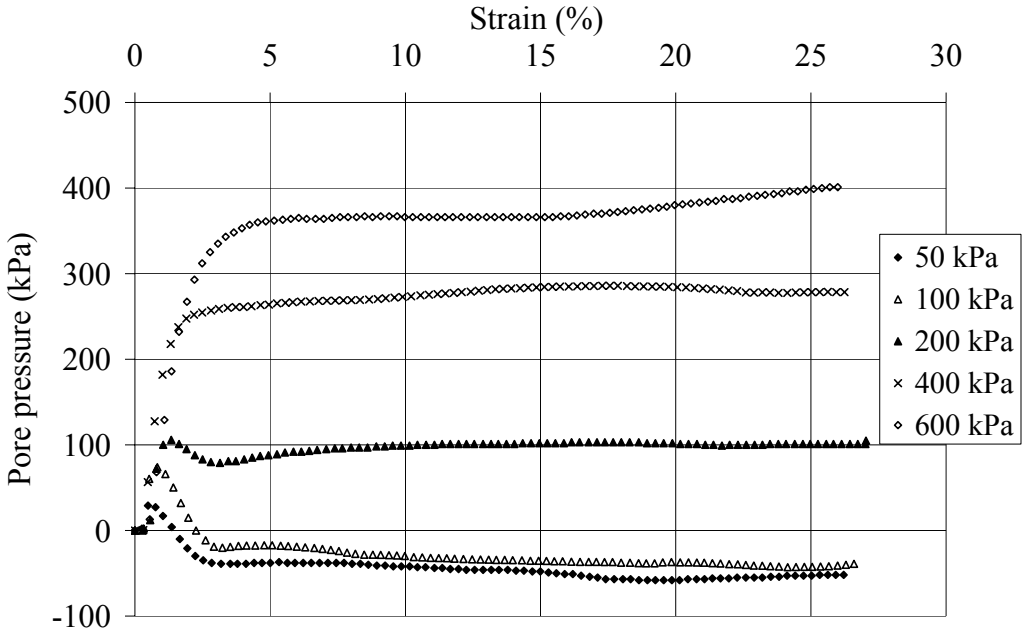

Figure 4.25: Pore pressure versus axial strain increment for 5% cement treated Aberdeen soil.

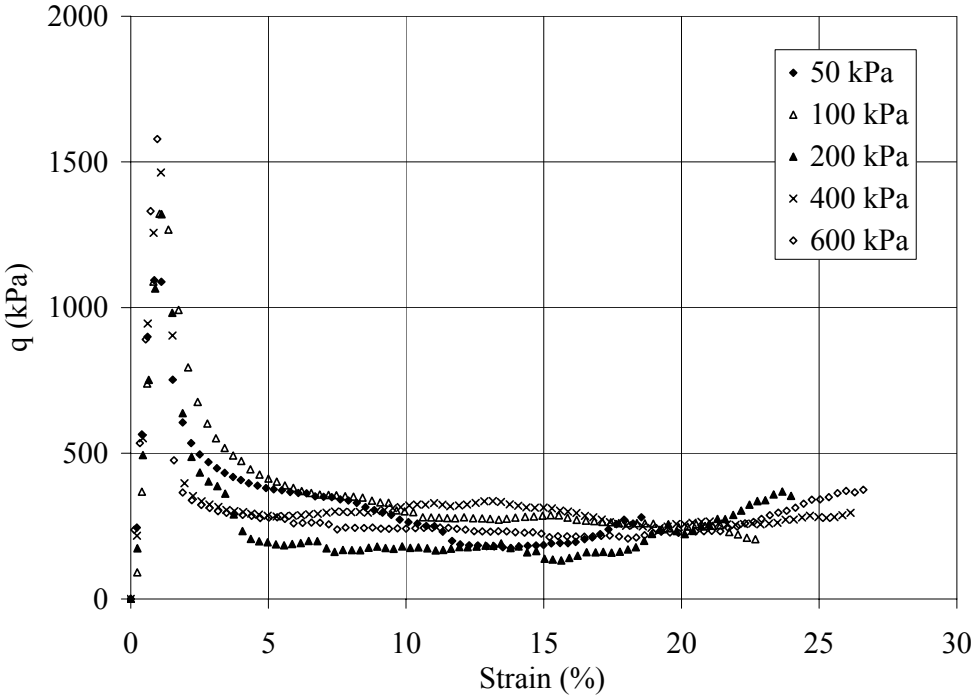

Figure 4.26: Deviator stress versus axial strain increment for 10% cement treated Aberdeen soil.

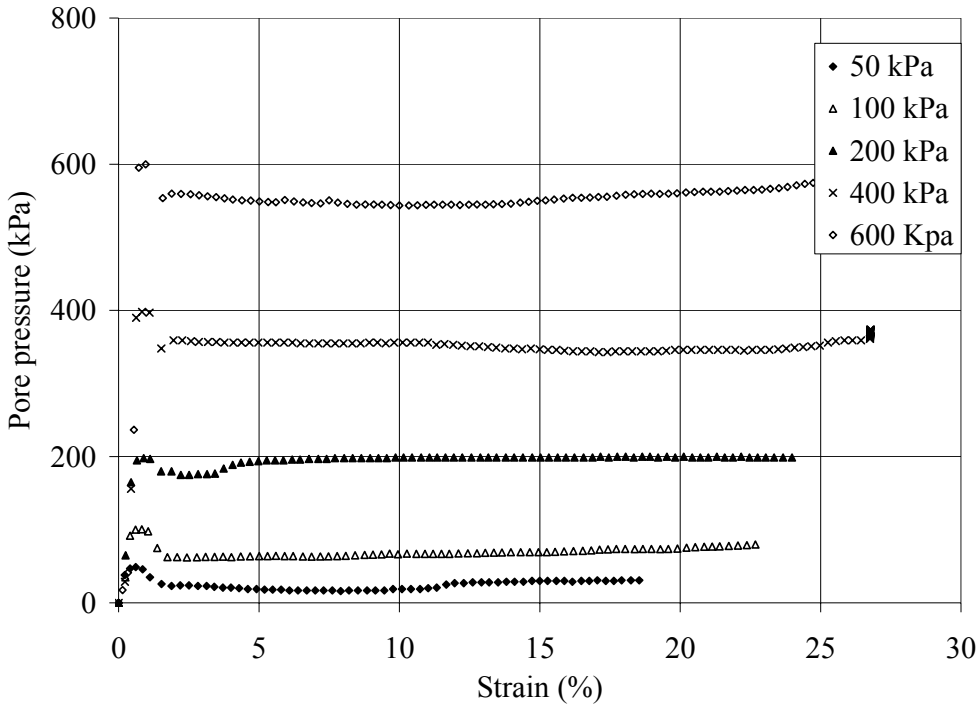

Figure 4.27: Pore pressure versus axial strain increment for 10% cement treated Aberdeen soil.

Figure 4.28: Ductile type of failure for non-treated Aberdeen soil.

Figure 4.29: Planar type of failure for 5% cement treated Aberdeen soil.

Figure 4.30: Splitting type of failure for 10% cement treated Aberdeen soil.

Figure 4.31 shows variation of peak deviator stress versus confining pressure for non-treated, 5%, and 10% cement treated Aberdeen soil. It was observed that as

confining pressure increased peak deviator stress increased. In addition cement treatment led to significant increase in peak deviator stress. However, as mentioned before use of high percentages of cement may lead to dramatic drop in strength after attaining peak values.

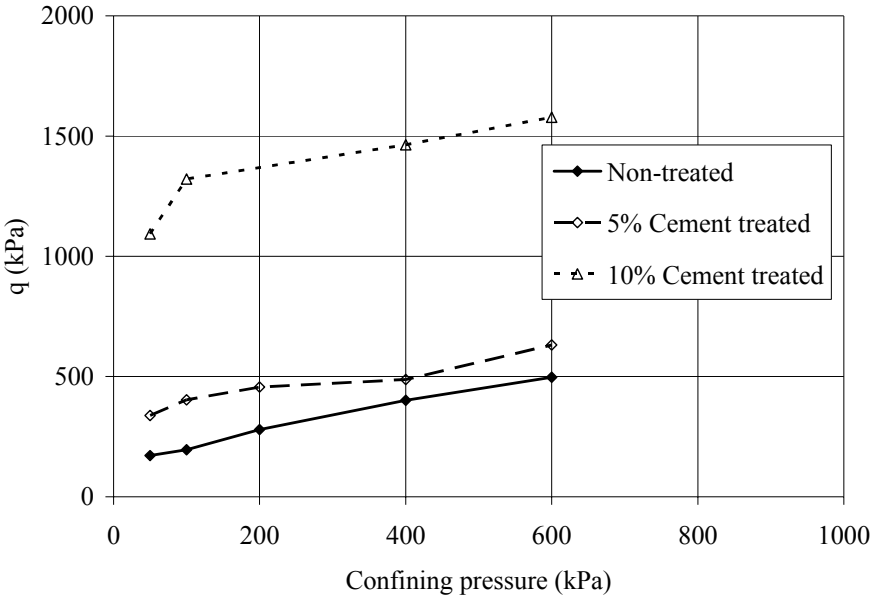

Figure 4.31: Variation of peak deviator stress versus confining pressure for Aberdeen soil at different cement content.

The decrease in post peak deviator stress is due to inter-particle bond breakage and can be quantified by brittleness index defined by Bishop (1971).

$$I_B = \frac{q_p - q_r}{q_p} \tag{4.1}$$

Where, I_B, q_p, and q_r are brittleness index, peak deviator stress, and residual deviator stress, respectively. Figure 4.32 shows the variation of brittleness index versus confining pressure for non-treated, 5%, and 10% Aberdeen soil. It can be observed that as a result of cement treatment brittleness index increased significantly. It is also observed that for non-treated and 10% cement treated soil brittleness index is relatively constant while for

5% cement treated specimens brittleness index increased initially and decreased at higher confining pressures.

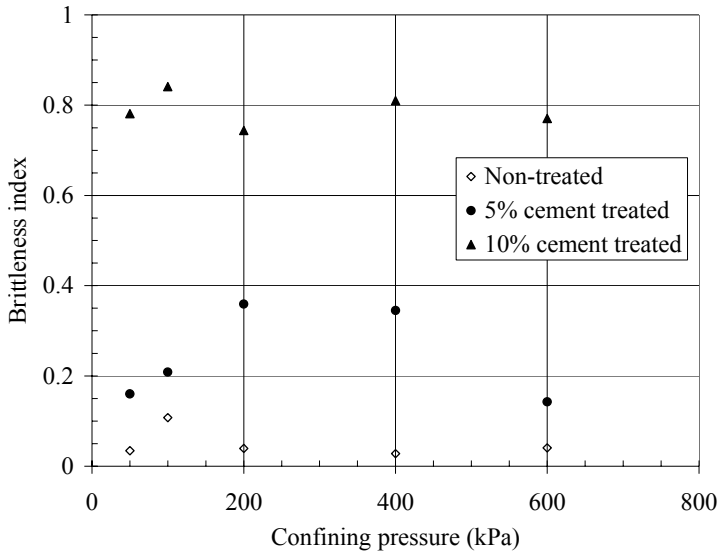

Figure 4.32: Variation of brittleness index versus confining pressure for non-treated, 5%, and 10% cement treated Aberdeen soil.

4.7.2 Everett soil

Figures 4.33 to 4.38 show the deviator stress (q) and pore pressure versus axial strain increment for non-treated and cement treated Everett soil for different confining pressures. It is observed that deviator stress increased with increasing in confining pressure and also as cement content increased, deviator stress increased significantly.

Non-treated and 5% cement treated specimens displayed ductile type of failure at lower confining pressures while brittle type of failure was observed at higher confining pressures. This was opposite of expectation. For 5% cement treated development of negative pore pressure was observed at lower confining pressures. For 10% cement treated pore pressure raised up to almost confining pressure therefore effective confining pressure at failure was near zero. As in the case of Aberdeen soil peak deviator stress was

approximately at 1% strain increment and splitting type of failure was observed, leading to dramatic increase in pore pressure equal to confining pressure.

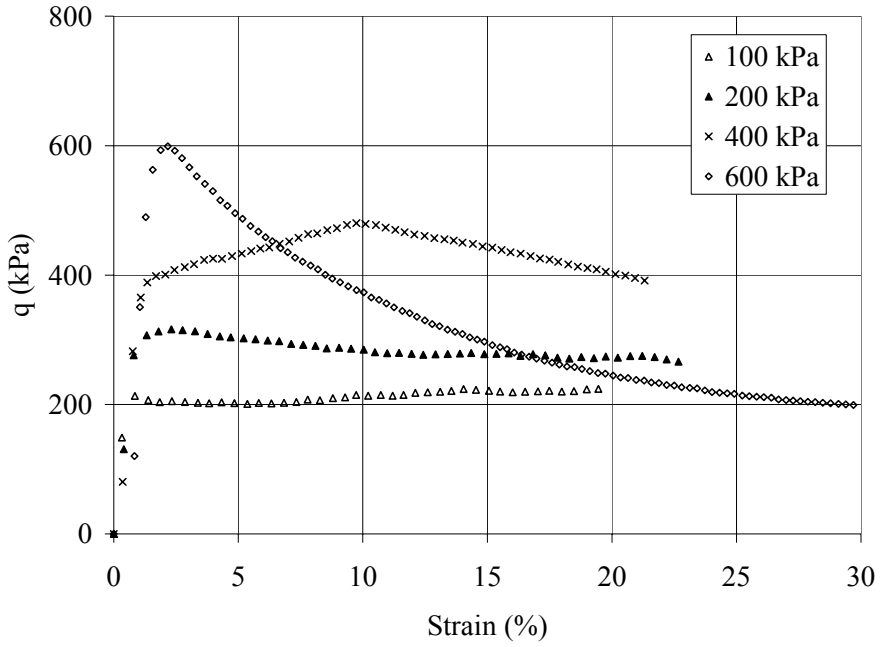

Figure 4.33: Deviator stress versus axial strain increment for non-treated Everett soil.

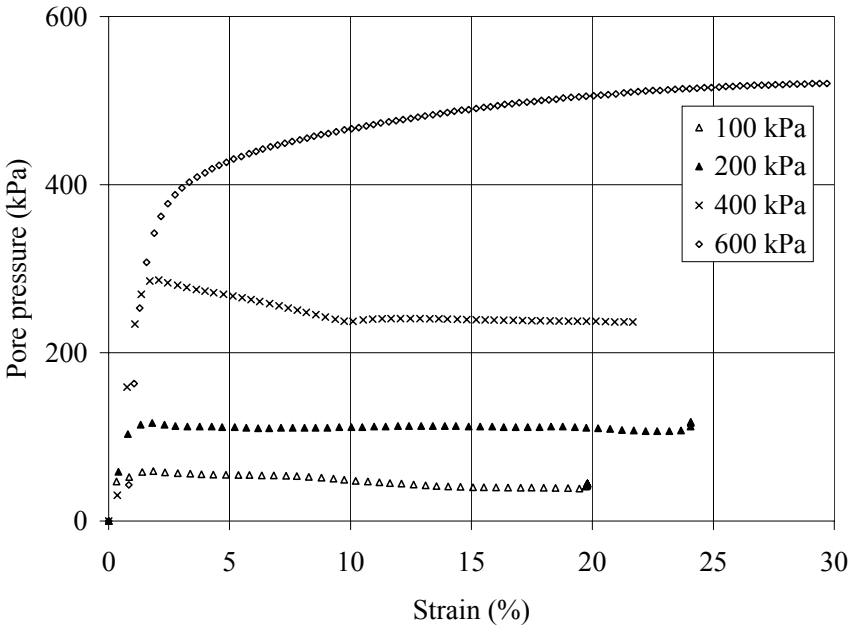

Figure 4.34: Pore pressure versus axial strain increment for non-treated Everett soil.

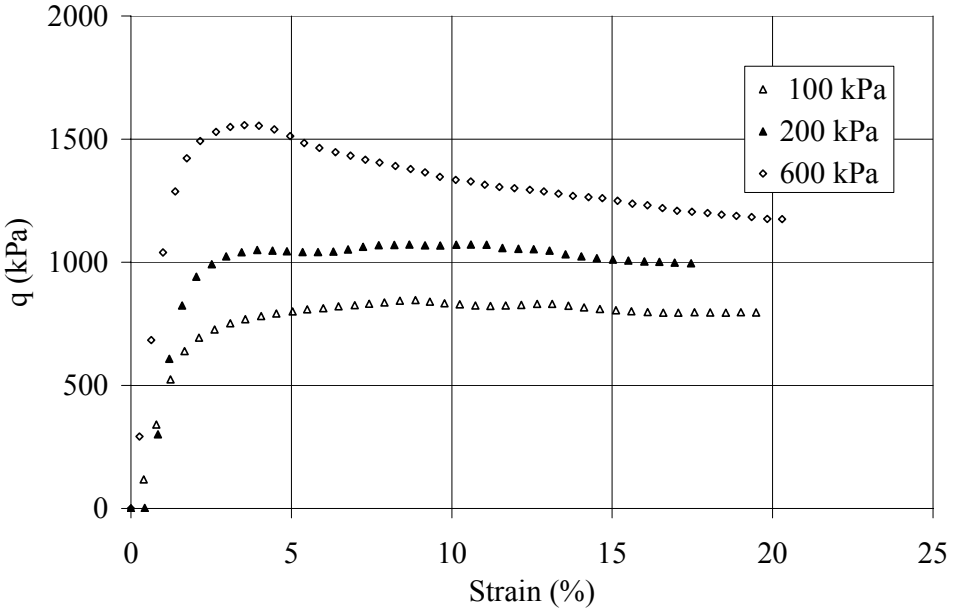

Figure 4.35: Deviator stress versus axial strain increment for 5% cement treated Everett soil.

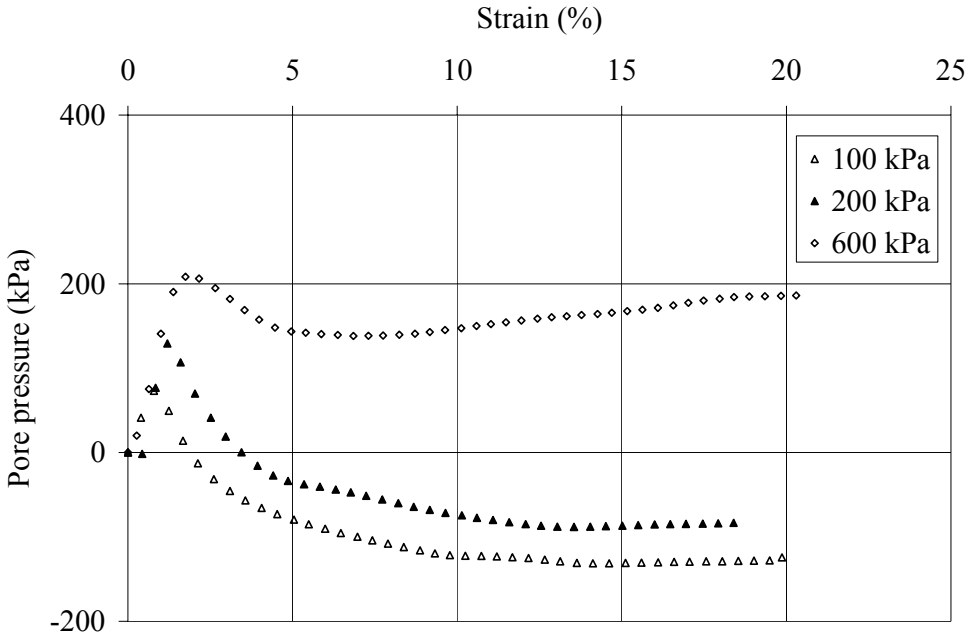

Figure 4.36: Pore pressure versus axial stress increment for 5% cement treated Everett soil.

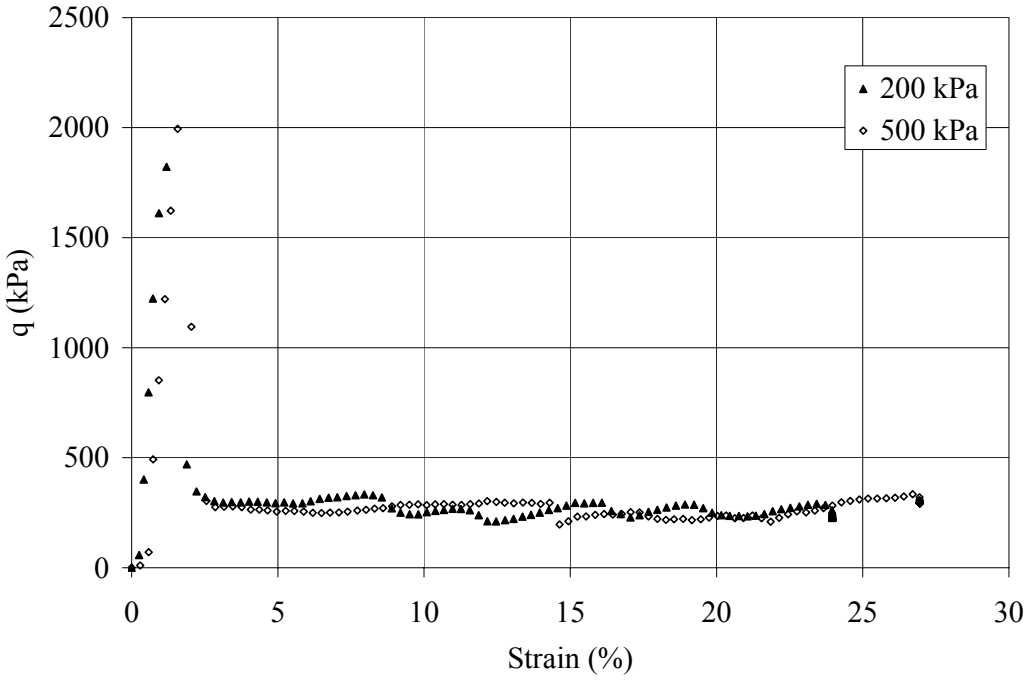

Figure 4.37: Deviator stress versus axial strain increment for 10% cement treated Everett soil.

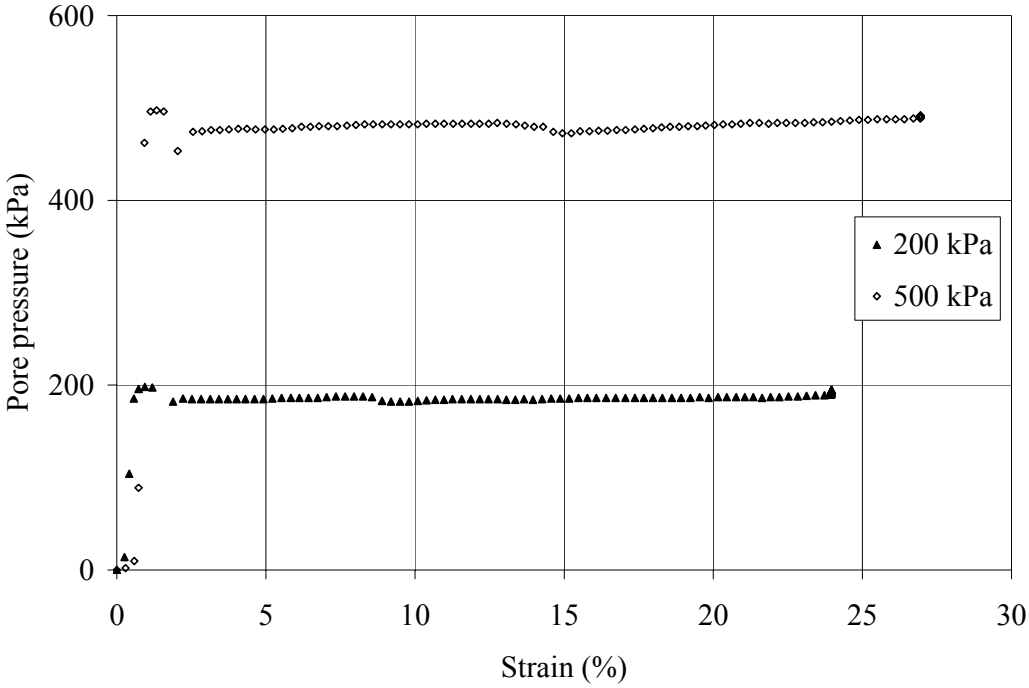

Figure 4.38: Pore pressure versus axial strain increment for 10% cement treated Everett soil.

Variation of peak deviator stress versus confining pressure for Everett soil is shown in Figures 4.39. It can be observed that as confining pressure increased peak deviator stress increased. In addition cement treatment led to significant increase in peak deviator stress.

Figure 4.40 shows variation of brittleness index versus confining pressure for non-treated, 5%, and 10% cement treated Everett soil. It can be observed that for non-treated and 5% cement treated specimens brittleness index increased with increasing in confining pressure. It also can be seen that 10% cement treated soils exhibited much higher brittleness index compared with non-treated and 5% cement treated soils.

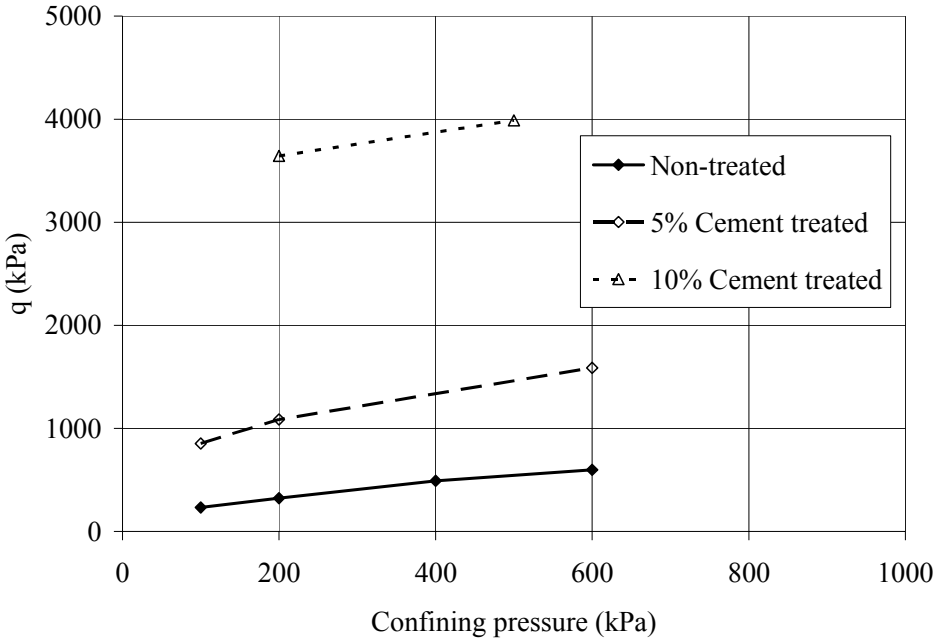

Figure 4.39: Variation of peak deviator stress versus confining pressure for Everett soil at different cement content.

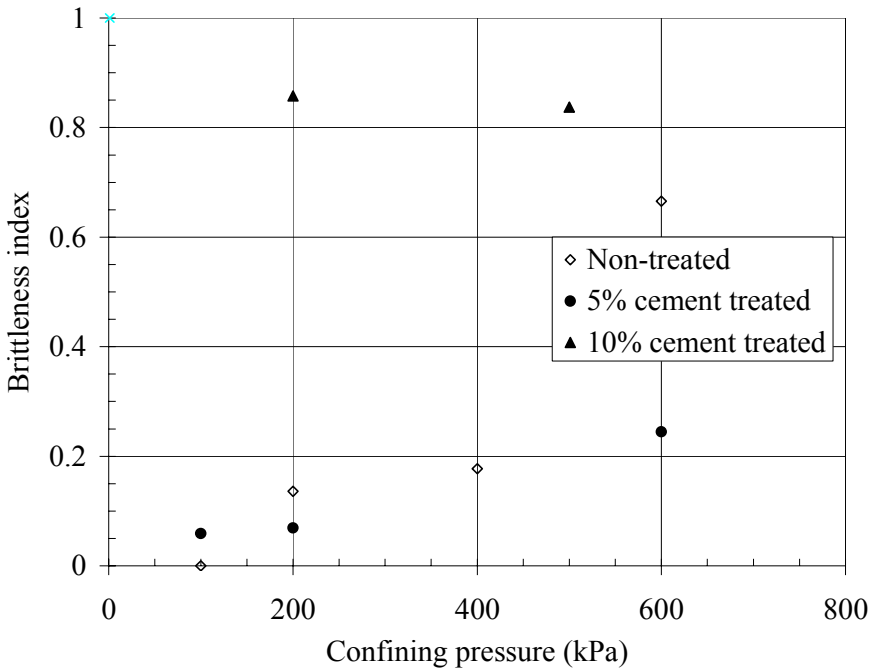

Figure 4.40: Variation of brittleness index versus confining pressure for non-treated, 5%, and 10% cement treated Everett soil.

Based on the undrained triaxial compression tests on host and cement treated Aberdeen and Everett soils the following conclusion are drawn:

- Addition of cement resulted to a significant increase in peak deviator stress.
- As cement content increased strain corresponding to peak deviator stress decreased remarkably.
- For 10% cement treated soils post peak deviator stress was drastically lower than peak deviator stress.
- For 10% cement treated soils at the peak deviator stress pore pressure raised almost equal to confining pressures. Therefore, effective confining pressures were near zero.

- For both soils, generally, brittleness index increased with increasing in cement content.
- Brittleness index for non-treated and 10% cement treated Aberdeen soil found to be relatively constant respect with confining pressure.
- For 5% cement treated Aberdeen soil, brittleness index increased initially and decreased at higher confining pressures.
- For non-treated and 5% cement treated Everett soil brittleness index increased with increasing in confining pressure.

4.8 Oedometer

The compressibility of non-treated and cement treated Aberdeen soil as determined by Oedometer test are shown in Figures 4.41 and 4.42. It is noted that for cement treated soils the solid phase was split into soil and cement in calculating the void ratio:

$$e = \frac{V_{void}}{V_{soil} + V_{cement}} \tag{4.2}$$

In addition the specific gravity of the cement is assumed to be 3.15. It can be seen that cement treatment led to substantial reduction in compressibility. The results of values of coefficient of volume change (m_v), compression index (C_c), and swelling index (C_s) are presented in Table 4.4. The reduction of compressibility of cement treated soils would result in reduced settlements in the field.

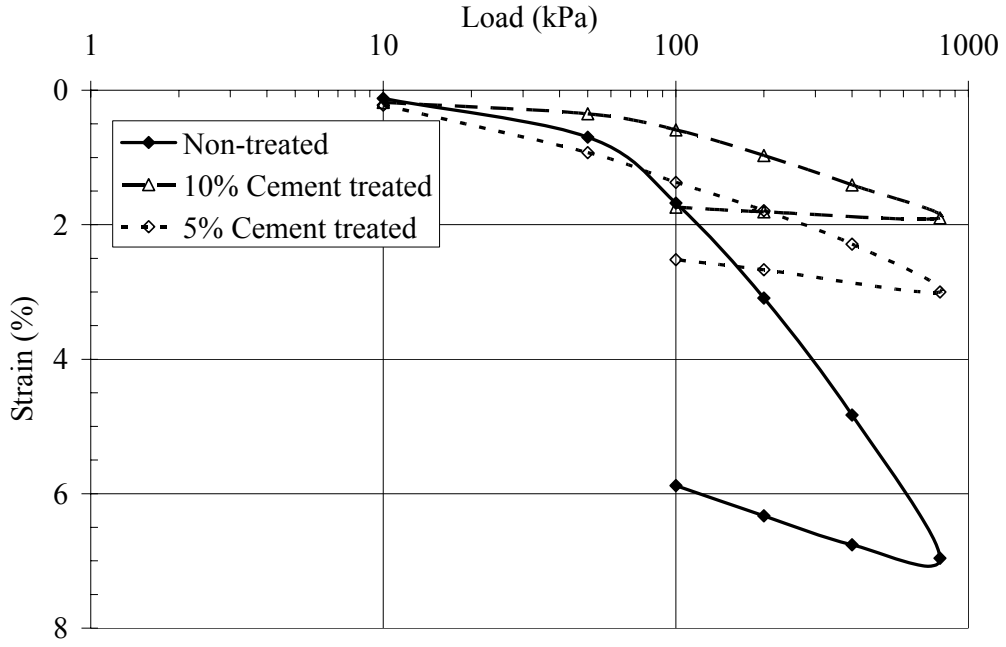

Figure 4.41: Strain increment versus vertical pressure for non-treated and cement treated Aberdeen soil.

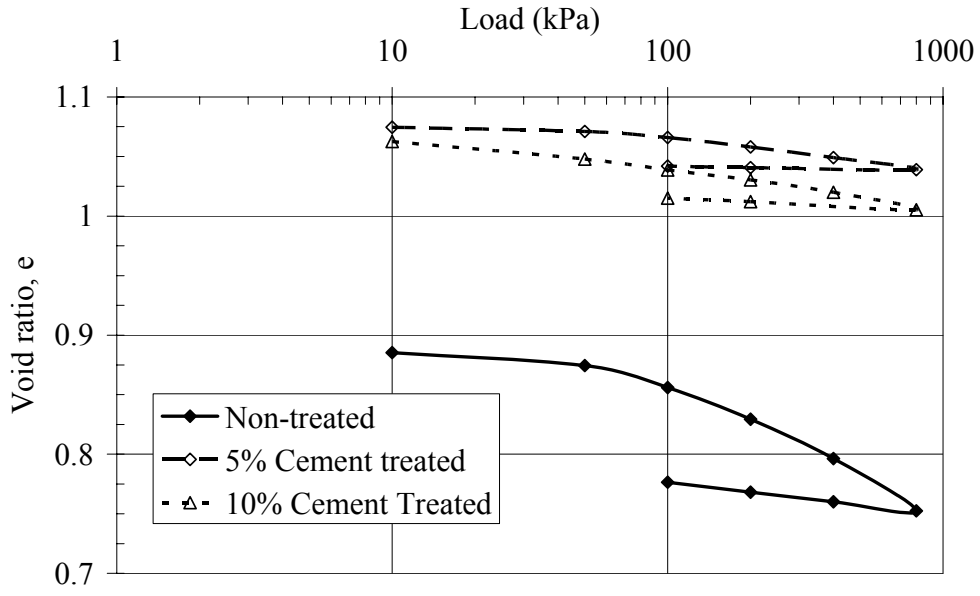

Figure 4.42: Void ratio versus vertical pressure for non-treated and cement treated Aberdeen soil.

Table 4.4: Consolidation parameters for non-treated and cement treated Aberdeen soil.

	Non-treated	5% Cement	10% Cement
m_v $(kPa)^{-1}$	$7.54x10^{-5}$	$2.33x10^{-5}$	$1.87x10^{-5}$
C_c	0.1146	0.0372	0.0300
C_s	0.0266	0.0110	0.0035

4.9 Failure criteria

4.9.1 Mohr-Coulomb failure envelope

4.9.1.1 Aberdeen soil

The Mohr circles of effective stress for non-treated, 5%, and 10% cement treated Aberdeen soil are as shown in Figures 4.43, 4.44, and 4.45, respectively. The best fit tangent line was drawn to represent the failure envelope of the soils. This was possible for non-treated soil. For 5% cement treated soils the Mohr-Coulomb failure found to be a curve, therefore reporting a particular strength parameters was not possible, however for design purposes a conservative linear failure envelope was presented. As noted earlier, 10% cement treated specimens attained pore pressures equal to the confining pressures resulting in near zero effective confining pressure at failure. Thus, regardless of the initial confining pressures all failure stress circles passed through origin (Figure 4.45). Consequently, representing the failure envelope was not possible. Table 4.5 presents the values of effective cohesion (c′) and friction angle (ϕ'). For 5% cement treatment cohesion intercept increased compared with non-treated Aberdeen soil. 5% cement treated specimens displayed lower internal friction angle compared with non-treated soil.

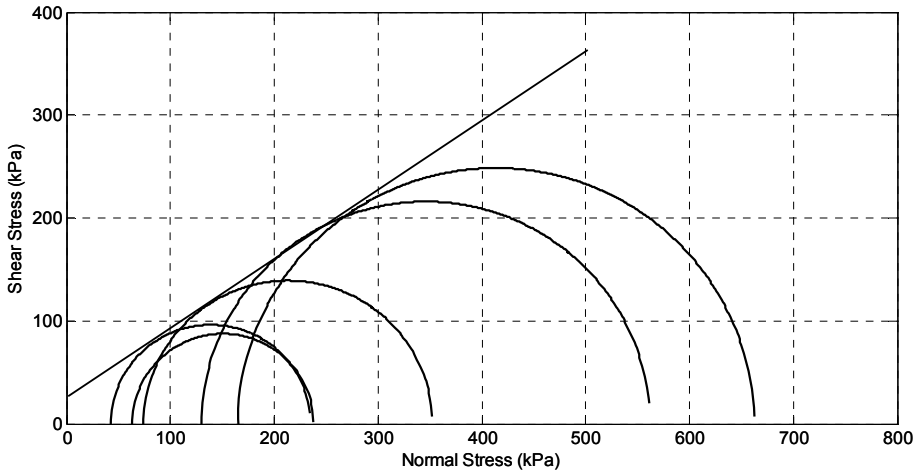

Figure 4.43: Mohr-Coulomb failure envelope for non-treated Aberdeen soil.

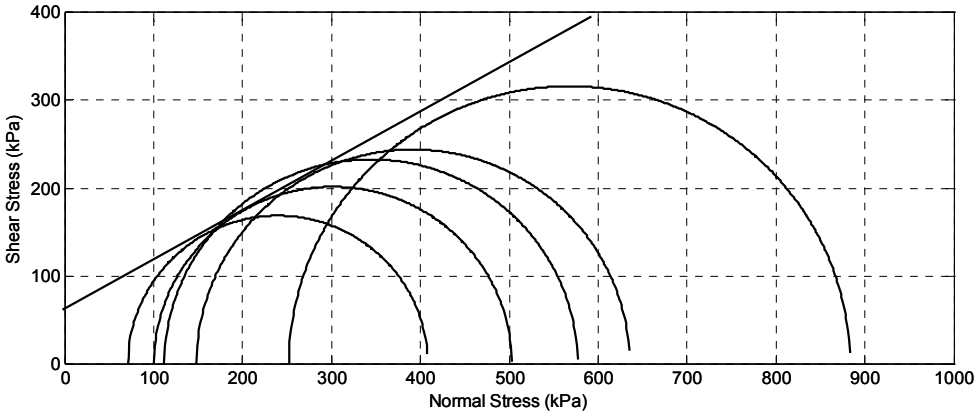

Figure 4.44: Mohr-Coulomb failure envelope for 5% cement treated Aberdeen. soil

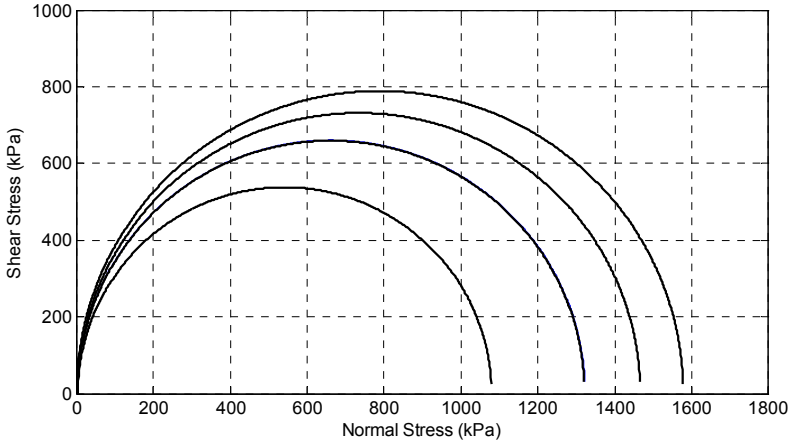

Figure 4.45: Mohr circles for 10% cement treated Aberdeen soil.

Table 4.5: Effective shear strength parameters of non-treated and cement treated soil based on Mohr-Coulomb failure criterion.

	Aberdeen		Everett	
	Non-treated	5% Cement treated	Non-treated	5% Cement treated
c' (kPa)	33	60	50	100
φ' °	34	29	29	35

4.9.1.2 Everett soil

Figures 4.46 to 4.48 show effective Mohr circles stress for non-treated, 5%, and 10% cement treated Everett soil, respectively. The best fit tangent line was drawn to represent the failure envelope of the soils. However, 10% cement treated soils behaved similar to 10% cement treated Aberdeen soil therefore drawing a line to represents failure envelope was not possible. For 5% cement treated cohesion intercept and friction angle increased (Table 4.5). It is evident from the above discussion use of Mohr-Coulomb failure criterion is not useful to describe shear strength of 10% cement treated Aberdeen and Everett soils.

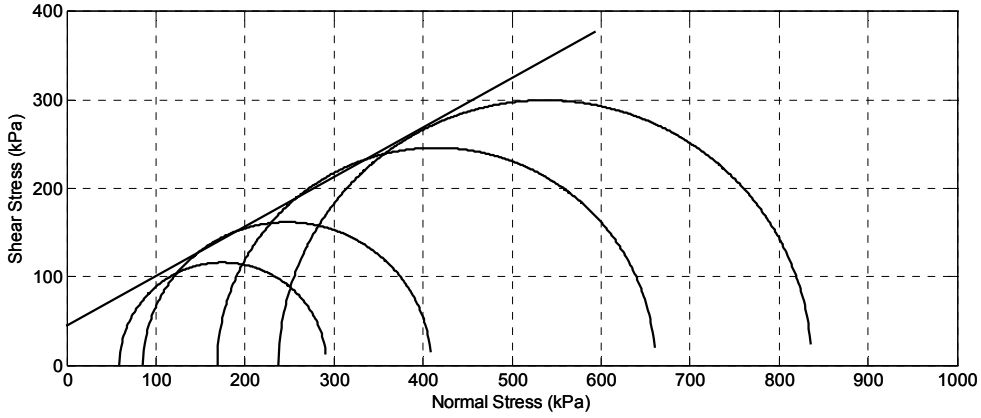

Figure 4.46: Mohr-Coulomb failure envelope for non treated Everett soil.

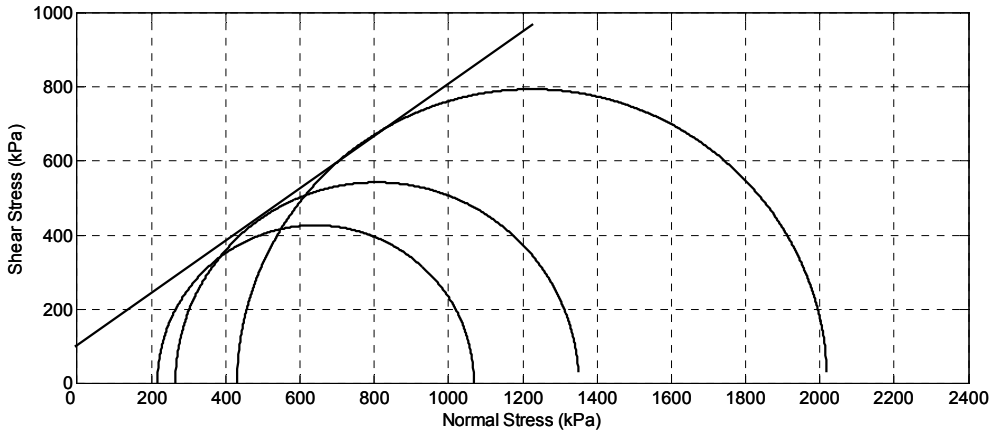

Figure 4.47: Mohr-Coulomb failure envelope for 5% cement treated Everett soil.

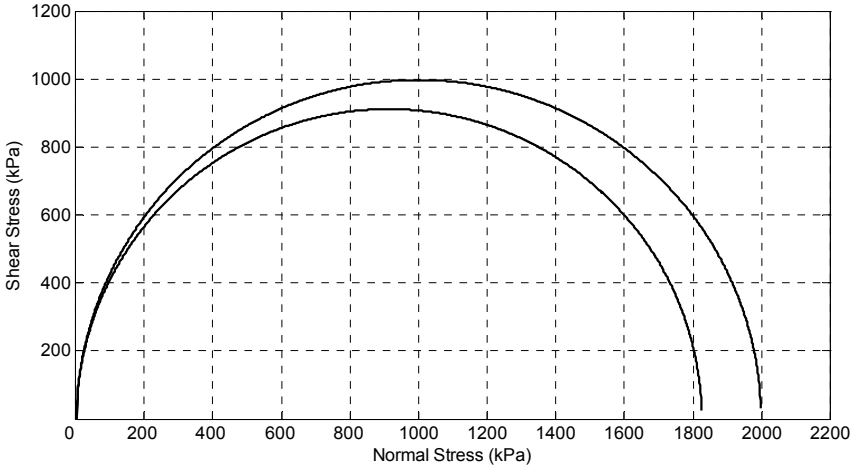

Figure 4.48: Mohr circles for 10% cement treated Everett soil.

4.9.2 Griffith and modified Griffith crack theory

4.9.2.1 Aberdeen soil

The measured shear stress values for non-treated, 5%, and 10% cement treated Aberdeen soil are as shown in Figure 4.49, 4.50, and 4.51, respectively. On the same plots values of failure shear strength predicted by Griffith (Equation 2.10) and Modified

Griffith theory (Equation 2.13) are also shown. Based on mean squared error (MSE) analysis it is evident that predicted shear strength using modified Griffith theory has closer agreement with measured shear strength compared with Griffith theory (the smaller the MSE the closer the agreement) for non-treated and cement treated Aberdeen soil. Values of the coefficient of friction (μ) in modified Griffith theory (Equation 2.13) for non-treated soils and cement treated soils are presented in Table 4.6. It is observed that coefficient of friction increased with cement content. It is noted that estimated μ for the Aberdeen and Everett soils was lower than those suggested by McClintock and Walsh (1962) and Mitchell (1976) for published data.

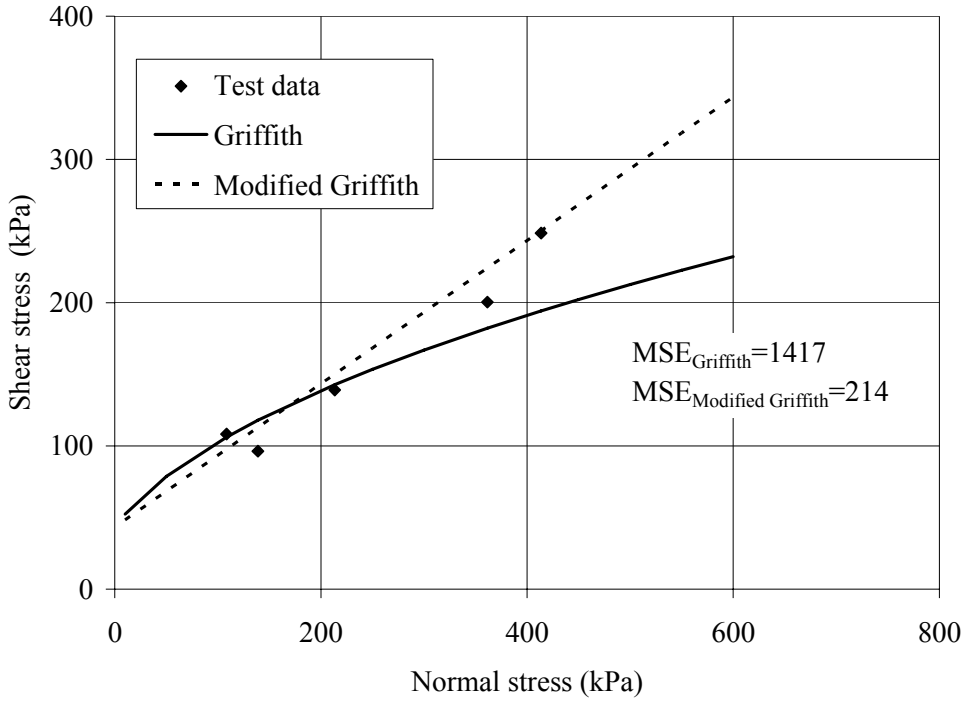

Figure 4.49: Measured values and predicted strength using Griffith and modified Griffith crack theory for non-treated Aberdeen soil.

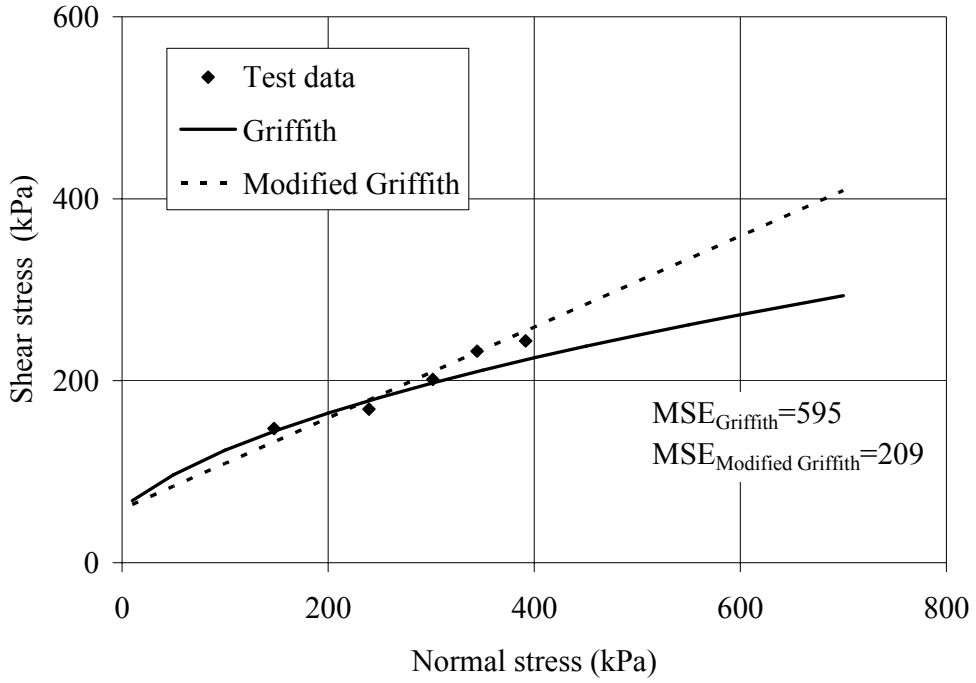

Figure 4.50: Measured values and predicted strength using Griffith and modified Griffith crack theory for 5% cement treated Aberdeen soil.

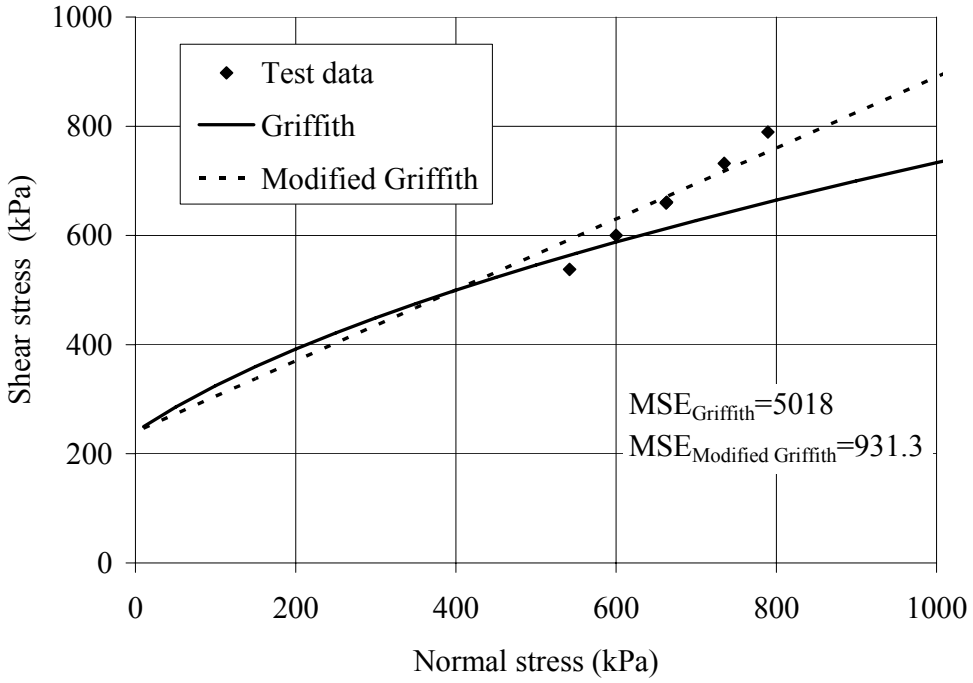

Figure 4.51: Measured values and predicted strength using Griffith and modified Griffith crack theory for 10% cement treated Aberdeen soil.

Table 4.6: Values of μ for Aberdeen and Everett soil at different cement content.

	Non-treated	5% Cement	10% Cement
Aberdeen	0.50	0.50	0.65
Everett	0.50	0.54	0.65

4.9.2.2 Everett soil

The measured shear stress values for non-treated, 5%, and 10% cement treated Everett soil are as shown in Figure 4.52, 4.53, and 4.54, respectively. On the same plots values of failure shear strength predicted by Griffith (Equation 2.10) and Modified Griffith theory (Equation 2.13) are also shown. Based on MSE analysis it can be seen that for non-treated and cement treated Everett soil Griffith and modified Griffith is more applicable, respectively. It is noted that coefficient of friction (μ) increased with cement content (Table 4.6).

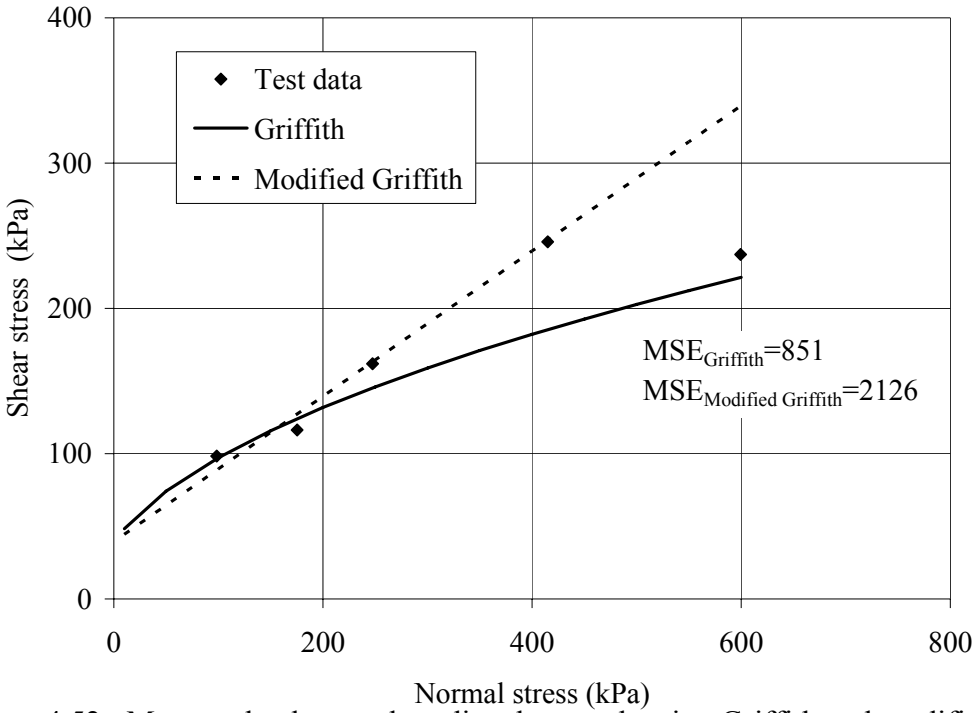

Figure 4.52: Measured values and predicted strength using Griffith and modified Griffith crack theory for non-treated Everett soil.

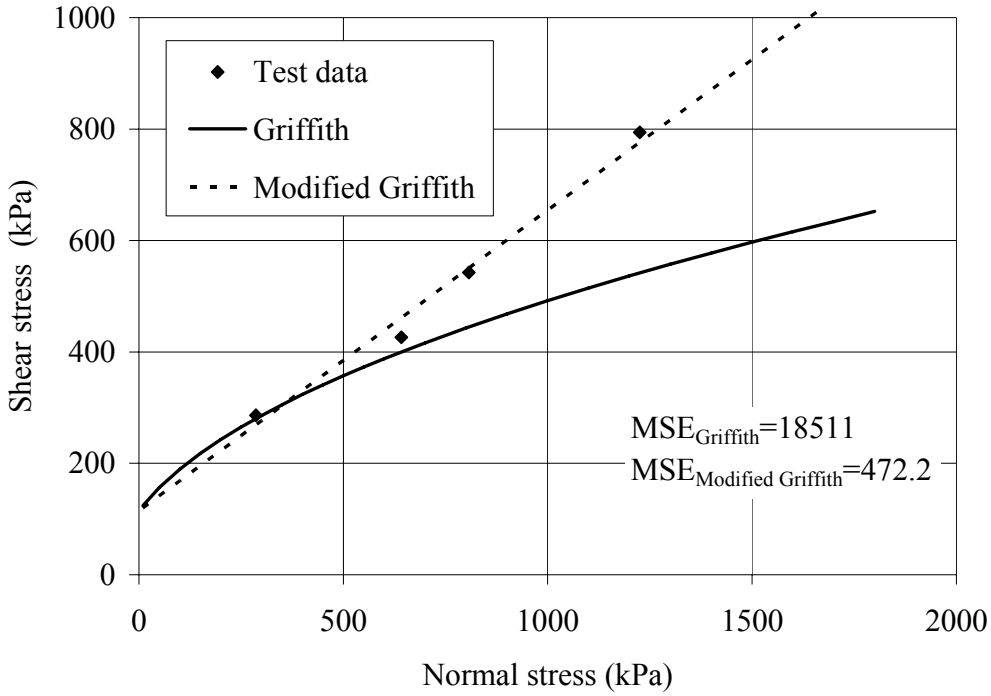

Figure 4.53: Measured values and predicted strength using Griffith and modified Griffith crack theory for 5% cement treated Everett soil.

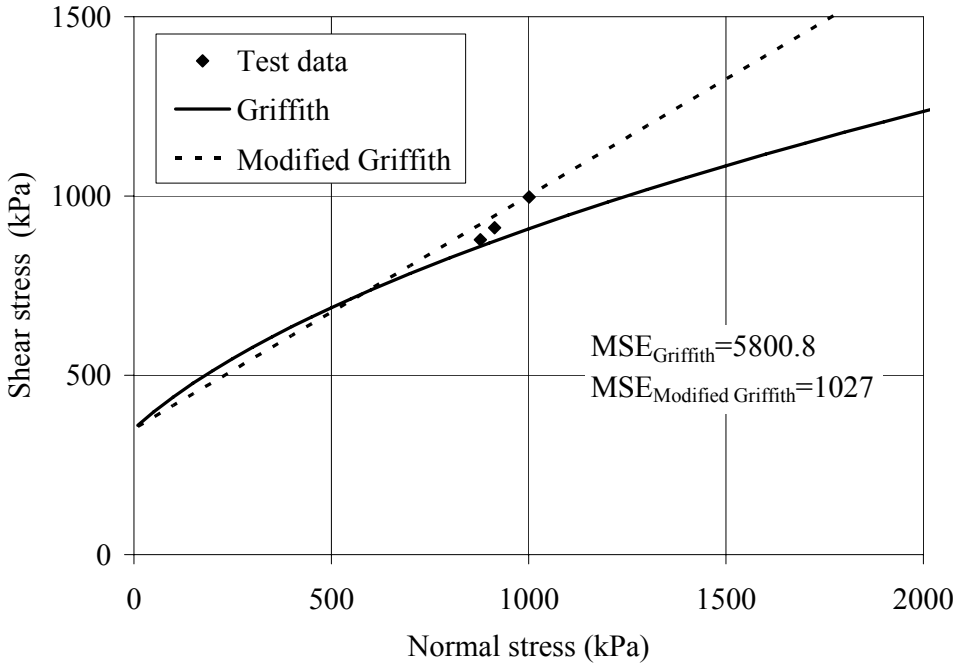

Figure 4.54: Measured values and predicted strength using Griffith and modified Griffith crack theory for 10% cement treated Everett soil.

4.9.3 Johnston failure criterion

4.9.3.1 Aberdeen soil

The comparison of measured and predicted normalized principal stresses values at failure for non-treated and 5% cement treated soils using Johnston criterion (Equation 2.16) are as shown in Figures 4.55 and 4.56. The B and M values of the criterion were obtained from Equations 2.18 and 2.20, respectively. The S value was determined by trial and error method to obtain the lowest MSE value. It is observed that Johnston method is applicable to predict normalized principal stresses for non-treated and 5% cement treated Aberdeen soil. In case of 10% cement treatment, as a result of zero effective confining pressure at failure Johnston criterion is not applicable (normalized minor stress falls on σ_{1N} axis).

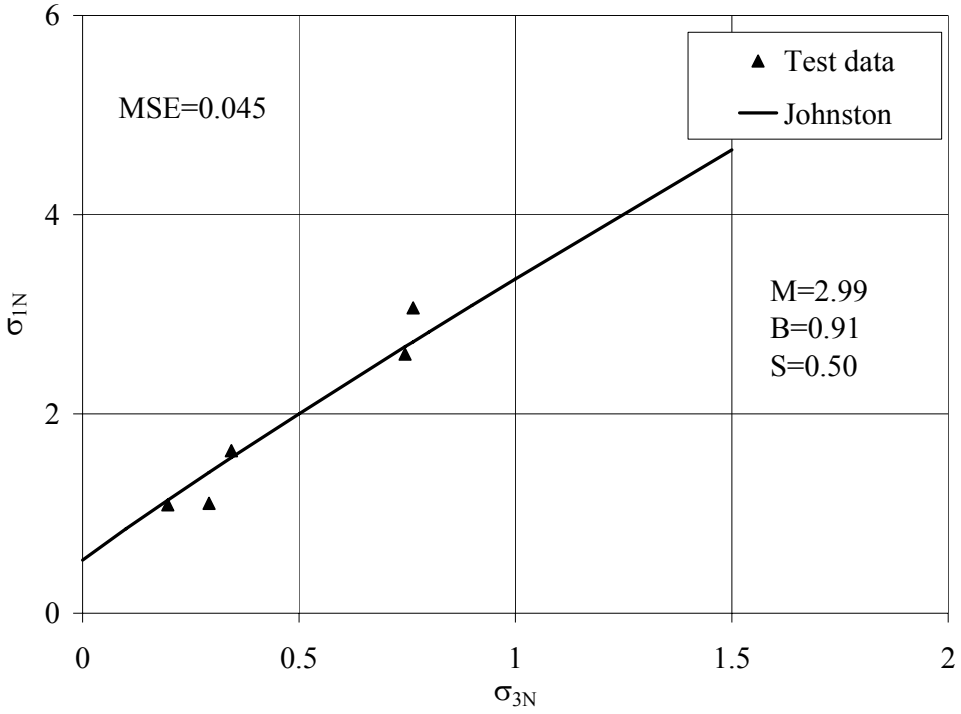

Figure 4.55: Comparison between measured and predicted normalized principal stresses at failure for non-treated Aberdeen soil using Johnston criterion.

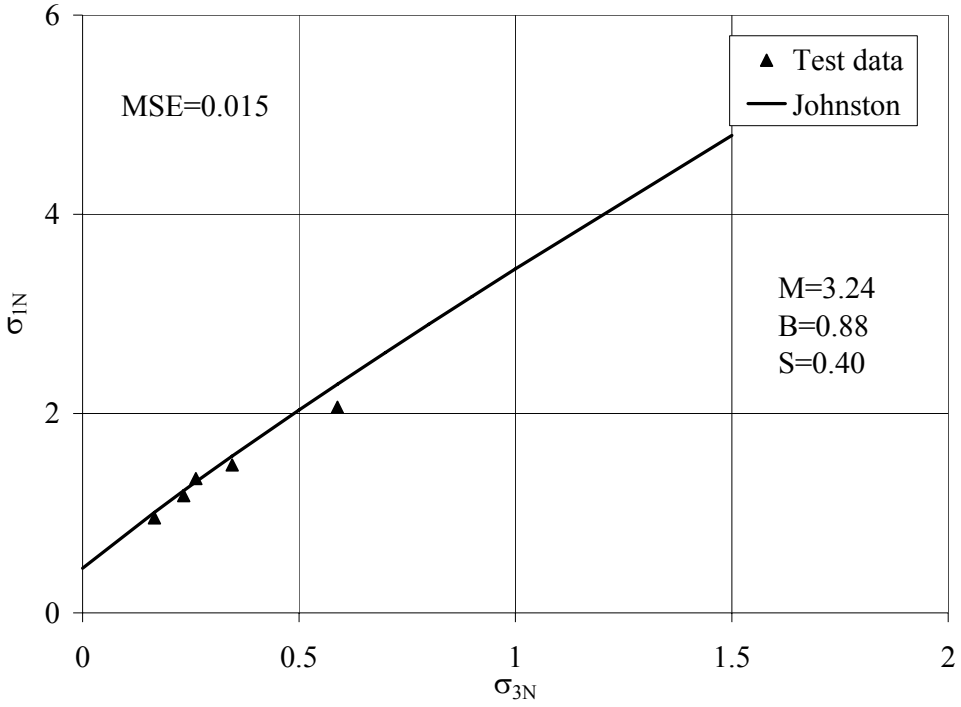

Figure 4.56: Comparison between measured and predicted normalized principle stresses at failure for 5% cement treated Aberdeen soil using Johnston criterion.

4.9.3.2 Everett soil

The comparison of measured and predicted normalized principal stress values at failure for non-treated and 5% cement treated Everett soil using Johnston criterion (Equation 2.16) are as shown in Figures 4.57 and 4.58. The B value was obtained from Equation 2.18 and M value was determined from Equations 2.20 and 2.21 for non-treated and 5% cement treated Everett soil, respectively. The S value was determined by trial and error method to obtain the lowest MSE value, it must be noted S value for 5% cement treated soils was significantly higher than that for non-treated Everett soil. It is observed that Johnston method is applicable to predict normalized principal stresses for non-treated

and 5% cement treated Aberdeen soil. In case of 10% cement treatment similar to Aberdeen soil Johnston criterion is not applicable.

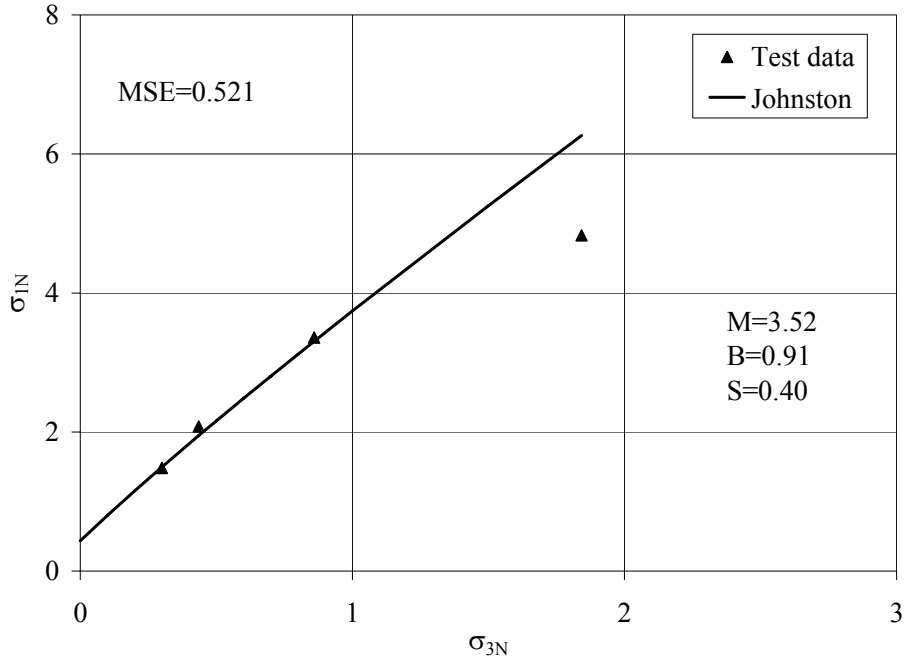

Figure 4.57: Comparison between measured and predicted normalized principle stresses at failure for non-treated Everett soil using Johnston criterion.

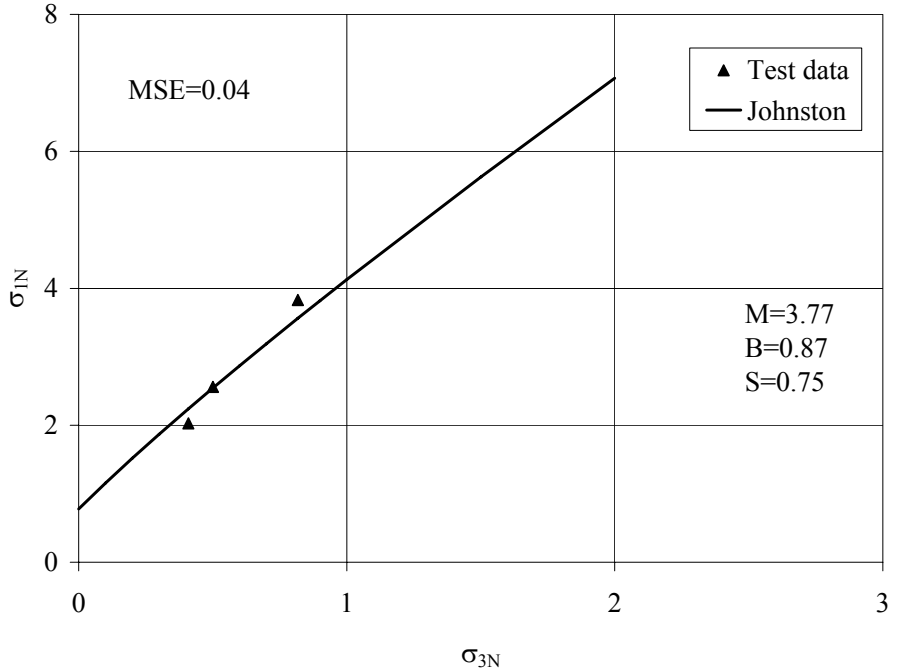

Figure 4.58: Comparison between measured and predicted normalized principle stresses at failure for 5% cement treated Everett soil using Johnston criterion.

CHAPTER FIVE

CRITICAL STATE FRAMEWORK AND MECHANICAL BEHAVIOR OF CEMENT TREATED SOILS

5.1 Introduction

Soil strength is considered to be a unique function of cohesion and friction angle in using the Mohr-Coulomb failure criterion. However, as discussed in Chapter Two, critical state soil mechanics suggested that the strength of soils (be it sand, silt, or clay) is governed by the critical state friction and inter-particle locking. Further, depending on the combinations of void ratio and effective confining pressure, soil behavior changes its characteristics from brittle to faulting to ductile. Different criteria are needed to quantify such behavior in these different regions. The critical state framework has been used to describe these different characteristics successfully for clays and sand in the past. The framework is examined here to highlight its feasibility to quantify the behavior of cement treated soils. The description is limited to the case of Aberdeen soil.

5.2 Critical state parameters

Critical state soil parameters for non-treated and cement treated Aberdeen soil were determined from laboratory test results. The critical state parameters λ and κ were determined by (Wood 1990):

$$\lambda = \frac{C_c}{2.303} \tag{5.1}$$

$$\kappa = \frac{C_s}{2.303} \tag{5.2}$$

where C_c and C_s are the compression and swelling index obtained, from Oedometer test respectively. The parameters N and Γ were found by constructing V-ln p′ plots from triaxial test data. The critical state friction parameter M was obtained by plotting triaxial test results in q-p′ space (Figures 5.1 to 5.3). A summary of the critical state parameters for non-treated and cement treated Aberdeen soil are given in Table 5.1. Note that N and Γ are usually used in critical state numerical models. They are reported here for completeness only and are not used in following discussions.

Table 5.1: Critical state parameters for non-treated and cement treated Aberdeen soil.

Critical state parameter	Non-treated	5% Cement treated	10% Cement treated
λ	0.0498	0.0162	0.0130
κ	0.0116	0.0048	0.0015
N	1.8886	2.0680	2.0793
Γ	1.8504	2.0566	2.0678
M	1.40	1.40	

5.3 Effect of cement treatment on stress path

Plots of deviator stress (q) versus effective confining stress (p′) for non-treated, 5% and 10% cement treated Aberdeen soil are shown in Figures 5.1, 5.2, and 5.3, respectively. It can be observed that for both non-treated and 5% cement treated soils the effective stress paths of specimens consolidated at lower stresses rise up above the critical state line to reach a constant stress ratio defined by the Hvorslev surface (Muhunthan and Schofield 2000). Thereafter, these materials progressively degrade and tend toward the critical state with slope M =1.40. On the other hand, 10% cement treated soil specimens attain a much higher constant ratio with a slope equal to 3 (i.e. $q = 3p'$)

line. This slope corresponds to the surface on which soil is prone to develop tensile cracks (Muhunthan and Schofield 2000). Indeed as reported earlier these specimens were observed to fail with split cracks (Figure 4.30).

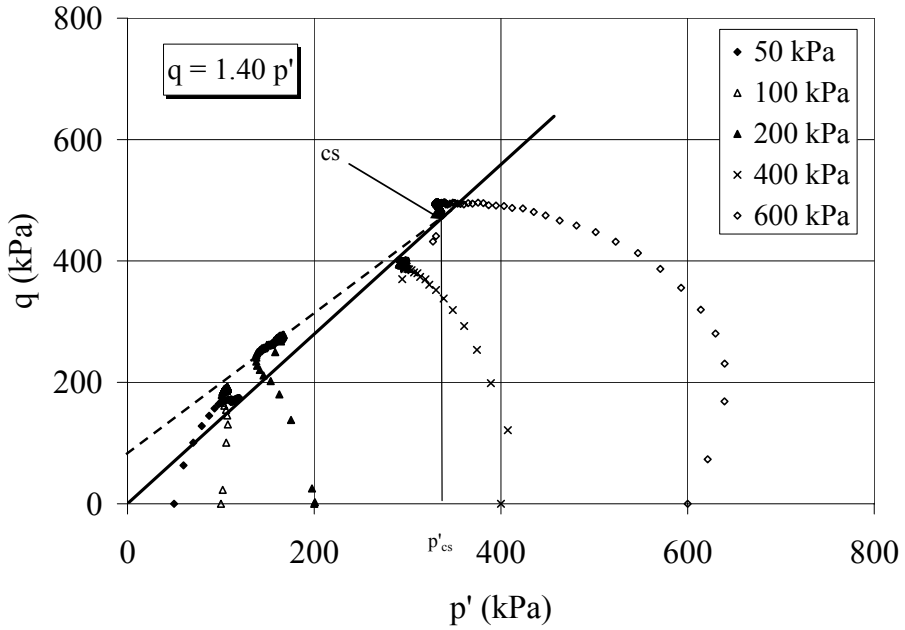

Figure 5.1: Undrained stress path for non-treated Aberdeen soil.

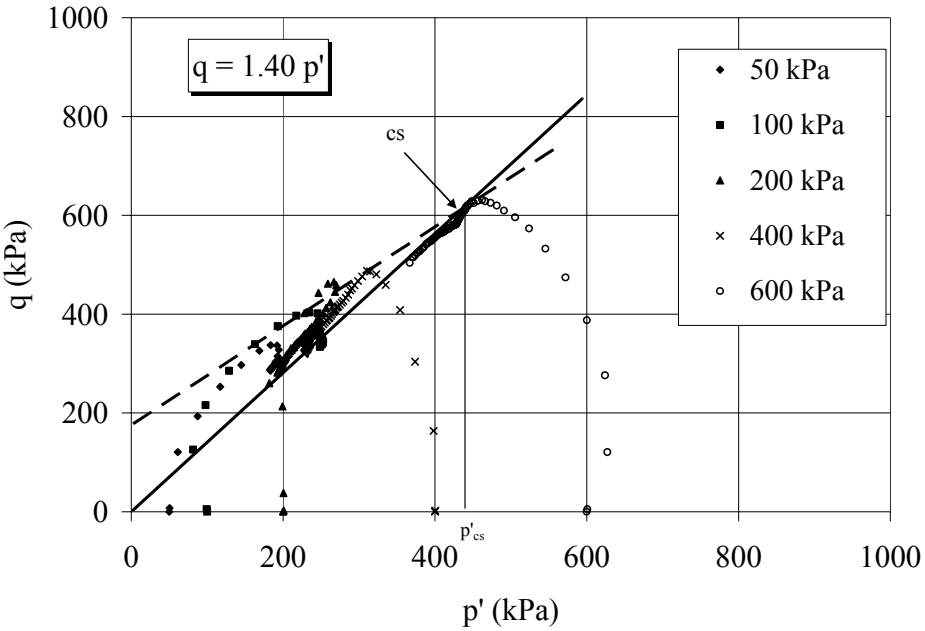

Figure 5.2: Undrained stress path for 5% cement treated Aberdeen soil.

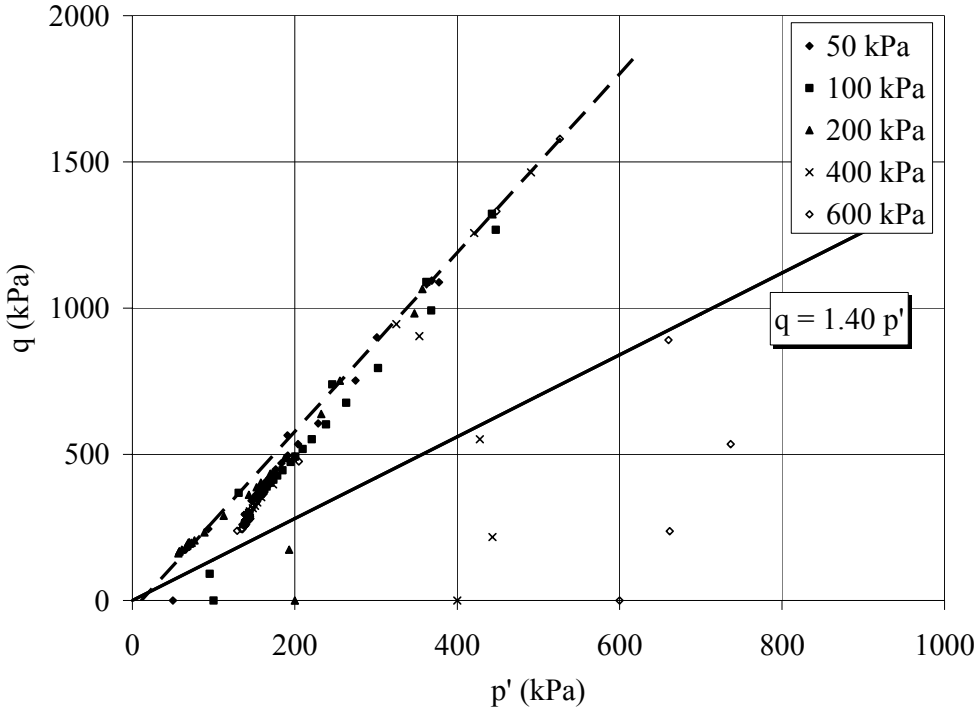

Figure 5.3: Undrained stress path for 10% cement treated Aberdeen soil.

The region between the Hvorslev surface and the critical state surface could be considered as a measure of the amount of interlocking associated with a specimen. A comparison of these regions in Figures 5.1 and 5.2 show that addition of cement leads to increase in interlocking. The intersection of Hvorslev and the critical state surfaces is the critical state of these specimens. The corresponding pressure at this state is the critical confining pressure. It is seen that addition of cement leads to an increase in the value of the critical pressure meaning the brittle to ductile transition will occur at higher pressures.

The unique undrained stress path of cemented soil observed in the case of 10% cement treated soils (Figure 5.3) is the result of failure of cemented bonding and is independent from general effective stress patterns (Sangrey 1972; Pillai and Muhunthan 1999). In addition, cemented soils (naturally or artificially) exhibit anisotropic behavior

(Wong and Mitchell 1975; Rotta et al. 2003). Schematic illustration of undrained stress path for cemented soils is shown in Figure 5.4. This is slightly different from the conceptual model presented by Pillai and Muhunthan (1999). Based on their observation of slope failures in natural cemented soils in Eastern Canada, they assumed that the point C is on or very close to critical state line whereas the results of the present study and that by Sangrey (1972) show that the undrained stress path may continue and end up on point B which is on the fracture line $q = 3p'$. At point B, as a result of failure of cemented bonding pore pressure increases to confining pressure, consequently effective confining pressure drops to zero and specimen splits vertically (Figure 4.30).

Schofield (1980) divided behavior of remolded soils into fold (ODC), fault (OAC), and fracture (between q axis and OB) zones (Figure 5.4). It is seen that highly cement treated soils extend the limit of the fracture region from point A to B. It must be noted for 10% cement treated Aberdeen soil, it was observed that point B corresponds to 1% strain (Figure 4.26).

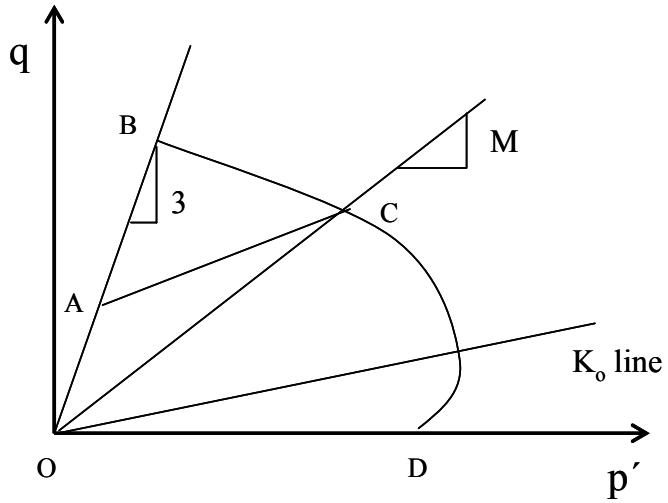

Figure 5.4: Schematic illustration of undrained stress path for highly cemented soils.

5.4 Plastic energy dissipation and yield surface

Researchers have proposed a number of ways to define the yield surface of soils and subsequently the shape of the effective stress path. The family of yield surface developed based on plastic energy dissipation as was done in the case of cam clay (Roscoe et al. 1963) and modified cam clay (Roscoe and Burland 1968) models are prime examples of this approach. These basic formulations did not account for development of anisotropy.

In order to incorporate the effects of anisotropy within the family of critical state models, Muhunthan and Masad (1997) have proposed a modification to the plastic energy dissipation equation with an anisotropic parameter (α):

$$p'\delta\varepsilon_v + q\delta\varepsilon_q = p'\sqrt{(\delta\varepsilon_v + \alpha\delta\varepsilon_q)^2 + (M\delta\varepsilon_q)^2} \tag{5.7}$$

where $\delta\varepsilon_v$ and $\delta\varepsilon_q$ are the plastic volumetric and shear strain increments, respectively. M is the friction constant from soil and $p'$is the mean effective pressure. A detailed description of the fabric parameter and its mathematical formulation are presented in Muhunthan et al (1996). Similar energy dissipation formulations for modeling soil behavior have been used by Dafalias (1987) and Collins and Kelly (2002). Rearrangement of Equation 5.7 and application of the normality, and integration results in the anisotropy yield function as:

$$\frac{p}{p_o} = \left[\frac{M^2 + (\eta_{in} - \alpha)^2}{M^2 + (\eta - \alpha)^2}\right] \tag{5.8}$$

Where η_{in} is the initial value of $\frac{q}{p'}$ and p_o is the value of p' when $\eta = \eta_{in}$. If $\alpha = 0$ Equation 5.8 reduces to the modified cam clay yield function (Roscoe and Burland 1968).

The general shape of the anisotropic yield surface consists of a rotated and distorted ellipse. The effective state path surface can be obtained by combining the yield function and volumetric behavior (Muhunthan et al. 1996):

$$\frac{p}{p_o} = \left[\frac{M^2 + (\eta_{in} - \alpha)^2}{M^2 + (\eta - \alpha)^2} \right]^{\frac{\lambda - \kappa}{\lambda}} \tag{5.9}$$

The comparison between observed and predicted stress path using modified cam clay and the model presented by Muhunthan and Masad (1997) for non-treated and 5% cement treated Aberdeen soil are shown in Figures 5.5 and 5.6, respectively. It can be seen that the model presented by Muhunthan and Masad (1997) captures the stress path for non-treated and 5% cement treated specimens well. Since compaction of specimens inside the mold induces anisotropy use of the anisotropic parameter becomes necessary to capture the behavior. Appropriate values of η_{in} and α were found by fitting Equation 5.9 on observed undrained stress paths of specimens. For both specimens η_{in} found to be 0.2 and α found to be 0.3 and 0.4 for non-treated and 5% cement treated specimens, respectively. It is evident that the addition of cement resulted in an increase in fabric parameter (α). However, further investigation needs to be conducted to find the more accurate relationship between cement content and fabric parameter.

It is evident that none of the models capture the behavior above the critical state line in the region of the Hvorslev state. It is proposed to model the behavior in this region using the different Griffith criteria discussed in the previous chapters.

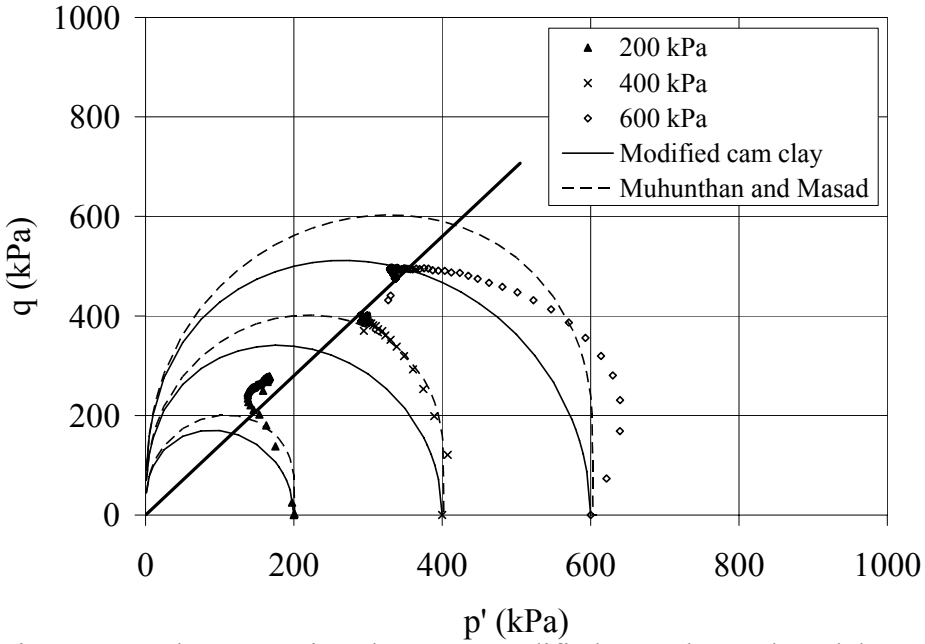

Figure 5.5: The comparison between modified cam clay and model presented by Muhunthan and Masad for non-treated Aberdeen soil.

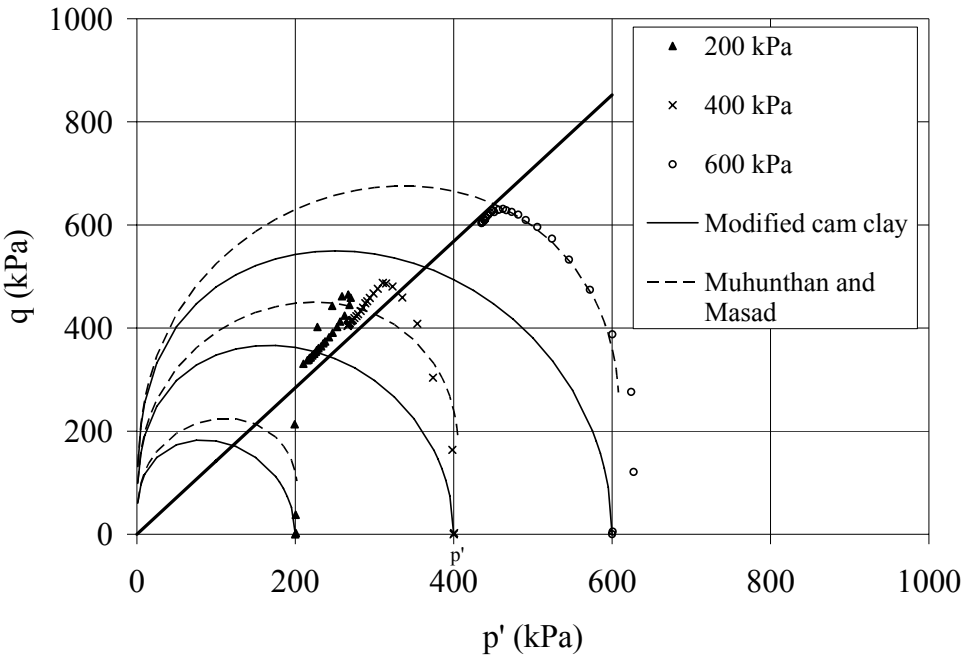

Figure 5.6: The comparison between modified cam clay and model presented by Muhunthan and Masad for 5% cement treated Aberdeen soil.

5.5 Brittle behavior in q-p´ space

The extended Griffith criterion (Equation 2.14) for triaxial compression test ($\sigma'_2 = \sigma'_3$) in terms of q and p´ becomes:

$$q^2 = -12\sigma'_t(3p) \tag{5.10}$$

In addition, modified Griffith criterion (Equation 2.11) for triaxial compression test becomes:

$$q = \frac{2\mu p' + 4\sigma_t}{\sqrt{1+\mu^2} - \frac{\mu}{3}} \tag{5.11}$$

The complete derivation of the above form is presented in Appendix B.

It can be seen that extended Griffith theory curve requires only the knowledge of unconfined compressive strength whereas modified Griffith theory requires knowledge of both unconfined compressive strength and coefficient of friction (μ). The predicted values of these criteria for soil are as shown in Figure 5.7. Note that, for extended Griffith theory σ_t was found to be -1/14 of unconfined compressive strength, while for modified Griffith theory σ_t found to be -1/10 of unconfined compressive strength. The latter value is the same as suggested by McClintock and Walsh (1962). In addition μ was found to be 0.5. Since both criteria predict the shear strength values well, it is preferred to use extended Griffith criterion as it only needs knowledge of unconfined compressive strength.

Therefore, based on the test results conducted in this study it is suggested to use a combination of Muhunthan and Masad (1997) and the extended Griffith criterion to predict the behavior of cement treated soils. In this hybrid model, for confining pressures lower than p'_A (confining pressure corresponds to point A at which extended Griffith line

and critical state line intercept) stress path raises to extended Griffith line then falls on critical state line. For confining pressures greater than p'_A stress path ends on critical state line. The location of point A can be determined by knowledge of unconfined compressive strength and M.

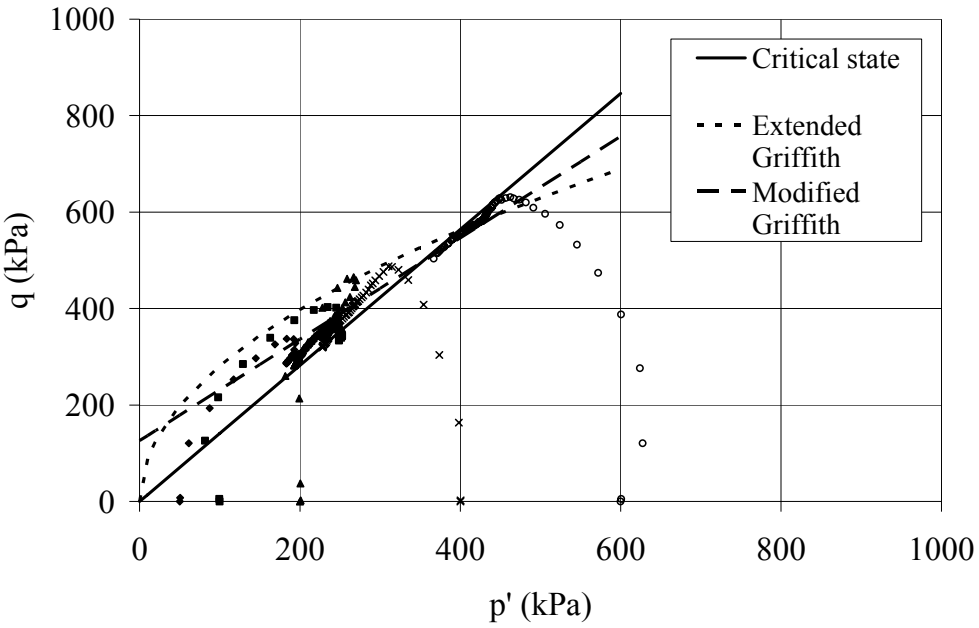

Figure 5.7: Extended and modified Griffith theory for 5% cement treated Aberdeen soil.

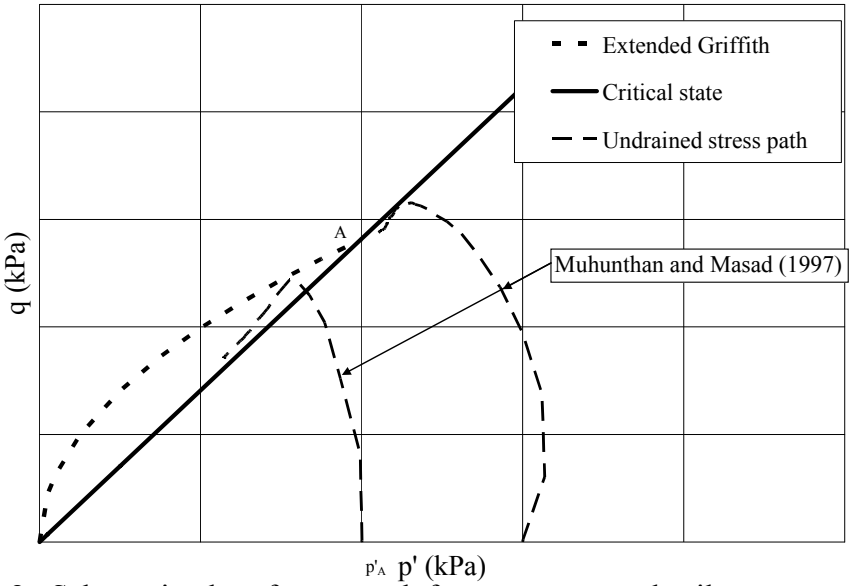

Figure 5.8: Schematic plot of stress path for cement treated soils.

5.6 Liquidity index and limits of soil behavior

The limits of soil behavior described above using q-p′ space can also be described in liquidity index-p′ space as proposed by Schofield (1980) (See Figure 2.23). Liquidity index for non-treated and cement treated Aberdeen soil at different confining pressure is given in Table 5.2. These values obtained from fall cone test data and for seven days curing. In addition a summary of predicted behavior using Figure 2.23 and observed behavior is presented in Table 5.3. Non-treated specimens displayed ductile type of behavior with vertical cracks as shown in Figure 5.9. Vertical splitting was observed for 10% cement treated soil (Figure4.30). While 5% cement treated specimens displayed planar type of failure (Figure 4.29).

Table 5.2: Liquidity index for non-treated and cement treated Aberdeen soil at different confining pressure.

Confining pressure (kPa)	Liquidity index		
	Non-treated	5% Cement	10% Cement
50	-3.7	-2.3	-3.8
100	-3.8	-2.3	-3.9
200	-4.0	-2.4	-4.0
400	-4.1	-2.5	-4.0
600	-4.2	-2.5	-4.1

Table 5.3: Summary of predicted behavior according to Figure 2.23 and observed behavior for non-treated and cement treated Aberdeen soil.

Cement content (%)	Predicted behavior	Observed behavior	Reference
0	Fracture	Fracture	Figure 5.9
5	Fracture	Planar (Fault)	Figure 4.29
10	Fracture	Fracture	Figure 4.30

Figure 5.9: Ductile type of failure with vertical crack for non-treated Aberdeen soil.

For non-treated and 10% cement treated specimens, as it was predicted, fracture behavior was observed. In case of 5% cement treatment also fracture behavior was predicted but planar (fault) behavior was observed. It is concluded that, as a result of cement treatment rupture zone in Figure 2.23 was widened. However, further study is required to be able generalize the latter for different type of soils.

CHAPTER SIX

CONCLUSIONS AND RECOMMENDATIONS

6.1 Introduction

This study made a comprehensive examination of the effectiveness of cement treatment on geotechnical properties of soils encountered in Washington State. The results of the study provides details on the compaction, strength and deformation characteristics of in situ soils as well as those mixed with different percentages of cement.

Three soils from Aberdeen and Everett in western and Palouse area in eastern part of the state were collected. Series of soil mechanics laboratory tests including grain size analysis, Atterberg limits, solidification, standard proctor, unconfined compressive strength, consolidated-undrained triaxial, and oedometer on host soils as well as cement treated soils were performed. The strength and deformation characteristics were examined in detail using several classical failure criteria such as Mohr-Coulomb, Griffith crack theory, modified Griffith crack theory, and a recent criterion by Johnston proposed for soft rocks. None of these criteria accounted for the combined effects of density and confining pressure on soil behavior.

The study made use of the critical state framework to interpret the strength and deformation behavior of non-treated and cement treated Aberdeen soil. This framework explicitly accounts for the combined effects of density and pressure and as such provided some significant insight into the different types of observed soil behavior. A new anisotropic critical state model proposed by Masad and Muhunthan (1997) was found to be able to predict the effective stress path of compacted Aberdeen soil (non-treated and

5% cement treated) in wet side of the critical state line. It was also found that extended Griffith theory is applicable to identify the Hvorslev's surface in q-p′ space. Thus, it is necessary to use a combination of the two formulations to describe the behavior of cement treated soils.

6.2 Observations

Based on the results of the study the followings were observed:

- Cement treatment led to significant increase in initial drying rate of the soils (Figures 4.2, 4.3, and 4.4).
- Generally, drying rate increased with increasing in cement content (Figures 4.2, 4.3, and 4.4).
- For Aberdeen and Palouse soil, addition of cement increased plasticity index initially, while higher percentages of cement led to reduction in plasticity index (Figures 4.5 and 4.6).
- Generally, as cement content increased, optimum water content increased and maximum dry density decreased (Figures 4.7 and 4.8).
- Addition of cement led to significant increase in unconfined compressive strength and modulus of elasticity of specimens (Figures 4.9, 4.10 and 4.12 to 4.21).
- Non-treated specimens disintegrated after being immersed in water. This was also the case for 2.5% cement treated Aberdeen soil (Figure 4.11).
- Addition of cement resulted in a significant increase in peak deviator stress (Figures 4.22, 4.24, 4.26, 4.33, 4.35, and 4.37).

- As cement content increased strain corresponding to peak deviator stress decreased remarkably (Comparison of Figures 4.22, 4.24, and 4.26 and comparison of 4.33, 4.35, and 4.37) .
- For non-treated and 5% cement treated Aberdeen and 5% cement-treated Everett soils, at low confining pressures, negative pore pressures developed (Figures 4.23, 4.25, and 4.36).
- For 10% cement treated soils post peak deviator stress was drastically lower than peak deviator stress (Figures 4.26 and 4.37).
- For 10% cement treated soils at the peak deviator stress pore pressure raised to near confining pressures. Therefore effective confining pressures were near zero at failure (Figures 4.27 and 4.38).
- Non-treated, 5%, and 10% cement treated soils displayed ductile, planar, and splitting type of failure, respectively in triaxial test (Figures 4.28, 4.29, and 4.30) depending on the confining stress.
- Generally, brittleness index increased with increasing in cement content (Figures 4.32 and 4.40).
- Brittleness index for non-treated and 10% cement treated Aberdeen soil found to be relatively constant respect with confining pressure (Figure 4.32).
- For 5% cement treated Aberdeen soil brittleness index increased initially and decreased at higher confining pressures (Figure 4.32).
- For non-treated and 5% cement treated Everett soil brittleness index increased with increasing in confining pressure (Figure 4.40).

- As a result of cement treatment, coefficient of volume change, compression index, swelling index decreased significantly. In addition these values decreased with increasing in cement content (Figures 4.41 and 4.42 and Table 4.4).
- Cement treatment led to increasing in cohesion intercept (Comparison of Figures 4.43 and 4.44, and comparison of Figures 4.46 and 4.47).
- As a result of addition of cement internal friction angle (ϕ') of Everett soil increased (Comparison of Figures 4.46 and 4.47).
- Failure envelope for 5% cement treated Aberdeen soil found to be curved; therefore reporting particular strength parameters were not possible. However for design purposes conservative strength parameters were presented (Figure 4.44).
- Soils (Aberdeen and Everett) treated with 10% cement developed pore pressures equal to confining pressures reducing the effective confining pressures to zero at failure. Thus, all Mohr circles passed through origin; consequently, drawing a single line to represent Mohr-Coulomb failure was not possible (Figures 4.45 and 4.48).
- Based on mean squared error (MSE) analysis modified Griffith theory was more applicable compared with Griffith theory to predict the shear strength of non-treated and cement treated Aberdeen soil within confining pressures ranging from 0 to 600 kPa (Figures 4.49 to 4.51).
- Based on MSE analysis shear strength of non-treated Everett soil could be predicted using Griffith theory whereas shear strength of cement treated

specimens could be predicted using Modified Griffith theory within confining pressures ranging from 0 to 600 kPa (Figures 4.52 to 4.54).

- Coefficient of friction (μ) increased with increasing in cement content (Table 4.6).
- Johnston failure criterion accurately predicted normalized principal stresses of non-treated and 5% cement treated Aberdeen and Everett soils within confining pressures ranging from 0 to 600 kPa (Figures 4.55 to 58).
- Johnston criterion was not applicable for 10% cement treated Aberdeen and Everett soils due to zero effective confining pressure at failure.
- As a result of cement treatment interlocking between particles increased while critical state friction remained constant (Figures 5.1 and 5.2).
- Interlocking between particles decreased with increasing confining pressure (Figures 5.1 and 5.2).
- As a result of cement treatment critical state confining pressure (confining pressure correspond to point at which Hvorslev's surface and critical state line intercept) increased (Figures 5.1 and 5.2).
- For non-treated and 5% cement treated soils for confining pressures smaller than critical stress path raised to Hvorslev's surface and ultimately reached to critical state line (Figures 5.1 and 5.2).
- For 10% cement treated soils undrained stress path ended on unconfined compressive stress line (Figure 5.3).
- Cement treated Aberdeen soil displayed anisotropy type of behavior (Figures 5.5 and 5.6).

- The model presented by Muhunthan and Masad (1997) showed close agreement between predicted and observed undrained stress path of compacted Aberdeen soil in wet side of critical state (Figures 5.5 and 5.6).
- Extended Griffith theory and modified Griffith theory (for triaxial) can be used to predict the maximum deviator stress in q-p´ space, the ratio of unconfined compressive strength to tensile strength found to be -14 and -10 for extended Griffith and modified Griffith (in q-p´ space), respectively (Figure 5.7).
- For confining pressures less than confining pressure correspond to the point at which critical state line and extended Griffith theory intercepts, stress path raised to extended Griffith theory line and dropped on critical state line (Figures5.7 and 5.8).

6.3 Conclusions

Based on the above observations following conclusions can be drawn:

- Evaluation of effectiveness of a stabilization agent based solely on improvement of unconfined compressive strength of treated soil as done by current state of practice is not safe. Since soil behavior is mainly controlled by confining pressure and water content performing triaxial test to simulate the field condition, in addition to unconfined compressive strength test is necessary.
- As a result of addition of cement soil behavior changes from ductile to rigid (displaying fracture type of behavior at failure) resulting in significant

reduction in post peak deviator stress. Therefore, for an earth structure treated with high percentage of cement allowable load and deformation need to be identified.

- Behavior of cement treated Aberdeen soil in q-p′ space can be predicted by combining Muhunthan and Masad (1997) model and extended Griffith theory for samples consolidated at near or greater than the critical confining pressure. Samples consolidated below this pressure behave elastically until the peak stress is attained. For these cases, a combination of elastic with extended Griffith criterion is suggested.
- In comparison between non-treated and 5% cement treated Aberdeen soil, it was observed that as a results of cement treatment inter-particle locking increased while critical state friction angle remained constant. Therefore improvement can be quantified in different confining pressures by using critical state framework.

6.4 Recommendations for future work

The following recommendations are made for future research:

- As observed, high percentages of cement lead to significant increase in pore pressure at the failure and as a result effective confining pressure drops to zero consequently specimen splits vertically, therefore upper limit of cement treatment needs to be identified respect with confining pressure for different soils.

- Since cement treatment changes the microstructure of soil use of non-destructive testing such as X-ray tomography for identifying range of improvement is recommended.
- Cam clay model and all modifications that have been made predict soil behavior well on the wet side of critical state. However, their prediction is not good on the dry side. Since cracks are formed in this side it may be necessary to expand the dissipated energy equation to account for the fact that during brittle failure of soil energy dissipates in forms of friction, initiation and propagation of crack.

REFRENCES

Abboud, M. M. (1973). *Mechanical properties of cement-treated soils in relation to their use in embankment construction,* Ph. D dissertation, University of California, Berkeley, CA.

ACI 230.1R-90. (1990). *State-of-the-Art report on soil Cement,* ACI Material Journal, 87 (4).

ASTM D4609-01. (2006). *Standard guide for evaluating effectiveness of admixtures for soil stabilization,* Annual Book of ASTM Standards, 4.08, 757-761.

Balmer, G. G. (1958). *Shear strength and elastic properties of soil-cement mixture under triaxial loading,* Portland Cement Association Research and Development Laboratories.

Baran, B., Ertuk, T, Sarikaya, Y., and Alemdarglu, T. (2001). "Workability test method for metals applied to examine a workability measure (plastic limit) for clays." Applied Clay Science, 20(1-2), 53-63.

Beikman, H. M., Rau, W. W., and Wagner, H. C. (1967). *Lincoln Creek formation, Grays Harbor basin southwestern Washington,* Geological survey bulletin 1244-I.

Bennert, T. A., Maher, M. H., Jafari, F., and Gucunski, N. (2000). "Use of dredged sediments from Newark harbor for geotechnical application." Geotechnics of high water content materials, ASTM special technical publication, STP 1374.

Bergado, D. T., Anderson, L. R., Miura, N., and Balasubramaniam, A. S. (1996). *Soft ground improvement*, ASCE Press.

Bishop, A. W. (1971). "The influence of progressive failure on the choice of stability analysis." Geotechnique, 21(2), 168-172.

Black, D. K. and Lee, K. L. (1973). "Saturating laboratory samples under back pressure." Journal of The Soil Mechanics and Foundation Division, ASCE, 99(SM1), 75-93.

Burland, J. B. (1965). Discussion, Geotechnique, 15, 211-214.

Burland, J. B., Rampello, S., Georgiannou, V. N. and Calabresi, G. (1996). "A laboratory study of the strength of four stiff clays." Geotechnique, 46(3), 491-514.

Chiu, H. K., and Johnston, I. W. (1984). "The application of critical state concepts to Melbourne mudstone." Fourth Australia- New Zealand conference on Geomechanics, (84/2), 29-33.

Clough, G. W., Sitar, N., Bachus, R. C., and Shafii-Rad, N. (1981). " Cemented sands under static loading." Journal of The Geotechnical Engineering Division, ASCE, 107(GT6). 799-817.

Cokrell, C. F., Muter, R. B., Leonard, J. W, and Anderson, R. E. (1970). *Application of floatation for recovery of calcium constituents from limestone modified fly ash.* West Virginia University, Coal Resource Bureau and School of Mines.

Collins, I. F. and Kelly, P. A. (2002). "A thermomechanical analysis of soil models." Geotechnique, 52(7), 507-518.

Currin, D. D., Allen, J. J., and Little, D. N. (1976). " Validation of soil stabilization index system with manual development." Report No. FJSRL-TR-0006, Frank J. Seisler Research Laboratory, United States Air Force Academy, Colorado.

Das, B. M. (1990). *Principle of foundation engineering*, PWS-KENT publishing company, Boston.

Eades, J. L. and Grim, R. E. (1966). "A quick test to determine lime requirements for lime stabilization." Highway Research Record, Washington, D.C., 139, 61-75.

Engineering manual 1110-3-137. (1984). *Soil stabilization for pavements mobilization construction*, Department of the Army, Corps of engineers office of the chief of engineers.

EPA-530-K-05-002. (2005). *Using coal ash in highway construction: a guide to benefits and impacts*, United States Environmental Protection Agency.

Feng, T. W. (2000)."Fall-cone penetration and water content relationship of clays." Geotechnique, 50(2), 181-187.

Harris, P., Sebesta, S., Holdt, V. J., and Scullion, T. (2006). "Recommendations for stabilization of high sulfate soils in Texas." Transportation Research Board, Washington, D.C., (1952), 71-79.

Head, K. H. (1992). *Manual of soil laboratory testing.* 1, 2nd Edition, Pentech Press Limited.

Hilt, G.H. and Davidson, D.T. (1960). "Lime fixation in clayey soils." Bulletin No. 304, Highway Research Record, Washington, D.C., 20-32.

Holtz, R. D. and Kovacs, W. D. (2004). *Introduction to geotechnical engineering.* Pearson Education Taiwan Ltd.

Jaeger, J. C. and Cook, N. G. W. (1976). *Fundamentals of rock mechanics,* John Wiley & Sons, Inc.

Jennings, A. T. (1994). *Dynamic properties of unsaturated loess,* MS thesis, University of Idaho, Moscow, Idaho.

Johnston, I. W. (1985). "Strength of intact geomechanical materials." Journal of Geotechnical Engineering, 111(6), 730-749.

Johnston, I. W. and Chiu, H. K. (1984). "Strength of weathered Melbourne mudstone." Journal of Geotechnical Engineering, 110(7), 875-898.

Kamon, M. and Nontananandh, S. (1991). "Combining industrial wastes with lime for soil stabilization." Journal of Geotechnical Engineering, 117(1), 1-17.

Koumoto, T. and Houlsby, G. T. (2001). "Theory and practice of fall cone test." Geotechnique, 51(8), 701-712.

Kasama, K., Zen, K., and Iwataki, K. (2007). "High-strengthening of cement-treated clay by mechanical dehydration." Soils and Foundations, 47(2), 171-184.

Little, D. N. (1995). *Stabilization of pavement subgrades and base courses with lime,* Kendall/Haunting publishing company.

Little, D. N., Males, E. H., Prusinski, J. R., and Stewart, B. (2000). *Cementitious stabilization*, Transportation in the New Millennium: State of the Art and Future Directions, Perspectives from Transportation Research Board Standing Committees.

Little, L., Connor, B., Carlson, R. F. (2005). *Tests of soil stabilization products, phase 1*, University of Alaska Fairbanks.

Lawrence, D. M. (1980). *Some properties associated with Kaolinite soils.* MS Thesis, Cambridge University, UK.

Lo, S. R., and Wardani, S. P. R. (2002). "Strength and dilatancy of a stabilized by a cement and fly ash mixture." Canadian Geotechnical Journal, 39(1), 77-89.

Lowell, S. (2005). Personnel communication, Washington Department of Transportation, Olympia, WA.

Maher, M., Marshall, C., Harrison, F. and Baumgaertner, K. (2005). *Context sensitive roadway surfacing selection guide,* FHWA-CFL/TD-05-004.

Mallela, J., Quintus, H. V., and Smith, K. (2004). *Consideration of lime-stabilized layers in mechanistic-empirical pavement design.* The National Lime Association.

McClintock, F. A. and Walsh, J. B. (1962). " Friction on Griffith cracks in rocks under pressure." Proceedings of Fourth U.S. National Congress on Applied Mechanics, 2, 1015-1022, Berkeley, CA.

Miller, G. A., and Azad, S. (2000)." Influence of soil type on stabilization with cement kiln dust." Construction and Building Materials, 14(2), 89-97.

Mitchell, J. K. (1976). "The properties of Cement-stabilized soils." Proceeding of Residential Workshop on Materials and Methods For Low Cost Road, Rail, and Reclamation Works, 365-404, Leura, Australia, Unisearch Ltd.

Muhunthan, B., Chameau, J. L., and Masad, E. (1996). "Fabric effects on the yield behavior of soils." Soils and Foundations, Japanese Society of Geotechnical Engineering, 36(3), 85-97.

Muhunthan, B. and Masad, E. (1997). "Fabric effects on stress-strain behavior of clays." Proceedings of Sixth International Symposium on Plasticity and Its Current Application, Juneau, Alaska.

Muhunthan, B. and Schofield, A. N. (2000). "Liquefaction and dam failure." ASCE Geotechnical Special Publication, GeoDenver Conference, Slope Stability 2000, (101), 266-280, Denver, CO.

Murrell, S. A. F. (1963). "A criterion for brittle fracture of rocks and concrete under triaxial stress and the effect of pore pressure on the criterion." Proceedings of Fifth Rock Mechanics Symposium, University of Minnesota, 563-577.

Nash, J. K. T. L., Jardine, F. M., and Humphrey, J. D., (1965). "The economic and physical feasibility of soil-cement dams." Proceedings of the Sixth International Conference on Soil Mechanics and Foundation Engineering, 2, 517-521, Montreal, Canada.

Nicholson, P. G. and Ding, M. (1997). "Improvement of tropical soils with waste ash and lime." American Society for Testing Materials, 1257, 195-204.

Novello, E. A. and Johnston, I. W. (1995). "Geotechnical materials and the critical state." Geotechnique, 45(2), 223-235.

Parry, R. H. G. (1995). *Mohr circles, stress paths and Geotechnics,* E&FN Spon

Pillai, V. S. and Muhunthan, B. (2002). "Discussion of an investigation of the effect of soils state on the capacity of driven piles in sand, by Klotz. E.U and Coop, M.R., Geotechnique, 52(8), 620-621.

Pillai, V. S. and Muhunthan, B. (2001). "A review of the initial static shear(K_α)and confining stress(K_σ)on failure mechanism and earthquake liquefaction of soil."

Proceeding of 4th International Conference on Recent Advances in Geotechnical Earthquake Engineering and Soil Dynamics, San Diego, CA.

Pillai, V.S. and Muhunthan, B. (1999). "Landslides in cemented and normally consolidated soils: a review of failure mechanism using stress-path." Proceedings of 13th annual Vancouver Geotechnical Society Symposium, Vancouver, British Columbia.

Portland Cement Association, (1992). *Soil-Cement Laboratory Handbook,* Skokie, Illinois.

Puppala, A. J. and Musenda, C. (2000)." Effects of fibers reinforcement on strength and volume change behavior of expansive soils." Transportation Research Board, Washington D.C., (1736), 134-140.

Rocha, M., Folque, J., and Esteves, V. P. (1961). "The application of cement stabilized soils in the construction of earth dams." Fifth International Conference on Soil Mechanics and Foundation Engineering, Paris, France.

Roscoe, K. H. and Burland, J. B. (1968). *On the generalized stress strain behavior of wet clay, Engineering plasticity,* Cambridge University Press.

Roscoe, K. H., Schofield, A. N., and Thurairajah, A. (1963). "Yielding of clays in states wetter than critical." Geotechnique, 13(2), 211-240.

Rotta, G. V., Consoli, N. C., Prietto, P. D. M., Coop, M. R., and Graham, J. (2003). "Isotropic yielding in an artificially cemented soil cured under stress." Geotechnique, 53(5), 493-501.

Running, D. L. (1996). *An energy-based model for soil liquefaction,* Ph D dissertation, Washington State University, Pullman, WA.

Sangrey, D. A. (1972). "Naturally cemented sensitive soils." Geotechnique, 22(1), 139-152.

Santoni, R. L., Tingle, J. S. and Nieves, M. (2004). "Accelerated strength improvement of silty sand using nontraditional additives." Transportation Research Board, Washington, D.C., (1936), 34-42.

Santoni, R. L., Tingle, J. S. (2002). *Building roads on soft and silty soils,* www.almc.army.mil/alog/issues/JanFeb02/MS698.htm - 18k.

Sariosseiri, F. and Muhunthan, B. (2008). "Geotechnical properties of Palouse loess modified with cement kiln dust and Portland cement." Proceedings of Geocongress 2008, Geochallenge of sustainability in the Geoenvironment, New Orleans, LA

Schofield, A. N. (2005). *Disturbed soil properties and geotechnical design,* Thomas Telford Ltd.

Schofield, A. N. (1998). ”Mohr Coulomb error correction.” Ground Engineering, 31(8), 30-32.

Schofield, A. N. (1980). “Cambridge geotechnical centrifuge operations.” Geotechnique, 30(3), 227-268.

Schofield, A. N. and Wroth, C. P. (1968). *Critical state soil mechanics,* McGraw-Hill, New York.

Singh, G. V. and Das, B. M. (1999). “Soil stabilization with sodium chloride.” Transportation Research Board, (1673), 46-55.

Sivapullaiah, P. V. and Sridharan, A. (1985). “Liquid limit of soil mixtures.” Geotechnical Testing Journal, 8(3), 111-116.

Sreekrishnavilasam, A., King, S., Santagata, M. (2006). “Characterization of fresh and landfilled cement kiln dust for reuse in construction applications.” Geoenvironmental Engineering, 85(1-2), 165-173.

Thompson, M. R. (1966). “Shear strength and elastic properties of lime-soil mixtures.” Highway Research Record, Washington, D.C., 139, 1-14.

Tabatabi, A. M. (1997). *Pavement [Roosazi Rah]*, University’s publication center, Tehran, Iran.

Technical manual 5-822-14/AFJMAN 32-1019. (1994). *Soil stabilization for pavement,* Department of Army and Air force, Washington D.C.

Troost, K. G., Booth, D. B., and Laparade, W. T. (2003). *Quaternary geology of Seattle,* Geology Society of America, Field guide 4.

Uddin, K., Balasubramaniam, A. S., and Bergardo, D. T. (1997). “Engineering behaviors of cement-treated Bangkok soft clay.” Geotechnical Engineering Journal, (28)1, 89-119.

University of Florida, http://grunwald.ifas.ufl.edu.

United States Geological Survey, http://esp.cr.usgs.gov.

Wasti, Y. (1987). “Liquid and plastic limits as determined from the fall cone and Casagrande methods.” Geotechnical Testing Journal, 10(1), 26-30.

Wissa, A. E. Z., Ladd, C. C., and Lambe, T. W. (1965). "Effective stress-strength parameters of stabilized soils." Proceedings of the Sixth International Conference on Soil Mechanics and Foundation Engineering, Montreal, Canada.

White, W. G. and Gnanendran, C. T. (2005). "The influence of compaction method and density on the strength and modulus of cementitiously stabilized pavement material." The International Journal of Pavement Engineering, 6(2), 97-110.

Wood, D. M. (1990). *Soil behavior and critical state soil mechanics,* Cambridge university press.

Wong, P. K. K. and Mitchell, R. J. (1975). "Yielding and plastic flow of sensitive cemented clay." Geotechnique, 25(4), 763-782.

APPENDIX A

GRIFFITH AND MODIFIED GRIFFITH CRACK THEORY

Griffith crack theory

The Griffith crack theory states the relationship between nominal stress and crack length at failure, or in other words it explains when a loaded brittle body becomes energetically favorable for a crack to propagate. An elliptical crack with its major axis perpendicular to a tensile stress σ_T in a thin plate is shown in Figure A.1.

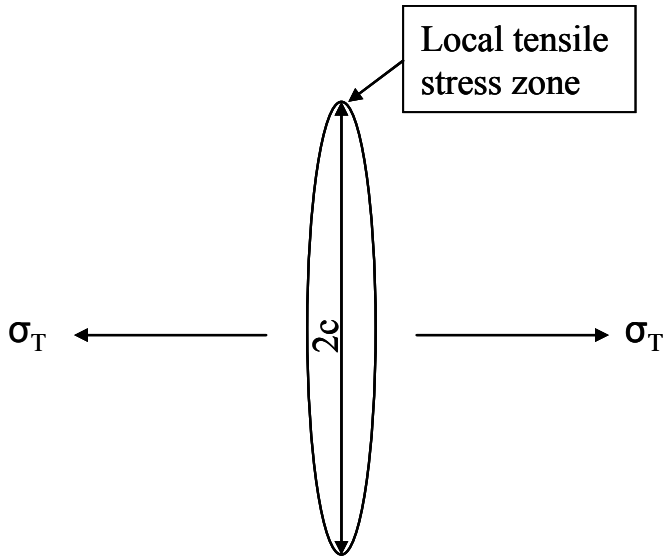

Figure A.1: Elliptical flaw with tensile stress effecting perpendicular to its major axis

It can be shown that (Mitchell 1976):

$$T_m = 2\sigma_T \sqrt{\frac{c}{r_m}} \tag{A.1}$$

Where:

T_m : Maximum tensile stress

r_m : Radius of curvature at the end of the major axis

$2c$: Major diameter

Failure occurs when part of stored strain energy is released as the crack propagates, it can be describes as (Mitchell 1976):

$$\sigma_T = \sqrt{\frac{2S_e E}{\pi c}} \tag{A.2}$$

Where:

S_e : Surface energy

E : Modulus of elasticity

It must be noted that tensile stress can be mobilized around the crack even in compressive stress field as shown in Figure A.2. By using Inglis's notation, Griffith has shown that the tensile stresses have the most influential when (Abboud 1973 and Mitchell 1976):

$$\cos 2\theta = -\frac{1}{2}\left(\frac{\sigma_1 - \sigma_3}{\sigma_1 + \sigma_3}\right) \tag{A.3}$$

Where σ_1 and σ_3 are major and minor principal stresses, respectively.

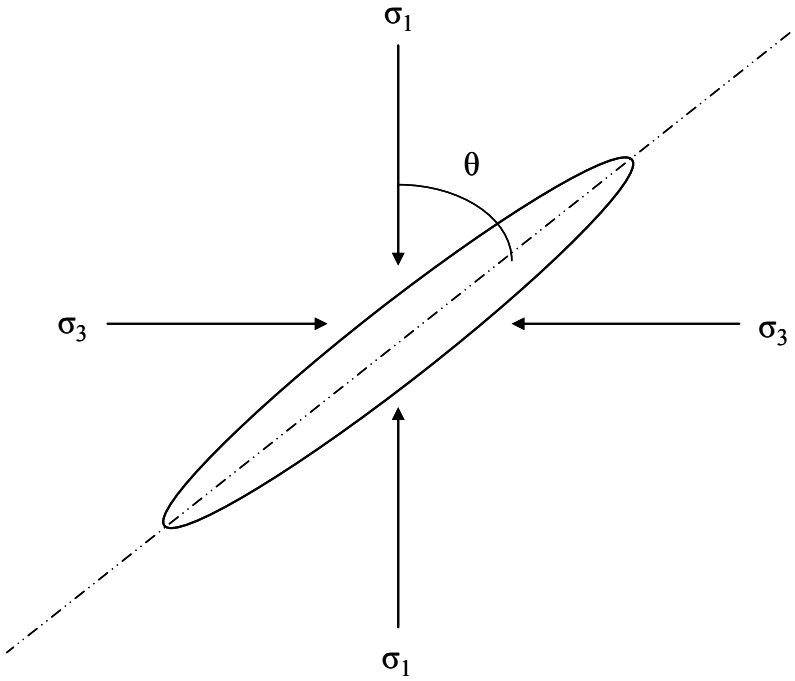

Figure A.2: Compressive stress field around a crack

By assuming compression is positive, if $\sigma_1 \neq \sigma_3$ and $3\sigma_1 + \sigma_3 > 0$ then,

$$(\sigma_1 - \sigma_3)^2 + 8\sigma_t(\sigma_1 - \sigma_3) = 0 \quad \text{(A.4)}$$

Where σ_t is the tensile strength, for $\sigma_3 = 0$, σ_1 becomes unconfined compressive strength, $\cos 2\theta = 0.5$ and

$$\sigma_1 = \sigma_c = -8\sigma_t \quad \text{(A.5)}$$

In addition equation B.4 can be rewritten as:

$$(\sigma_1 - \sigma_3)^2 = \sigma_c(\sigma_1 + \sigma_3) \quad \text{(A.6)}$$

Equations A.4 and A.5 can be expressed by shear stress versus normal stress as follow:

$$\tau^2 + 4\sigma_t\sigma_n - 4\sigma_t^2 = 0 \quad \text{(A.7)}$$

Where τ is shear stress and σ_n is normal stress. Evidently knowledge of unconfined compressive strength leads to obtain failure envelope.

Modified Griffith crack theory

The Griffith crack theory applies for tensile condition, McClintock and Walsh (1962) modified Griffith theory for condition at which crack become close and resist against sliding across the crack surface. They stated that an effective normal stress mobilized across the crack σ_e, when normal stress σ_n reaches to a particular critical value of σ_d, this statement can be shown mathematically as:

$$\sigma_e = \sigma_n - \sigma_d \quad \text{(A.8)}$$

Therefore a shear stress τ_c is developed along the crack, given by:

$$\tau_c = \mu(\sigma_n - \sigma_d) \quad \text{(A.9)}$$

Where μ is the coefficient of friction, superposition leads to the following failure condition (Detail derivation of Griffith and modified Griffith crack theory is given in Jaeger and Cook 1976):

$$\sigma_1\left[\left(\mu^2+1\right)^{\frac{1}{2}}-\mu\right]-\sigma_3\left[\left(\mu^2+1\right)^{\frac{1}{2}}+\mu\right]=4\sigma_t\left[1+\frac{\sigma_d}{\sigma_t}\right]^{\frac{1}{2}}-2\mu\sigma_d \qquad \text{(A.10)}$$

If the crack close at a very low stresses therefore it can be assumed that $\sigma_d = 0$, thus

$$\sigma_1\left[\left(\mu^2+1\right)^{\frac{1}{2}}-\mu\right]-\sigma_3\left[\left(\mu^2+1\right)^{\frac{1}{2}}+\mu\right]=4\sigma_t \qquad \text{(A.11)}$$

Based on data from rock and Concrete McClintock and Walsh (1962) suggested that it can be assumed $\sigma_c = -10\sigma_t$ and $\mu = 1$. Modified Griffith theory in terms of shear and normal stress can be present as:

$$\tau = 2\sigma_t + \mu\sigma_n \qquad \text{For } \sigma_n > 0 \qquad \text{(A.12)}$$

$$\tau^2 + 4\sigma_t\sigma_n - 4{\sigma_t}^2 = 0 \qquad \text{For } \sigma_n < 0 \qquad \text{(A.13)}$$

APPENDIX B

EXTENDING MODIFIED GRIFFITH THEORY FOR TRIAXIAL TEST

B.1 Introduction

Derivation of extending modified Griffith theory for triaxial test is presented in this Appendix. The sign conventional of soil mechanics, all the stresses and strains are positive in compression and negative in tension, and also all stresses are effective, was adopted.

B.2 Stress invariants

It is possible to decompose a stress tensor into two component including hydrostatic stress tensor and deviator tensor as shown in Equation B.1.

$$\sigma_{ij} = S_{ij} + p\delta_{ij} \tag{B.1}$$

Where,

S_{ij} : Stress deviator tensor

p : Hydrostatic stress or $p = \frac{1}{3}\sigma_{ii} = \frac{1}{3}(\sigma_1 + \sigma_2 + \sigma_3)$

δ_{ij} : Kronecker delta

The first, second, and third stress tensor σ_{ij} invariant is given by Equations B.2, B.3, and B.4, respectively.

$$I_1 = \sigma_1 + \sigma_2 + \sigma_3 = 3p \tag{B.2}$$

$$I_2 = \sigma_1\sigma_2 + \sigma_2\sigma_3 + \sigma_3\sigma_1 \tag{B.3}$$

$$I_3 = \sigma_1\sigma_2\sigma_3 \tag{B.4}$$

The first invariant of stress tensor S_{ij} is zero, the second, and third invariant is given by Equations B.5 and B.6, respectively.

$$J_2 = \frac{1}{3} S_{ij} S_{ji} = \frac{1}{6}\left[(\sigma_1 - \sigma_2)^2 + (\sigma_2 - \sigma_3)^2 + (\sigma_3 - \sigma_1)^2\right] \quad \text{(B.5)}$$

$$J_3 = \frac{1}{3} S_{ij} S_{jk} S_{ki} = \frac{1}{3}\left(S_1{}^3 + S_2{}^3 + S_3{}^3\right) = S_1 S_2 S_3 \quad \text{(B.6)}$$

The invariants J_1, J_2, and J_3 are related to the invariants I_1, I_2, and I_3 by Equations B.7 to B.9.

$$J_1 = 0 \quad \text{(B.7)}$$

$$J_2 = \frac{1}{3}\left(I_1{}^2 - 3I_2\right) \quad \text{(B.8)}$$

$$J_3 = \frac{1}{27}\left(2I_1{}^3 - 9I_1 I_2 + 27I_3\right) \quad \text{(B.9)}$$

B.3 Extending modified Griffith theory for triaxial test

The relationship between principal stresses and invariants are given in Equations B.10 to B.12 (Running 1996).

$$\sigma_1 = p + \frac{2}{\sqrt{3}}\bar{\sigma}\sin\left(\theta + \frac{2\pi}{3}\right) \quad \text{(B.10)}$$

$$\sigma_2 = p + \frac{2}{\sqrt{3}}\bar{\sigma}\sin\theta \quad \text{(B.11)}$$

$$\sigma_3 = p + \frac{2}{\sqrt{3}}\bar{\sigma}\sin\left(\theta - \frac{2\pi}{3}\right) \quad \text{(B.12)}$$

Where $\bar{\sigma} = \sqrt{J_2}$, $\theta = \frac{-\pi}{6}$ for q>0 and $\theta = \frac{\pi}{6}$ for q<0. For triaxial test condition in which $\sigma_2 = \sigma_3$, the first stress invariant I_1 and the second deviator stress invariant J_2 can be related to the mean stress (p) and the deviator stress (q) as presented in Equations B.13 and B.14.

$$p = \frac{I_1}{3} = \frac{1}{3}(\sigma_1 + 2\sigma_3) \tag{B.13}$$

$$q = \sqrt{3J_2} = \sqrt{3}\bar{\sigma} \tag{B.14}$$

In the other hand modified Griffith theory (Equation 2.11) can be rewrite in a form as presented in Equation B.15.

$$(\sigma_1 - \sigma_3)\sqrt{1+\mu^2} - \mu(\sigma_1 + \sigma_3) = 4\sigma_t \tag{B.15}$$

Constructing the terms $\sigma_1 - \sigma_3$ and $\sigma_1 + \sigma_3$ by substituting from Equations B.10 and B.12 yields to:

$$\sigma_1 - \sigma_3 = p + \frac{2}{\sqrt{3}}\bar{\sigma}\sin\left(\theta + \frac{2\pi}{3}\right) - p - \frac{2}{\sqrt{3}}\bar{\sigma}\sin\left(\theta + \frac{2\pi}{3}\right) \tag{B.16}$$

$$\sigma_1 + \sigma_3 = p + \frac{2}{\sqrt{3}}\bar{\sigma}\sin\left(\theta + \frac{2\pi}{3}\right) + p + \frac{2}{\sqrt{3}}\bar{\sigma}\sin\left(\theta + \frac{2\pi}{3}\right) \tag{B.17}$$

By using trigonometric relations and simplifications Equations B.16 and B.17 arrive in Equations B.18 and B.19, respectively.

$$\sigma_1 - \sigma_3 = q \tag{B.18}$$

$$\sigma_1 + \sigma_3 = 2p + \frac{q}{3} \tag{B.19}$$

Substitution of Equations B.18 and B.19 in B.15 and rearrangement results in Equation B.20, which defines the modified Griffith theory in q-p´ space.

$$q = \frac{2\mu p + 4\sigma_t}{\sqrt{1+\mu^2} - \frac{\mu}{3}} \tag{B.20}$$